Ultrafiltration of partially degraded starch solution

Contribution of fouling mechanisms to the flux decline and effect of operating parameters

Doctoral Thesis

by

Berhanu A. Demessie

Submitted to
Department of Chemical Engineering
Norwegian University of Science and Technology (NTNU)
In partial fulfillment of the requirement for degree of Doctor Engineering (Dr. Ing.)

Trondheim, 2002

URN:NBN:no-3327

Dr. Ing thesis
NTNU
2002:87

By: Berhanu A. Demessie
Supervisor: Professor Norvald Nesse
August, 2002

ISBN 82-471-5487-0
ISSN 0809-108X

Summary

Desizing wastewater is largely responsible for the chemical oxygen demand (COD) load in the textile industry wastewater. A larger portion of COD comes from degraded starch in desizing wastewater. Removing the starch from the wastewater by an ultrafiltration process may reduce the environmental problem caused by the textile factory. If the treatment is made in such a way that all starch components are removed from the wastewater, the treated water can be reused by the factory. If the starch in the concentrate is stable, it can also be reused as a sizing agent. This will give the factory an economic advantage.

In this thesis we have studied the fouling mechanisms involved in the ultrafiltration of solution with partially degraded starch in order to find the treatibility of such solutions. The work has mainly been directed to uncover how the different fouling mechanisms depend on the operating parameters, and to find the performance of selected membranes. In addition, different models were evaluated for their validity in predicting the performance of the membranes and the data was fitted to the model that give the best prediction and are physically more meaningful. In addition, the starch solution was concentrated, and the flux, concentration, retention and rejection profiles as a function of concentrating time were investigated.

For the study, we used a partially degraded starch solution as a model solution. The solution was prepared in the laboratory by enzymatic degradation of potato starch to different levels. In order to evaluate the reproducibility of the degraded starch, three replicates were prepared. The reproducibility was determined by comparing the molar mass distribution from HPLSEC analysis and the concentration of reducing sugar from a DNS test for the replicates. The analyses show very good reproducibility. Three starch model solutions with three different degradation levels were chosen for our ultrafiltration experiments to investigate the effect of average molar mass of the starch.

For the ultrafiltration of the solution ES625 (from PCI) and MPT-U20 (from KOCH) membranes were used. Both membranes were used in the

investigation of the contribution of different fouling mechanisms to the flux decline during ultrafiltration of the solution. In the evaluation of the performance of ultrafiltration of the starch solution, however, only the ES625 membrane was used. According to the manufacturers, both membranes have nearly equal pure water flux and MWCO. But in our test, we observed a higher and different pure water flux for each type of membrane. The ES625 had a lower flux (higher retention) than the MPT-U20 membrane.

In the ultrafiltration of partially degraded starch solution the permeate flux declines very fast and, for a low feed concentration, it reaches a steady state in a very short time. The steady state time was observed to increase with concentration, molar mass and transmembrane pressure drop, and to decrease with cross flow velocity. All the three fouling mechanisms (concentration polarization, adsorption and deposition) were responsible for the flux decline. The major observed contributors are, however, adsorption and deposition. Adsorption is largely responsible at low-pressure operation while the deposition fouling effect is dominant at higher pressures, near or beyond the limiting flux.

For the ES625 membrane, the contribution of adsorptive fouling increases with concentration and decreases with molar mass of the starch, temperature and pH at a given transmembrane pressure and cross flow velocity. The effect of the operating parameters on the depositional fouling is in line with literature. It increases with pressure, concentration, molar mass and temperature, and decreases with cross flow velocity. Its dependence on pressure can be expressed by a power function with exponent larger than 1.0. This seems to due to an increase in thickness and compaction of the starch gel/deposit at the membrane surface as the transmembrane pressure drop is increased. The contribution of the concentration polarization is also dependent on concentration, cross flow velocity and pressure. Its relative contribution increases with concentration while it decreases with an increase in cross flow velocity. In the turbulent flow regime the relation between the resistance contributed by concentration polarization increases almost linearly with transmembrane pressure drop. In the laminar flow regime, however, the relative contribution of the resistance due to concentration polarization increases for the lower range of pressure and decreases for the higher range of pressure. Its relative contribution also increases with temperature and decreases with increasing molar mass. But the overall fouling resistance in the ultrafiltration of the starch solution increases with feed concentration, molar mass of the starch and transmembrane pressure drop and decreases with cross flow velocity and temperature.

The trend of the flux loss due to all fouling mechanisms for MPT-U20 membrane is similar to ES625 membrane except for adsorption and concentration polarization with changes in concentration and molar mass. The difference could be a result of the difference in morphological properties between the two membranes and the experimental procedures used in determining flux data that used for calculating the contributions. From the pure water flux and the retention data, the ES625 membrane seemed to have a smaller pore size than the MPT-U20 membrane.

Among the ultrafiltration models, the resistances-in-series model was chosen for its provision to include all the fouling mechanisms into the model. When our permeate flux data was fitted to the model, it gives a good fit. However, the model fails to give realistic estimates of the contribution of the individual fouling mechanisms. In order to improve this problem, the model was modified by introducing osmotic pressure across the membrane in such a way that the effect of concentration polarization is accounted for. This modified model is more physically meaningful and gives a realistic estimate of the contribution the reversible and irreversible fraction of the overall resistance.

In concentrating mode operation,the permeate was continuously withdrawn and hence, the concentration of starch in the feed tank was increased. At an early stage of ultrafiltration, the permeate flux appeared to increase slightly, which seems, a result a shear thinning of the starch solution when the solution was pumped through the system. For the rest of the operation, the flux was decreasing, the retention was increasing and the rejection of the membrane was shifted to a lower molar mass as the solution in the feed tank got more concentrated as expected. The shift of rejection to the lower molar mass region is due to the fouling layer that reduces the accessibility of the pores of the membrane.

Generally, the flux we obtained in ultrafiltration of a partially degraded starch solution with the ES625 tubular membrane is equal or better than the reported values from an existing ultrafiltration plant that has been used in the textile industry to recover a synthetic sizing agent (PVA) from the desizing wastewater. The retention is, however, rather low. Two or more stages of treatment are needed to get all starch components removed from the wastewater and make the treated water reusable (recycled).

URN:NBN:no-3327

Preface

I started my study for the Doctor Engineering (Dr. Ing.) degree at the Department of Chemical Engineering, the Norwegian University of Science and Technology (NTNU) in February 1997 under the supervision of Professor Norvald Nesse. The study was planned to for three and half years. The research has been aimed to be purely experimental, which involves membrane pilot plant. At first, I thought experimental research would be simple. Now, I do have a true picture of it. It is expensive and time consuming, tedious and boring, and has a lot of disappointment… to get it run. In the end, however, I could see that the experience is invaluable. I would say, for beginner like me, the experience itself is much more regarding than the results. If I have a chance again, I would be glad to be in the laboratory but not as a student. Rush is the enemy for experimental work. Since I secured properly working pilot plant it is one and half years ago. Now, it is June 2002.

Our initial plan was to work on wastewater from Ethiopian textile factories Due to lack financial support for the project we changed our mind. We therefore decided to explore the behavior of the most pollutant ingredient, starch, in desizing wastewater (from one of the unit processes in textile industry) during ultrafiltration of the solutions. The study was conducted on a model solution containing stable partially degraded starch. The concentration of the starch solution used in the experiment was relatively low due to the limitation of the equipment used for the preparation of model starch solution. We believe that the results obtained from the experimental study introduce new information on the contribution of the fouling mechanisms involved and performance of ultrafiltration of partially degraded starch. It may also be used as springboard for further study on partially degraded starch solution and for the treatment of wastewater rich in partially degraded starch, in particular from textile industries.

In this thesis, the results are presented as a monograph. The results have not been published yet. We hope it will be made ready for publication in the mean time.

URN:NBN:no-3327

Acknowledgement

First of all, I would like to thank my supervisor Professor Norvald Nesse for his inspiration, scientific support, valuable advises and encouragement during my study. I would like to thank also Professor Bjørn Erik Christensen from the Department of Biotechnology. This work would not be possible without his support, advises and the use of the facilities of his department for the preparation of model starch solution used in our experiment. I would like to express also my gratitude to Anne Sissel Ulseth, Mildrid Mybr and to all their colleagues for their spirit of hospitality in their laboratory, for their wonderful technical assistance in using their facilities and in analyzing test samples.

I appreciate the financial support I got from Norwegian State Loan Fund for the first two years by my study. The Department of Chemical Engineering financed the rest (the last three years) of the study, in part by giving me a per-time job (as scientific assistant). I am very much grateful to the department for their support and for giving me the job. I would like to thank also the administrative and technical personnel of the department for their cooperation and willingness to help me whenever I needed.

The encouragement and the support, in some way, I enjoyed from my friends in Trondheim and somewhere else helped me a lot at all phases of my study. In particular, I am grateful to Edvard Sivertsen (former dr. ing student and my colleagues) for helping me to solve experimental data acquisition problem, for the discussion we had on the results, for proofreading my thesis and for his valuable comment. My deep gratitude is also due Ayele Taye for his inspiring suggestion on the presentation and discussion of the results, his help in proof reading and his comments at all stages of the writing up of the thesis. I can not forget also to acknowledge Hirpa Lemu and his family for the wonderful time we have had together since I came to Norway and their encouragement and support whenever I need them.

My final but the deepest thanks goes to my wife Genet, who paid a heavy price for the success of my study. I am also grateful for her precious gift for

me, Joel, at this special moment in our life. Therefore, I would like to dedicate this thesis to our common Love, for remembrance of Joel, the Source of hope that does not disappoint.

Contents

URN:NBN:no-3327

List of abbreviations and symbols

List of abbreviations

AB	Acid-base (polar) interaction
COD	Chemical oxygen demand
CFV	Cross flow velocity
DNS	Dinitrosalisylic acid (reducing sugar analysis methods)
DP	Degree of polymerization
FLR	Flux loss ratio
HPLC	High pressure liquid chromatography
HPLSEC	High pressure liquid size exclusion chromatography
RI	Refractive index
LW	Lifshitz-van der Waals (non-polar) interaction
MWCO	Molecular weight cut off
NFL	Normalized flux loss
PS	Phenol sulfuric acid (analysis method of the sugar content)
PVA	Polyvinyl alcohol
SEC	Size exclusion chromatography
UNEP	United nations environment programme

List of symbols

Roman

A_2	The second virial coefficient [mol $m^{-3}g^{-1}$]
A_3	The third virial coefficient [mole $m^{-6}g^{-1}$]
B	The solute permeability of the membrane [g $Pa^{-1}s^{-1}$]
C	Solute concentration at x unit distance from the membrane surface [g/m^3]

$\bar{C}$	The log mean concentration difference across the membrane [g/m^3]
C^*	Semi-dilute concentration [g/m^3]
C_h^*	Hydrodynamic semi-dilute concentration [g/m^3]
C_{A2}^*	Thermodynamic semi-dilute concentration [g/m^3]
C_b	Bulk solute concentration [g/m^3]
C_F	Solute concentration in the feed stream [g/m^3]
C_g	Gel concentration at the membrane surface [g/m^3]
C_i^*	Semi-dilute concentration at which the overlap between the macromolecules starts [wt %]
C_m	Solute concentration at the membrane surface [g/m^3]
C_P	Solute concentration in the permeate stream [g/m^3]
C_R	Solute concentration in the retentate stream [g/m^3]
d	Distance between strands of macromolecules in a solution [m]
D	Diffusion coefficient [m^2/s]
d_h	Hydraulic diameter [m]
d_o	The minimum equilibrium distance between the strands of two macromolecules [m]
E	lastic module of polymer gel [Pa]
ΔG_{121}	Free energy of interaction between species 1 and 2 (per unit area) [J/m^2]
ΔG_{121}^{AB}	Polar component of free energy of interaction between species 1 and 2 (per unit area) [J/m^2]
ΔG_{121}^{T}	Total energy of adhesion [J]
ΔG_{121}^{LW}	Apolar component of free energy of interaction between species 1 and 2 (per unit area) [J/m^2]
$J_¥$	Limiting flux [m/s]
J_a	Pure water flux for a membrane which is fouled by static adsorption degraded starch solution [m/s]
J_f	Pure water flux for a membrane which is fouled by degraded starch solution [m/s]
J_i	Pure water flux for new or clean membrane [m/s]
J_s	Solute flux through the membrane [m/s]
J_v	Permeate flux of ultrafiltration of degraded starch solution under a given set of operating conditions [m/s]
k	Mass transfer coefficient [m/s]
L	Tubular membrane length [m]
Lp	Membrane permeability [m Pa^{-1}s^{-1}]
M_W	Molecular weight [g/mol]

DP	Transmembrane pressure drop across the membrane [Pa]
p	Gel permeability [m $Pa^{-1}s^{-1}$]
Q_F	Volumetric feed stream flow rate [m^3/s]
Q_P	Volumetric permeate stream flow rate [m^3/s]
Q_R	Volumetric retentate stream flow rate [m^3/s]
R	Observed retention of the membrane [%]
r_a	Adsorptive resistance determined in accordance with FLR principle [m^{-1}]
R_a	Resistance added by adsorption of the solute on the membrane Rd [m^{-1}]
r_{cp}	Resistance due to concentration polarization determined in accordance with FLR principle [m^{-1}]
R_{cp}	Resistance added concentration polarization about the membrane [m^{-1}]
r_d	Depositional resistance determine in accordance with FLR principle [m^{-1}]
R_d	Resistance due to the deposition in pores and on the surface of the membrane [m^{-1}]
Re	Reynolds number, $Re = d_h v r/h$ [-]
R_f	Resistance added by the fouling the membrane [m^{-1}]
R_g	Radius of gyration of a macromolecule [m]
R_h	Hydrodynamic radius of a macromolecule [m]
R_{int}	Intrinsic (actual) retention of the membrane [%]
R_m	Intrinsic membrane resistance [m^{-1}]
R_p	Resistance added by the pore plugging [m^{-1}]
R_t	Overall resistance [m^{-1}]
S	Macromolecules strand contact area [m^2]
Sc	Schmidt number, $Sc = h/(rD)$ [-]
Sh	Sherwood number, $Sh = kd_h/D$ [-]
T	Temperature [^oC]
v	Cross flow velocity [m s^{-1}]
V_2	Molar volume of a solvent [m^3/mol]
V_M	Molar volume of a macromolecule [m^3/mol]
z	The number of segments of a starch molecule [mol^{-1}]

Greek

c_{12}	Flory-Huggins interaction parameter [-]
d	Concentration boundary layer thickness [m]

f	Volume fraction of macromolecules in the solution, deposit or gel [-]
γ_i	Surface tension of species I [N/m]
γ_i^{AB}	Polar component of surface tension of species i [N/m]
γ_i^{LW}	Apolar component of surface tension of species i [N/m]
γ_i^+ -	Electron acceptor species i of surface property parameter [N/m]
γ_i^-	Electron donor species i of surface property parameter [N/m]
λ	Characteristic correlation length [m]
η	Viscosity of a solution [Pa s]
η_o	Viscosity of a solvent [Pa s]
η_{sp}	Specific viscosity of a solution [-]
$[\eta]$	Intrinsic viscosity [$m^3 g^{-1}$]
p	Osmotic pressure [Pa]
Δp	Osmotic pressure difference across the membrane [Pa]
ρ	Density of the solution [kg/m^3]
s	Reflection coefficient of the solute across the membrane [-]

Constants

N_A	Avogadro's number, N_A = 6.023 x 10^{23} [-]
R_G	Universal gas constant, R_G = 8.314 [J K^{-1} mol^{-1}]
k_B	Boltzman's constant, k_B = 1.38 x 10^{-23} [J/K]
π	Circle constant, π = 3.1416 [-]

Chapter 1

Introduction

In this thesis, we have studied the fouling mechanisms involved in ultrafiltration of degraded starch solution, the effect of the operating conditions and different models that can be used to predict the performance of ultrafiltration of degraded starch solution. The study was meant to simulate ultrafiltration of desizing wastewater from textile industries, which contains degraded starch. Desizing is washing of the sizing agent, in our case starch, used for sizing (coating) yarn to improve abrasion resistance during the weaving process. This chapter introduces the use of starch as sizing agent and its effect on the environment and the role ultrafiltration processes could play to improve the environmental impact of starch in the wastewater and in rendering an economic advantage to the industry.

1.1. Motivation

1.1.1. Starch as sizing agent and its effect on the environment

Starch has been the most commonly used sizing agent in the textile industry. Especially, where cotton fibers are used as a raw material, it is the most conventional sizing agent for its good sizing properties and low cost. In the future, it is expected to remain the dominant sizing agent provided the demand for natural fibers like cotton increases [Buckley et al., 1982; Radley, 1976].

On the other hand, starch is responsible for 50- 80 % of the Chemical Oxygen Demand (COD) in the effluents of textile finishing industries where starch is used as sizing agent [UNEP, 1994; Cooper, 1978; Snowden-Swan, 1995, Buckley et al., 1982, Opwis et al, 1999]. In the light of the present global environmental concern, the textile industry has started to pay attention to reduce its contribution to the environmental damage. Unlike

synthetic sizes, the desized starch in wastewater is unstable due to the enzyme bath used to break down the starch before washing so that it can be easily washed when flushed with hot water (about 90°C).

When pure synthetic sizes are used as sizing agents, the sizes are stable in the wastewater. This makes it attractive in the light of environmental concern since synthetic sizes can be recovered and the hot water used for washing can be recycled by using membrane processes [Porter, 1998]. However, besides a large cost difference, a complete substitution of synthetic size for the starch is not possible, because they do not have good enough sizing properties for cotton/synthetic fiber blends, 100% cotton and some other natural fibers [Radley, 1976].

In order to get starch that can be recovered, different modified starches have been tested. Bayazeed & Trauter (1991, 1 & 2) evaluated the sizing performance of chemically modified potato starches and the effect of series of ultrafiltration. They found that the starch loses some of its sizing performance due to degradation during ultrafiltration. On the other hand, Elgal et al. (1979) examined the sizing performance of starch modified by fermentation and enzyme (partially degraded starch). They used the starch at new sizing conditions (different from conventional sizing conditions). The partially degraded starches had a significant amount of chains with less than 40 glucose units but were dominated by much larger starch molecules (i.e. an average molar mass larger than 8000 g/mol). Degraded starches prepared by both methods gave very good sizing performance and had an encouraging advantage over the native starch. They could be washed away at much lower temperature without any use of enzyme. For details see Elgal et al. (1979). In such a case, since the degraded starch in the wastewater is stable, it may be concentrated as the synthetic sizing agent. The concentrated degraded starch solution could be stored for several weeks or dried to be stored for later use [Elgal et el., 1979]. Moreover, the concentrate can be used as substrate in fermentation to produce alcohol or used to generate energy in the plant. Thus, this process would give the industry an economic and environment friendly starch based sizing agent.

1.1.2. Ultrafiltration of degraded starch

There are some articles that discuss membrane filtration of starch. In Ousman & Bennasar (1995), microfiltration of a starch grain suspension was studied using inorganic tubular membrane at 50°C. They found that much of

the flux decline was caused by deposition of grains of starch. Gaddis et al. (1999) studied gelatinized starch suspensions using tubular inorganic membrane in the ultrafiltration range at 60°C. The major cause for flux decline was the fouling of the membrane surface by a gelatinized starch layer. The gel layer was observed to be compressible and might be a limiting phenomenon. Gomez-Gotor et al. (1996) studied the behavior of reagent grade soluble starch solution at ambient temperature using flat sheet polymeric membrane with a molecular weight cut off 20000 g/mol. They assumed the starch have molecular sizes that range from 100 to 300 glucose units. The membrane gave a retention of 95%. Of the three, the flux from ultrafiltration of gelatinized starch solution was the least. For example, for 1 wt % solution, it is about 21.6 l/(m^2h) at about 2 bar transmembrane pressure drop and 4.6 m/s cross flow velocity. Yet, this flux is larger than the flux obtained from ultrafiltration of PVA (polyvinyl alcohol) solution [Gaddis, 1999; Groves et al., 1978; Porter, 1998]. PVA is one of the synthetic-sizing agents that have been recovered by ultrafiltration from textile desizing wastewater. On the other hand, Chen et al. (1997) treated wastewater containing sizing agent that was largely starch degraded by the enzyme using nanofiltration. The nanofiltration membrane had nominal rejections of 50% for NaCl and 98% for lactose. The separation efficiency of the membrane was about 95%. The permeate flux was from 10 – 15 l/(m^2h) at transmembrane pressure of 2 bar, temperature of 35°C for desizing wastewater with COD of 5340 mg/l at pH 5.5 and 13820 mg/l at pH 10.2. The fouling was negligible, which was attributed to the presence of enzyme in the wastewater that had a cleaning effect.

In the light of the above discussions, one can presume that adsorption, concentration polarization, gel formation and deposition will affect to some extent the overall performance of the ultrafiltration of partially degraded starch solution. However, since partially degraded starch has a broad molar mass and size distributions, different composition and environment from the starch treated in the reviews, the contribution of the fouling mechanisms on the membrane performance may be different. In order to design ultrafiltration process plants for concentrating the degraded starch solution, understanding the behavior of the partially degraded starch solution, the knowledge of the contribution of each of the fouling mechanisms and their dependence on the operating conditions and membrane materials will be helpful.

1.2. Objective of the thesis

The theme for this study is to uncover the fouling mechanism that limits the performance of ultrafiltration of degraded starch solution for the selected membranes, feasible range of operating pressure and cross flow velocity and to evaluate the model that can be used for the prediction of the performance. In addition, we investigate the development of the rejection and retention of the membrane and the permeate flux as the solution is concentrated. The study is based on model solutions prepared by enzymatic degradation of potato starch (chosen for its wide use throughout the whole world except USA), hoping that it would be comparable to actual desizing wastewater containing degraded but stable starch. First, the model starch solution is prepared and checked for reproducibility for several levels of degradation. Then three model solutions with different molar mass distribution and average molar mass are chosen, and prepared throughout the experiments, according to the experimental study designed for ultrafiltration of degraded starch in solution. The experiments are designed to meet the following objectives:

- Evaluation of the contribution of the fouling mechanisms to the permeate flux decline and their variation with operating variables.
- The rejection and separation efficiency of the membrane as the selected degraded starch solution is concentrated.
- Effect of operating variables on the permeate flux and solute retention of the membrane.
- Selecting and/or modifying models in order to better account for the most fouling mechanisms.

1.3. Outline of the thesis

The thesis is written in the form of a monograph, with a list of abbreviations and symbols, common references and appendix. The main chapters are as follows:

Chapter 2 gives a literature survey on the characteristics of starch and partially degraded potato starch solutions with a brief introduction to the structural unit making all starch molecules.

Chapter 3 reviews ultrafiltration fouling mechanisms and models developed to account for the effect of the mechanisms with the introduction to the membrane filtration at the start of the chapter.

Chapter 4 presents experimental setup, the procedure used for preparation of feed solution, ultrafiltration experiment and analysis.

Chapter 5 presents the results and discussion on the contribution of the flux decline mechanisms, retention and flux profile variations with operating parameters, fits of flux data by selected models and the characteristics of rejection of the membrane as the solution is concentrated.

Chapter 6 gives overall conclusions of the thesis and recommendations for the future work.

URN:NBN:no-3327

Chapter 2

Characteristics of potato starch solution

2.1. Introduction

Potato is one of the sources of starch. Other sources of starch include corn, wheat, tapioca and rice. All starches are found tightly and radially packed into hydrated granules with about at least one water molecule per glucose unit making up the starch. The shape and the size of the granules depend on the sources of the starch. The major components that make up starch granules are two macromolecules: amylopectin and amylose. Amylopectin is responsible for the shape of the granule while amylose is mostly found as free molecules. This can be seen in Figure 2.1. In native potato starch, the granule size ranges from 10 to 100 μm in diameter [Snyder, 1984], its composition is 23 % amylose and 77 % amylopectin [Blanshard, 1987]. Potato starch has the largest amylopectin and amylose molecules when they are compared to other sources. This makes the solution of starch more viscous. But when it is subjected to shearing, the large molecules will break down and the viscosity of the solution will drop sharply. In addition, potato amylopectin has phosphate groups, which may increase its hydrophilicity. The starch granules also contain very small amounts of lipids and protein, i.e. about 0.1 % (w/w) [Swinkles, 1985], which does not have a significant influence on the properties of the starch.

In ultrafiltration of partially degraded potato starch, the knowledge of the solubility, conformation and size, osmotic pressure, adsorptive properties on the membrane surface, viscosity and diffusion coefficient is important. These properties depend on the degree of degradation, concentration, composition, molar mass distribution and conformation of the starch, temperature and the pH of the solution. Therefore, in the following sections, we will present an overview of (1) the structural units making the starch macromolecules, (2) the degradation mechanisms and the molar mass distribution of the degraded starch, and (3) the limited thermodynamic and hydrodynamic properties of starch, in particular for degraded ones. At last,

we will choose the degradation method that will be used for preparing the model solution for ultrafiltration experiments.

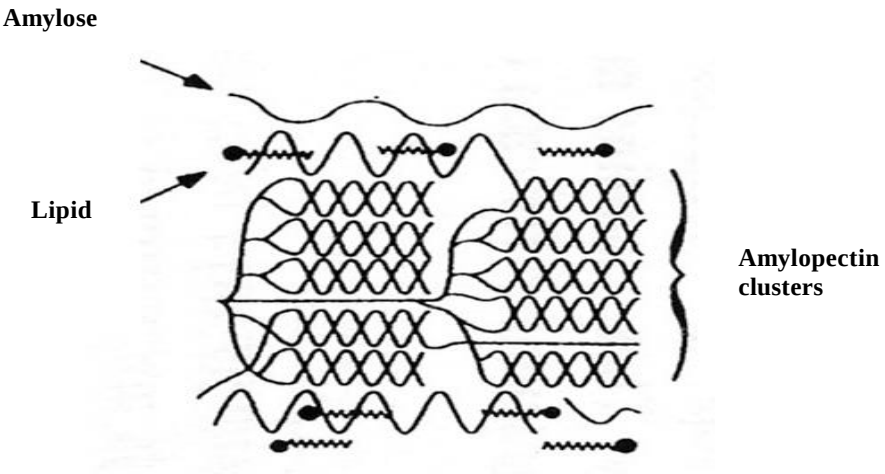

Figure 2.1. Schematic arrangement of amylopectin clusters that make up the starch granule.

2.2. Structural unit

Amylose is a linear polymer made of *a* -D-glucose units in the $^4C_1$ conformation, i.e. linear α-1,4-linkages with an average of hundreds to thousands D-glucose units connected. It can form an extended shape (hydrodynamic radius 7-22 nm) [Parker and Ring, 2001] but generally tends to wind up into a rather stiff helix due to a hydrogen bond between O3 and O2 oxygen atoms of sequential glucose units [Guilbot and Mercier, 1985]. Figure 2.2 shows the repeating unit that makes up amylose macromolecules. The macromolecules have hydroxyl group at O2 and O6 atoms on the outside surface of the helix; only the ring oxygen on the glucose molecules is pointing inwards. Thus, a single helix amylose possesses a relatively hydrophobic inner surface holding a spiral of water molecules that are relatively easily replaced by hydrophobic lipid or aroma molecules. The hydroxyl group on the outer surface of the helices form hydrogen bonding between aligned chains, and causes retrogradation and releases some of the bound water. The aligned chains may then form crystallites, which are resistant to even degradation by α-amylase.

Amylopectin is formed by non-random α-1,6-linkages branching of the amylose-type α-1,4-D-glucose structure. This branching is determined by branching enzymes, which leave each chain with up to 20-25 glucose units [Guilbot & Mercier, 1985]. See Figure 2.3. The figure shows a schematic representation of the branching point. In reality, the amylopectin molecules are oriented radially and as the radius increases so does the number of branches required to fill up the space, with the consequent formation of concentric regions of alternating amorphous and crystalline structure. Each molecule contains up to two million glucose units in a compact structure with a hydrodynamic radius of 21-75nm [Parker and Ring, 2001].

Amylose and amylopectin molecules are inherently incompatible molecules [Kalichevsky & Ring, 1987]. Amylose has a lower molar mass (MW 10^5-10^6 g/mol) with a relatively extended shape whereas amylopectin has a huge molar mass (larger than MW=10^7 g/mol) but compact molecular structure. As said earlier, the chain of both molecules tends to assume a helical conformation, which is relatively stiff and may present contiguous hydrophobic surfaces. However, the interaction of amylopectin molecules interact with each other and even with amylose is limited by steric effects.

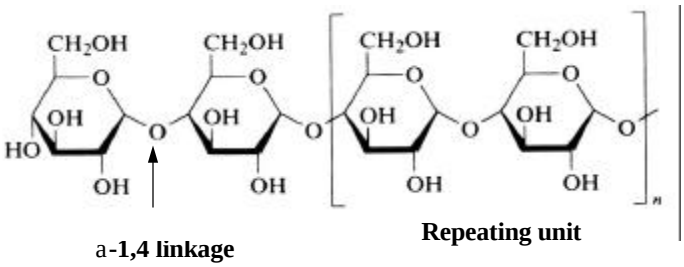

Figure 2.2. Schematic representation of a short amylose molecule that shows α-1,4-linkages and repeating units [Manners, 1989].

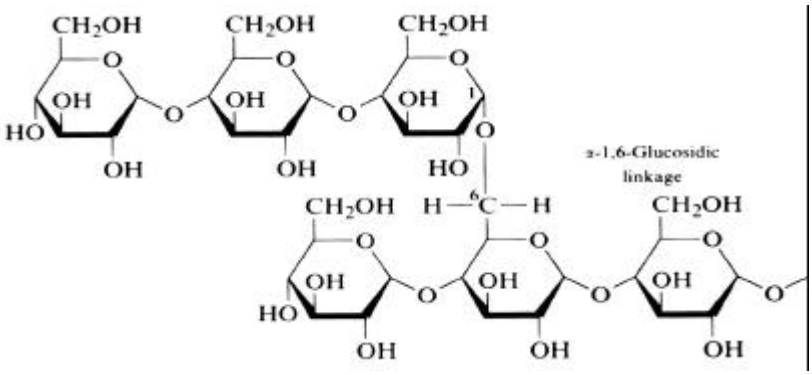

Figure 2.3. Schematic representation of an amylopectin molecule with a branch point at α-1,6-position.

2.3. Degraded potato starch and its molar mass distribution

Starch is commonly modified in order to give it the properties that are required when it is used in the industries. One of the modification methods is degradation of the large starch macromolecules. In the degradation, the solubility and hydrophilicity of the starch increases and the viscosity of the starch solution decreases.

The degradation can be accomplished by three different methods: physical, chemical and enzymatic methods. The common commercially produced modified starch is a partially degraded starch called lintnerized starch and soluble zulkowski starch. Lintnerized starch is produced by a prolonged treatment of native starch granules with hydrochloric acid for a period of up to 40 days at room temperature. Zulkowski starch is produced when native starch is hydrolyzed with glycerol at elevated temperature (190°C). The molar mass distributions of these starches are given in Figure 2.4. The figure shows that native potato starch solution and the lintnerized starch solution have bimodal distributions. This is due to the break down of the linkage of amylopectin molecules by acid and shearing in clusters as seen in Figure 2.6 [Heitmann et al., 1997]. According to the figure, the soluble starch has an average molar mass of about 30 DP, 4860 g/mol, while lintnerized starch is

about 500 DP, 81000 g/mol, where DP is the degree of polymerization. For details see Heitmann et al. (1997).

The enzymatic hydrolysis is used when fast degradation is required. The common enzyme used for hydrolysis of starch is α-amylase. The process is usually used to produce oligosaccharides with a few numbers of degrees of polymerization [Blanchard and Katz, 1995]. But, limited degradation could also be made to use as a sizing agent in textile by Elgal et el. (1979). The degree of enzymatic degradation depends on the source of α-amylase, its concentration, pH of the medium, its temperature, the mixing efficiency and degradation time [Marchal et al., 1999]. The degradation can be stopped when the required degree of degradation is achieved by heating to 100°C. By increasing the pH above 12 to inactivate the enzyme, the degradation can also be controlled.

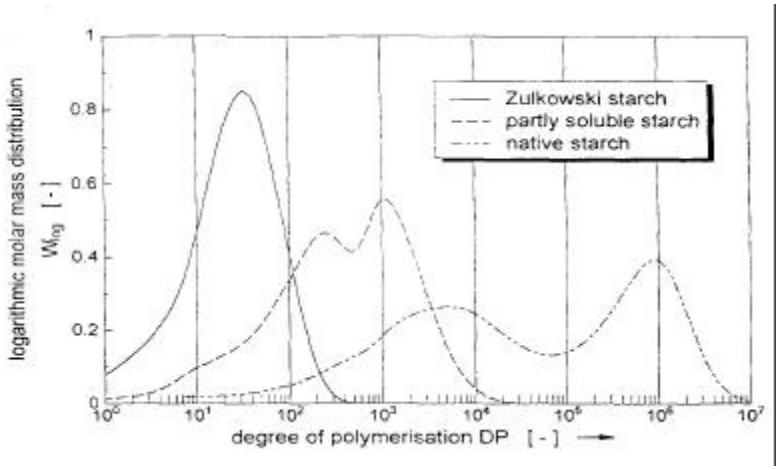

Figure 2.4. The molar mass distribution of native starch and the soluble starches [reproduced from Heitmann et al., 1997]

Heitmann et al. (1997) studied the degradation characteristics and the molar mass distributions of native potato starch degraded by α-amylase from B. subtilis. The plot in Figure 2.5 is reproduced here from their work. During the first stage of the α-amylolitic process, the fraction of higher molar mass is preferentially attacked. For amylopectin molecules, predominately, the external α-1, 4 linkages out side the cluster regions rather than the internal bonds are cleaved due to reactivity of long chains connecting the clusters compared to the internal bonds of the clusters, see Figure 2.6a. The

presence of clusters (branched fragment of amylopectin) gives the degraded starch the bimodal distribution. Figure 2.6c and Figure 2.6d show the cluster and fragments from amylopectin. If further enzymatic action is allowed the clusters will disappear and the formation of maltosaccharides increases. Heitmann et al. (1997) also showed how the time required to achieve a given degree of degradation could be reduced drastically by increasing the concentration of the enzyme.

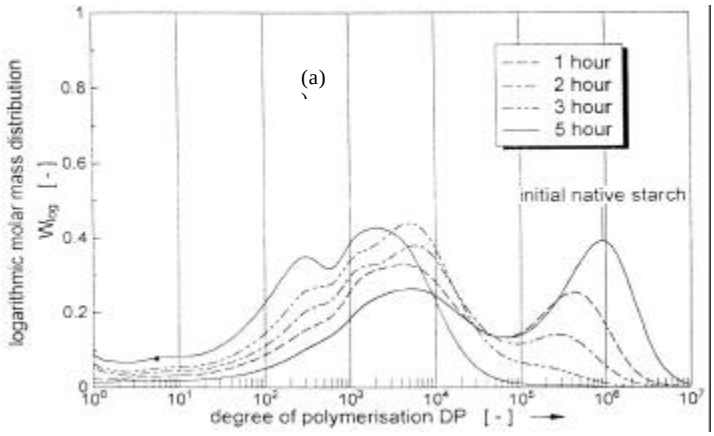

Figure 2.5: Course of enzymatic hydrolysis of native potato starch with 0.14 mg/l α -amylase concentration [reproduced from Heitmann et al., 1997].

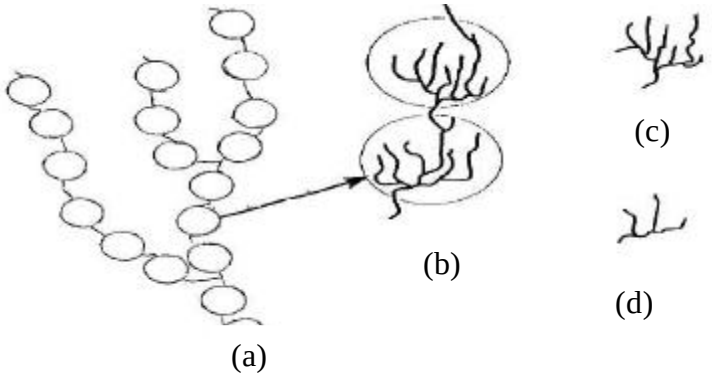

Figure 2.6. Schematic representation of the steps of degradation of a native amylopectin molecule: (a) amylopectin, (b) amylopectin fragment, (c) partially soluble starch and (d) Zulkowiski starch [reproduced from Heitmann et al., 1997].

The molar mass distribution of the degraded starch through the action of enzyme resembles that of lintnerized starch shown in Figure 2.5 at 5 hours degradation. When the degradation is run with larger amounts of enzyme and for longer time, the enzymatic methods gives degraded starch that has a molar mass distribution somehow similar to that of zulkowski starch [Heitmann et al., 1997].

The average molar mass of the degraded starch used as sizing byElgal et al. (1979) seemed to be much larger than thezulkowski starch and in the range of lintnerized starch. In addition, the preparation of both types of starches, zulkowski and lintnerized, is relatively difficult to control and takes a longer time than the enzymatic degradation method, which is simple and gives the possibility of degradation in a few minutes/hours in the laboratory. Therefore, we chose enzymatic degradation methods for the preparation of the model solution that was used in the study of ultrafiltration of degraded starch solution.

2.4. Solubility behavior of starch components

As discussed in section 2.1, the starch molecules are built from glucose units that three free hydroxyl groups. This makes the starch molecules hydrophilic [Swinkels, 1985]. However, the solubility of the molecules depends on the conformation of the molecules. When they have the conformation that help them to easily align, they are attracted to each other and release the water molecules bound to them for the thermodynamic reason discussed in section 2.5 and form strong hydrogen bonds. In the solid state, the chains are aligned and there is no significant bound water layer between the molecules. Hence, the hydrogen bond between the starch molecules is very strong. In order to dissolve the starch molecules, this bond must be broken by heating the suspension of the starch granules up to 60 to 70°C [German et al., 1992]. On cooling, amylose molecules aggregate (retrograde), while the amylopectin remains in solution due to steric effects. This means that amylose has less affinity to water than amylopectin due to its conformation in the aqueous solution.

The conformation of amylose varies with molar mass and so its association (retrogradation). For a DP up to 45, the retrogradation rate of the starch in the solution is negligible. As the molar mass increases the retrogradation

becomes visible. It has a maximum between DP 75 to 80 [Pfannemüller, 1971; Pfannemüller & Ziegast, 1981]. This could be a result of the interaction between the effect of an increase of molar mass and helicity have on the solubility of the starch. The helix conformation gives the molecules the structure that makes the alignment between the molecules easier so that the hydroxyl groups on the surface of the helices could form strong hydrogen bond [Swinkels, 1985]. This reduces the solubility of the starch, but its effect decrease, as the molar mass of the amylose is increased [see Section 2.4.1]. On the other hand, the solubility of the aymlose decreases as its molar mass is increased as a result of an increase of the interaction between the segments of the molecule. Pfannemüller (1971) also observed that the presence of a small amount of amylose molecules with higher molar mass decreases the retrogradation tendency of the solution. Because larger molecules are hardly involved with the process of association of the short chains and visa-versa. Rather, they could have a stabilizing effect, inhibiting the nucleation process. The presence of amylopectin, branched molecules, also reduces the retrogradation rate. For heterogeneous starch molecules, maximum retrogradation is observed to be around DP 350 – 460 [Pfannemüller, 1971]. Thus, the heterogeneity of the molecular size increases the DP at which retrogradation starts. The retrogradation is concentration dependent, and there may not be retrogradation if the concentration is very low.

Increasing the temperature and agitation, and using extreme pH increase the solubility of starch molecules. Because, they change the conformation of the molecules to the more water accessible ones [Sun, 1994]. When the temperature decreases or pH is brought to neutral, the starch molecules undergo retrogradation. This is observed by a gradual change of the colorless solution to a cloudy suspension of insoluble white precipitates. When it is heated and mixed the suspension may disappear and become a clear solution.

2.4.1. Conformation of starch molecules in solution

In a solution, the starch polymers have flexible chemical bonds [Sun, 1994]. The linear segment of the starch molecules assumes different configurations depending on the size of chain. For instance, depending on the bond strength and flexibility of the chain, in aqueous solution amylose could have one of the configurations shown in Figure 2.7 [Banks & Greenwood, 1975; Sun, 1994]. In some literatures [Pfannemüller, 1971], amylose was reported to have an ordered structure with a helical sequence of 10 – 15 turns without

interruption forming a rod like shape. They also observed that as the amylose chain length grows the helix structure becomes flexible and is interrupted. In some cases, amylose was found to behave a random flexible coil without a significant helical content [Banks & Greenwood, 1968]. This difference could be attributed to the variation of amylose-water interaction from species to species and the solvent characteristics from experiment to experiment. As the affinity of the amylose and the solvent increases, it becomes more flexible and acts as a random coil [Rogeret al., 1999]. In neutral aqueous solution, the worm-like helix (random coil of helix or broken helix) model is found to approximate the conformation of the amylose in solution [Pfannemüller, 1971].

(a) (b) (c) (d)

Figure 2.7. a) Rigid rod-like helix, b) flexible helical coil, c) random coil and d) worm-like coil

For amylopectin, since each branched chain is short (DP is 20 to 25), it is highly probable that each chain retains the helical shape. As the density of branching increases, the helical chain could be stiff and extended due to steric effects [French, 1984]. In dilute solution, the branch chains spread in the aqueous solution. In a two-dimensional view, their conformation can be approximated by the structure shown in Figure 2.8 [Thurn and Burchard, 1985].

In a flowing stream, studies suggest that amylose behaves as a non-free draining coil [Ring et al., 1985]. The coil is said to be a non-free draining coil when the water encompassed by the coil moves with the coil. The amylopectin molecule can also be assumed to have same property in flowing stream.

For degraded starch, the conformational behavior depends on the molar mass distribution and the composition of branched and linear starch molecules in the solution. We have never come across any literature that discussed how the starch molecules behaves in this kind of solution. From

section 2.2 and 2.3, we know that branched starch molecules dominate a native potato starch. As the starch is degraded, the starch molecules get more linear. Thus, we may assume that as the starch is degraded the conformation of the starch in the solution resembles more the conformation of the linear polymer.

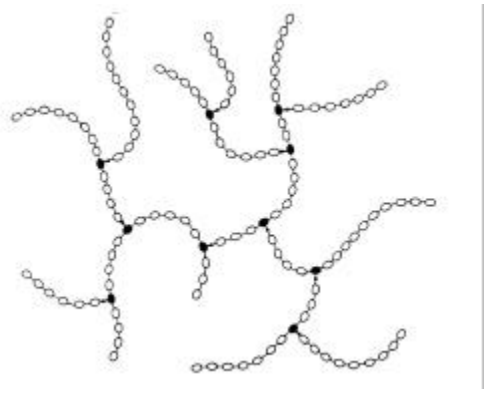

Figure 2.8. Schematic conformation of an amylopectin cluster molecule in solution [Thurn and Burchard, 1985].

2.4.2. The size of starch molecules

The size of starch molecules in solution is usually given as a radius of gyration, R_g. The radius of gyration depends on the conformation of the molecule. Sun (1994) reported R_g calculated theoretically for three different conformations for a polyethylene chain of 5000 DP. The conformations were an unperturbed random-coil, a rod like (a hypothetical helical form in which all the bonds are trans-configuration) and a globular. The radius of gyration calculated is given in Table 2.1 for comparison. The table shows that the random and compact coil conformations give the macromolecules very much smaller size than the rigid rod conformation.

For the two components of the starch, Aberle et al. (1994) also measured the R_g. They found around 220 nm for native amylopectin with a molar mass of $6.0 \times 10^7 - 11.0 \times 10^7$ g/mol), and 19 to 60 nm for native amylose with molar mass from 2.1×10^6 to 2.0×10^7 g/mol. From this, one can presume that the amylose had some kind of flexible coil conformation in static dilute solution so that its radius of gyration was measured to be very small. When amylopectin and amylose have the same molar mass, the radius of gyration of amylopectin and amylose may be comparable, even amylopectin could be smaller depending on the conformation and branching density.

Table 2.1. Radii of gyration of random-coil, rod-like and globular configurations calculated theoretically for a polyethylene chain of 5000 DP assuming the carbon bond length to be 0.11 nm, the excluded volume of the ethylene unit to be 0.023 nm^3 and the characteristic ratio of the random coil to be 6.7.

Structure	Radius of gyration (nm)
Random coil	8.2
Rigid rod	130.0
Compact coil	2.3

For degraded starch, however, the size of the starch molecules in the solution will be the average of the two components. Galinsky and Burchard (1995) determined the radius of gyration as a function of average molar mass using acid degraded potato starch, see Figure 2.9. In range given in the figure, we can guess that the configuration of the molecules is dominated by the average of flexible coils and granule molecules. Thus, the size of the molecule to the lower molar mass region depends on the conformation and composition of the linear component of the starch, which may have different conformation depending of its molar mass. If it is flexible, we expect a similar trend. As discussed in Section 2.4.1, if there is a range of molar mass where helical conformation is preferred, the trend may be different.

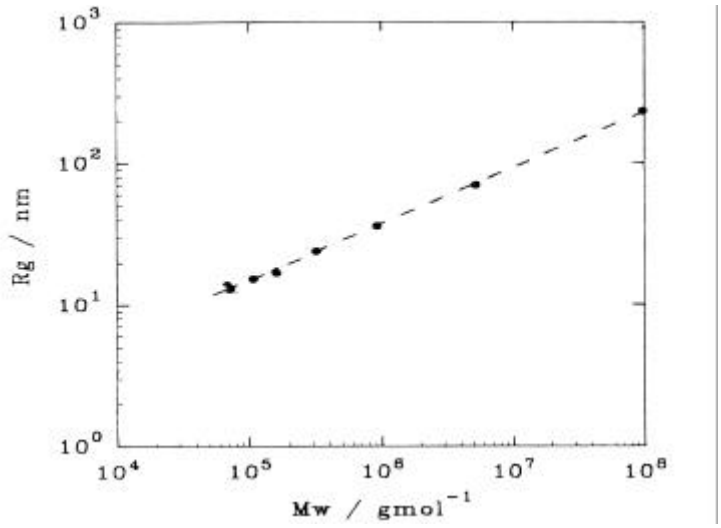

Figure 2.9. Radius of gyration, R_g, as function of average molar mass [reproduced from Galinsky and Burchard, 1995].

2.4.3. Chain crossover and chain entanglement

In dilute solution, the individual molecules behave independently. When a certain concentration C_i^* [1] is exceeded the molecules lose independence and a marked change in the behavior of the solution is observed. This concentration is still relatively low and the solution is certainly to be considered as dilute. However, C_i^* represents a change between two dilute solution regimes of remarkably different behavior. This concentration is referred to as semi-dilute in order to distinguish it from the highly concentrated one. At this concentration, the segments of the chains start to overlap. As the overlap concentration C^* [2] increases beyond C_i^*, the solution properties change drastically.

In the case of a linear polymer, the coils interpenetrate each other and form a transient network of entangled chains. At the overlap concentration, the polymers cannot any longer be distinguished from each other due to entanglement. The process of formation of long chain entanglement as the concentration is increased is illustrated in Figure 2.10. When the concentration is very high and the mesh of the network has a size comparable to the monomer, the bond will not be stable and the chain will collapse, see Figure 2.10d. This state is said to be a collapsed state. At this stage, the properties of the solution are dependentonly on the concentration of the solute (i.e. independent of the molar mass).

For branched amylopectin, the picture of chain overlap may be problematic. However, the outer chains of the branch can still penetrate each other in a manner similar to that of linear chains [Galinsky and Burchard, 1996]. Interpenetrating is limited due to segment overcrowding near the center of the star (branching point). This depends on the chain length of the branch. The shorter the chain length, the lesser the interpenetrating and entanglement will be.

For starch solutions, where both amylose and amylopectin are involved, the average semi-dilute behavior of the two components is expected [Aberle and Burchard, 1997, Aberle et al., 1997]. Thus, the composition and the degree of degradation will affect the semi-dilute concentration and behavior

[1] C_i^* - the concentration at which the semi-dilute regime starts.
[2] C^* - any concentration in the semi-dilute concentration regime.

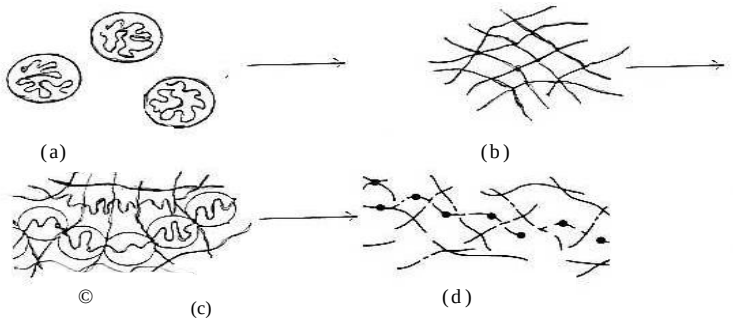

Figure 2.10. (a) Dilute solution region where an individual polymer chain is considered as confined in a blob of radius ξ, (b) semi-dilute region where many chains interpenetrate into each other to form a mesh with size ξ, (c) semi-dilute with somehow higher concentration C^* where the same individual chain is now in the form of a succession of subchains or a sequence of blobs of radius ξ, (d) collapsed state where chains are broken due to high stress on the bonds as a result of a very high concentration of starch in a given volume [Sun, 1994].

The semi-dilute concentration C^* represent the average segmental concentration of individual coils of macromolecules in the solution. Thus, the concentration is determined by the mass of the macromolecule and the volume that it occupies in the solution. The overlap concentration can be expressed as

$$C^* = \frac{M_W}{N_A V_M} \qquad 2.1$$

where M_W is the molar mass of the macromolecules, V_M is their volume and N_A is Avogadro's number. The value of C^* depends on the methods used to determine the volume. It can be determined using Equation 2.2 [Utracki and Simha., 1963], where the hydrodynamic properties of semi-dilute solution are of interest.

$$C_h^* \equiv \frac{1}{[h]} \qquad 2.2$$

where [η] is the intrinsic viscosity of the starch solution, see Section 2.7.

On the other hand, when static properties of the semi-dilute solution and thermodynamic interactions between two particles in semi-dilute solution are of interest, Equation 2.3 can be used [Yamakawa, 1971; Burchard, 1990].

$$C_{A_2}^{*} \equiv \frac{1}{[A_2 M_W]} \qquad 2.3$$

where A_2 is the second virial coefficient, see Section 2.6.

For acid degraded potato starch, Galinsky and Burchard (1996) have also determined, the relation between C_i* and molar mass based on different physical measurements, including viscosity and second virial coefficient measurement. They calculated C_i* from viscosity and the second virial coefficient, see Figure 2.11.

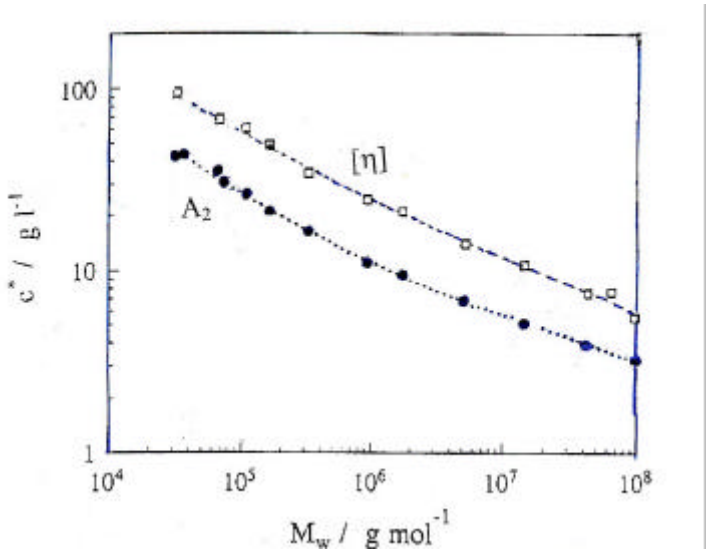

Figure 2.11. Relation between C_i* and average molar mass for acid hydrolyzed potato starch [reproduced from Galinsky and Burchard, 1996].

2.5. Adsorption of starch polymers in solution on membranes

Starch is composed of neutral polymers that are known to have strong adsorption properties on the surfaces and it has been used as flocculent and sizing agent. From a thermodynamic point of view, there are two phenomena that are responsible for their adsorption on solid surfaces. One

reason is the entropy that is gained when solvent molecules are released from the surface into the solution. When a solvent molecule is released from the surface into the solution, each solvent molecule gains three degrees of freedom, i.e. the solvent molecule can move freely in three-dimensional space. Thus, there is always an entropic force favoring the adsorption of polymers. If the solute is intensely hydrophilic, the adsorption could be small. However, as the molar mass and hydrophobicity of the macromolecule increase, the adsorption will increase due to a decrease in the solubility of the macromolecules. For hydrophobic polymers in aqueous solution, the interaction energy between the polymer segments and the solvent molecules are unfavorable compared to the interaction between segment-segment and solvent-solvent interactions [Jönsson, 1998].

Zydney (1996) also discussed the adsorption of macromolecules on hydrophobic membrane surfaces. He formulated the thermodynamic driving force in terms of Gibbs free energy. When the solute is in solution, the surface of both the solute and the membrane are in intimate contact with the solvent, water. The degree of interaction between the macromolecules and the membrane is measured by the Gibbs free energy of water in the proximity of the membrane surface. For a hydrophobic membrane, there is no attractive interaction. Thus, the water layer adjacent to the surface has a higher Gibbs free energy than the bulk water. This condition favors highly adsorption of the macromolecules and the escape of water from the surface between the macromolecules, and the macromolecules and the membrane reduces the total Gibbs free energy of the system. This effect is more pronounced when both the solute and the solid surface are hydrophobic.

Polymer adsorption isotherms have a sharp adsorption profile at very low polymer concentrations followed by a plateau, no change in the amount adsorbed with polymer concentration. This is on the basis of the assumption that the adsorbed solute is the solute attached to the solid surface as a result of the physico-chemical interaction between the solute and the solid surface. Adsorption rate increases with hydrophobicity and molar mass or as the attraction between the solid surface and the polymer is increased. An increase in the hydrophobicity of the macromolecules also increases the association and precipitation the macromolecules in aqueous solution, which gives additional loose adsorption layer. The effect of molar mass depends on the conformation of the polymer and the strength of the interaction between the solid and the polymer. When the macromolecules have a stretched conformation and strong attraction to the solid surface, the surface can be saturated by smaller amounts of the macromolecules [Jönssonet al., 1998]. The constant adsorption at the higher polymer concentrations is due to the

fact that the surface is saturated with the polymer. The adsorption is affected by the aqueous solution properties, the ionic strength and pH, depending on their effect on the surface and polymer properties. For instance, if the polymer solubility could decrease on addition of salt and as the pH is changed, adsorption increases.

As far as our knowledge is concerned, no literature is available on starch adsorption on membranes or any solid surface in aqueous solution, in particular. However, in the light of what is discussed herein, one can presume that amylose would have much higher tendency to be adsorbed on the membrane surface because of its tendency to re-associate and precipitate when the concentration of the starch solution is above semi-dilute concentration. The size of the amylose may also be important since the association tendency of the molecule depends on it. On the other hand, amylopectin is expected to have low adsorption because of its tendency to stay in solution. Thus, the starch, which is composed of the two components, may have an average adsorption property of the two. For degraded starch, its adsorption property will also depend on its degree of degradation. The more linear segments the degraded starch is composed of, the higher may be its adsorption. However, it is worth remembering that the association of degraded starch is maximum at DP 350 [Pfannemüller, 1971], that may also affect the adsorption pattern.

2.6. Osmotic pressure of starch solutions

2.6.1. Models used for osmotic pressure prediction

Osmotic pressure π in a dilute starch solution can be calculated fromvan't Hoff's equation:

$$\frac{p}{C} = \frac{R_G T}{M_W} \qquad 2.4$$

where R_G is the universal gas constant, T is temperature, M_W is molar mass and C is concentration. Since the deviation from an ideal solution is pronounced at higher concentration, this should be accounted for by modifying the van't Hoff's equation. One of the equations used for this purpose is the virial equation:

$$\frac{p}{C} = \frac{R_G T}{M_W}\left(1 + A_2 C + A_3 C^2 + \cdots\right) \qquad 2.5$$

where A_n is the n^{th} virial coefficient. These coefficients are functions of molar mass distributions of the solute, solute-solvent interaction, and temperature. According to this equation, the osmotic pressure increases with an increase in concentration.

For the degraded starch, Galinsky and Burchard (1995) determined the second virial coefficient A_2 as shown in Figure 2.12. The third virial coefficients A_3 are related to the second one [Burchard, 1990] and given as:

$$A_3 M_W C^2 = g_A (A_2 M_W C)^2 \qquad 2.6$$

where the coefficient g_A is structure dependent. For potato starch, Burchard (1990) found g_A = 0.18, which gives good fitting. The virial equation can be a good approximation of the osmotic pressure until the onset of phase separation, at semi-dilute concentration [Galinsky and Burchard, 1996].

Another common approach for the estimation of the osmotic pressure of the macromolecular solution is the relation developed based on the Flory-Huggins theory [Hermans, 1949]. This is given by the following equation:

$$p = RTC\left[\frac{1}{M_W} + V_2\left(\frac{z}{M_W}\right)^2 (0.5 - c_{12})C + V_2^2\left(\frac{z}{M_W}\right)^3 \frac{C^2}{3} + \cdots\right] \qquad 2.7$$

where V_2 is the molar volume of the solvent, z is the number of the segment in starch molecules with molecular weight M_W and c_{12} is the Flory-Huggins interaction parameter. A segment is approximately equal in size and shape to a single molecule of the solvent [Hermans, 1949]. The number z is commonly determined experimentally from the ratio between the molar volume of the solute to that of the solvent. The z can be also approximated by the following relation:

$$z = \left(\frac{M_W(solute)}{M_W(solvent)}\right)\left(\frac{r_w}{r_s}\right) \qquad 2.8$$

where r_w is the density of the solvent (water) and r_s is the density of the solute.

The Flory-Huggins interaction parameter c_{12} can be determined using the surface free energy measurements of the solute species in aqueous solutions [van Oss et al., 1990]. The magnitude and the sign of the interaction parameter is a measure of the total interaction energy between the solute molecules and a given solvent.

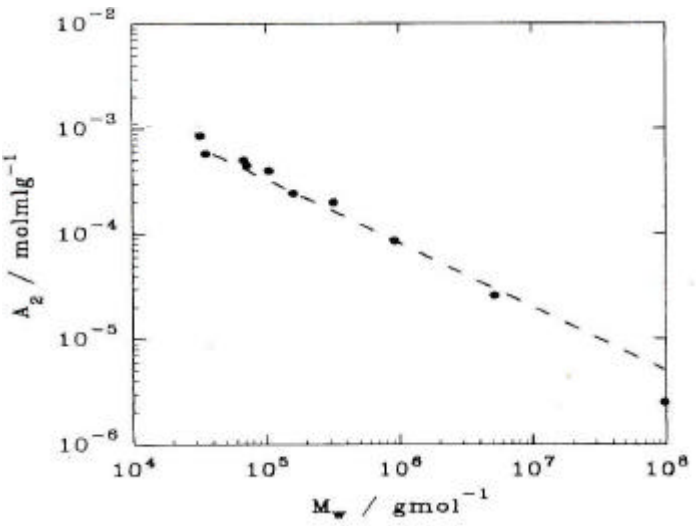

Figure 2.12. Molar mass dependence of the second virial coefficient A_2 for acid degraded potato starch [reproduced from Galinsky and Burchard, 1996].

2.6.2. Interaction parameters and surface energy

For neutral molecules like starch, the total free energy of interaction per unit area is the sum of the apolar (Lifshitz-van der Waals, LW) and polar (acid-base, AB) interactions and is given as

$$\Delta G_{121} = \Delta G_{121}^{LW} + \Delta G_{121}^{AB} \qquad 2.9$$

Hence, the total energy of adhesion ΔG_{121}^{T} between two molecules can be obtained by multiplying ΔG_{121} with the contact area, i.e. $\Delta G_{121} \cdot S$, where S

is the contact area between two strands of the molecules. From this, the Flory-Huggins interaction parameter is determined by the following relation (van Oss et al., 1990)

$$c_{12} = -\frac{\Delta G_{121}^{T}}{k_B T} \qquad 2.10$$

χ_{12} is a dimensionless form of the interaction energy.

The interaction energy per unit area between two linear chain molecules can be expressed as a function of the separation distance between linear chains. The following relation is used for apolar and polar components [van Oss et al., 1990; Bhattacharjee et al, 1994]

$$\Delta G_{121}^{LW}(d) = \Delta G_{121}^{LW}(d_o)\frac{d_o^2}{d^2} \qquad 2.11$$

and

$$\Delta G_{121}^{AB}(d) = \Delta G_{121}^{AB}(d_o)\frac{d_o - d}{l} \qquad 2.12$$

where d_o is the minimum equilibrium distance, where the extremely short range Born repulsion may be replaced by a vertical rise in the potential to infinity (hard sphere approximation). l is the characteristic correlation length. The relations in Equations 2.11 and 2.12 show that as the separation between the macromolecules increases, i.e. as the concentration of macromolecules in the solution decreases, the interaction energy between the two components decrease.

The LW component of the energy of adhesion, $\Delta G_{121}^{LW}(d_o)$, is always attractive (negative), whereas the AB component (polar) may be repulsive (positive) for an intensely hydrophilic solute in water (van Oss et al. 1990).

The total free energy of adhesion of two particles of solute 1 (i.e. only separated by a thickness d_o layer of solvent 2) in solvent 2, $\Delta G_{121}(d_o)$ can be calculated from the sum of the following two relations [van Oss et al. 1990]:

$$\Delta G_{121}^{LW}(d_o) = -2\left(\sqrt{g_1^{LW}} - \sqrt{g_2^{LW}}\right)^2 \qquad 2.13$$

and

$$\Delta G_{121}^{AB}(d_o) = -4\left(\sqrt{\gamma_1^+\gamma_1^-} + \sqrt{\gamma_2^+\gamma_2^-} - \sqrt{\gamma_1^+\gamma_2^-} - \sqrt{\gamma_1^-\gamma_2^+}\right)^2 \qquad 2.14$$

where γ_i^{LW} is the apolar component of the surface tension of species *i*, and γ_i^- and γ_i^+ are the electron donor (proton acceptor) and electron acceptor (proton donor) parameters of material *i*, respectively. Different surface parameters γ_i^{LW}, γ_i^-, and γ_i^+ needed for evaluation of the free energy of adhesion are readily determined by the measurements of contact angles of diagnostic liquids on a flat surface of the solute [van Oss et al., 1990)]. For starch and water, the average of the surface energy parameters found from literature are given in Table 2.1 [Lawton and Peoria, 1995; Biresaw and Carriere, 2001].

Using the relation given in the above equations for free energy and the data in the table, one can determine the trend of the osmotic pressure of starch in a solution as the solution gets concentrated. This is shown in the following section.

Table 2.1. Interfacial tension parameters for starch and water [Lawton and Peoria, 1995; Biresaw and Carriere, 2001].

Component	γ^{LW} (mN/m)	γ^+ (mN/m)	γ^- (mN/m)	γ^{TOTAL} (mN/N)
Starch	36.98	0.17	3.63	37.77
Water	21.80	25.50	25.50	47.30

2.6.3. Osmotic pressure beyond phase separation of starch solution

Gel starts to form at semi-dilute concentrations, where phase separationaor association of the starch molecules in the solution commences. From Figure 2.11, we know that association between starch molecules starts at very low concentration. For example, in the solutions of starch with molar masses of about 30, 000 and 300,000 g/mol, the starch starts to associate at about 40 and 16 g/l for static solution and 100 and 35 g/l for dynamic solution

(solution that flows), respectively. The maximum concentration of the gel can be approximated for a dehydrated starch at the temperature of interest. At 25°C, it is about 760 g/l.

At the phase separation, c_{12} can be approximated from the second virial coefficient given for degraded starch in Figure 2.12. At the other extreme concentration, for dehydrated starch, c_{12} is approximated from data of interfacial tensions given in Table 2.1. In this approximation, we assume that the strands of two chains of starch molecules are in contact in perpendicular to each other, and that the thickness of the strand is equal to 7 nm, which is an estimate of the size of one glucose molecule. Hence, the contact area between the strands S is 49 x 10^{-18} m^2. The values of c_{12} are calculated for the two molecular weights assumed earlier and given in Table 2.2.

Table 2.2. The estimated c_{12} at two concentrations for two model solutions

M_W (g/mol)	30,000		300,000	
Conc. (g/mL)	0.05	0.76	0.021	0.76
c_{12}	0.47	7.03	0.49	7.03

The total free energy calculated is almost dominated by the polar interaction energy. Therefore, from Equations 2.12 and 2.14, one can see that $\ln|\chi_{12}|$ is largely proportional to d_o-d. That means $\ln|\chi_{12}|$ is proportional to the concentration (in particular, for linear molecules) and expressed as

$$c_{12} = a\exp(bC) \qquad 2.15$$

where a and b are constants that can be determined from the data in Table 2.2. The result is plotted in Figure 2.13. This shows that the interaction parameters are positive and increase with an increase in the concentration, and it implies that the starch molecules are highly attracted to each other and easily get associated as the concentration is increased beyond semi-dilute concentration, C_i*. So, in this region, the molecules begin to stop acting as individual molecules, rather they act as very large macromolecules (pseudo-large macromolecules). The size of the pseudo-molecule depends on the degree of association. Hence, the osmotic pressure will decrease with an increase in concentration. This can be seen from the osmotic pressure

calculated using the estimated c_{12} from Equation 2.7 as a function of concentration. The value of z used in the calculation is approximated from Equation 2.8. The result from the calculation is plotted in Figure 2.14.

According to Figure 2.14, even the osmotic pressure could be negative at a little higher concentration than semi-dilute concentration. At least, theoretically it is possible to have such values [Hermans, 1949; Tager, 1972]. This does not mean, however, during ultrafiltration of the starch solution, that the effective operating pressure increases as a result of negative osmotic pressure. Rather, it shows that the degree of attraction between the macromolecules is very strong, the free energy of interaction is negative [van Oss and Good, 1989]. Hence, in order to break the association between the molecules in a solution, a large amount of energy is needed [Tager, 1972]. This is to say that the macromolecules form a network that acts as infinitely large molecules, which have negligible osmotic pressure. However, since there are free parts of the macromolecules (tails) that interact as individual molecules with water in the opening (pores) of the network, they can cause osmotic pressure due to their mixing (interaction) with water. In that case, the van 't Hoff's model (Equation 2.4) may be used to approximate the osmotic pressure. A straight lines in Figure 2.14 show the osmotic pressure approximated by the van't Hoff model. For the maximum possible concentration, the osmotic pressure would be about 0.4 bar for molar mass of 30,000 g/mol and 0.1 bar for 300,000 g/mol.

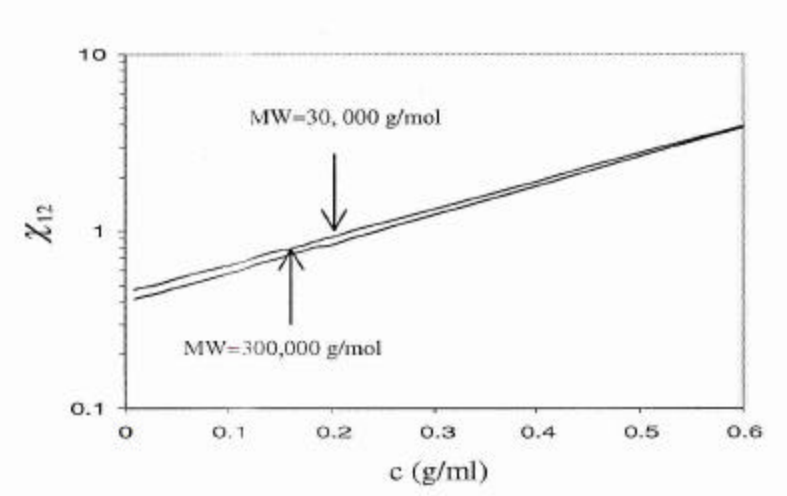

Figure 2.13. Concentration dependence of c_{12} for a rectangular strand of starch.

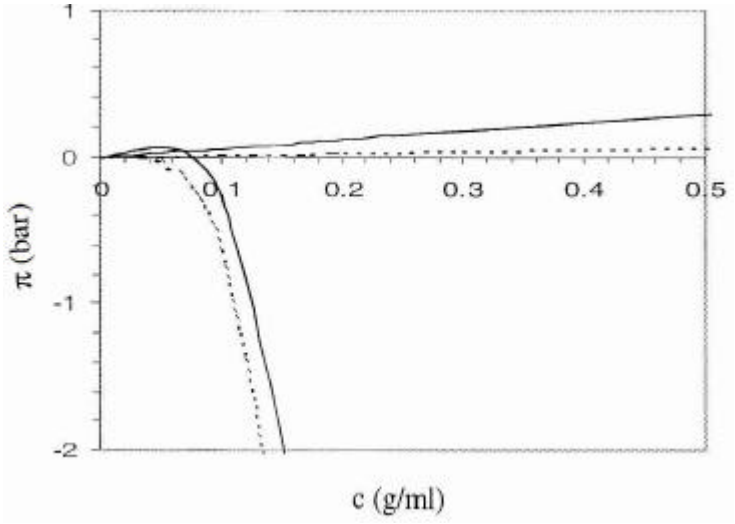

Figure 2.14. Osmotic pressure predicted by van 't Hoff's equation (straight line) and Flory-Huggins model (curved) equations for MW =30,000 (full line) and 300,000 (dotted line).

2.7. Viscosity

The presence of starch molecules in water will increase the viscosity of the solution. For a dilute solution, the dependence of viscosity on concentration is described (Tanford, 1961) as:

$$h_{sp} = \frac{h - h_o}{h_o} = n f \qquad 2.16$$

where h_{sp} is specific viscosity, h_o the viscosity of water, h is the viscosity of the solution, n is a constant depending on the asymmetry of the starch molecules (for spherical particles - n = 2.5) and f is the hydrodynamic volume fraction of the starch molecules.

The viscosity increases with molar mass. In literature, the dependence of viscosity on the molar mass is commonly reported as intrinsic viscosity[3], $[\eta]$. The intrinsic viscosity is related to molar mass by a power function, $M_W{}^g$, where g depends on the shape and the nature of the polymer. For some lower molar mass and linear starch molecules (maltose through to malto-hexaose and a dextrin of DP 18), Ring and Whittam (1991) determined their intrinsic viscosity $[\eta]$. Their values are given in Table 2.3.

Table 2.3. Intrinsic viscosity of malto-dextrins [Ring and Whittam, 1991].

Solute	$[\eta]$ 25°C (ml/g)
D-glucose	2.5
Maltose	2.6
Maltotriose	2.7
Maltohexaose	3.6
Dextrin (DP18)	6.0

On the other hand, Galinsky and Burchard (1995) determined the dependence of the intrinsic viscosity $[\eta]$ on the molar mass for the higher molar mass fractions for acid hydrolyzed degraded potato starch. This is given in Figure 2.15.

In semi-dilute solution, where the effect of the entanglement starts to be felt, the viscosity also depends on concentration. In this region, the specific viscosity is given by a power series of concentration and intrinsic viscosity [Tanford, 1961].

$$\eta_{sp} = [\eta]C + a_2[\eta]^2 C^2 \qquad 2.17$$

where a_2 is a constant known as the Huggins constant. For neutral spherical particles a_2 is approximately 2 and for flexible molecules in good solvents it is often about 0.35. However, at the collapse state concentration and beyond the viscosity of the solution is independent of the molar mass [Doesanto & Williams, 1981; Ring and Whittam, 1991]. On the other hand, however, the

[3] Intrinsic viscosity, or viscosity number, $[\eta] = \lim_{c\to 0} (\eta_{sp}/c)$

collapsed state concentration is a function of molar mass. That is, collapsed state concentration decreases as the molar mass increases.

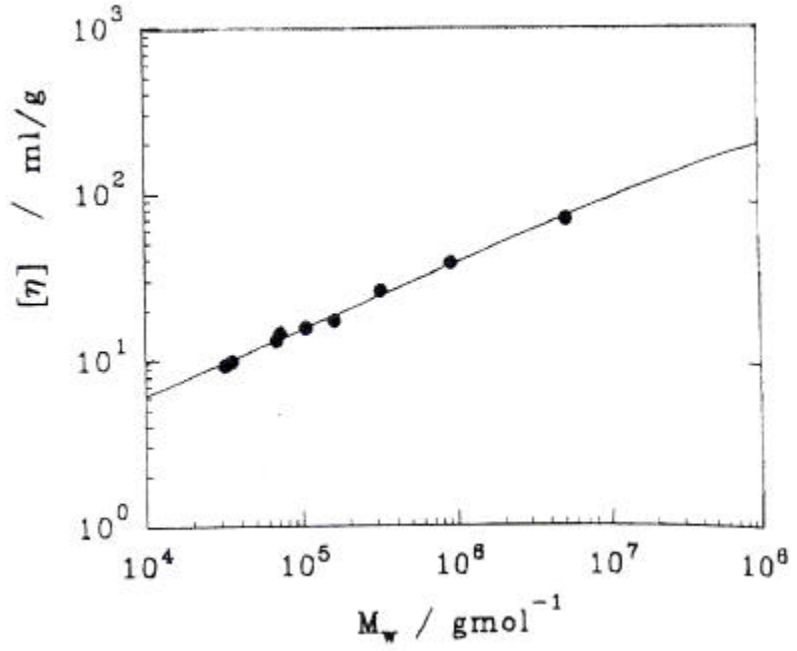

Figure 2.15. Intrinsic viscosity as function of molar mass of degraded potato starch [Galinsky and Burchard, 1995].

The viscosity behavior discussed above for a concentrated solution is derived for hydrophilic polymers, with which water has strong affinity. Starch is, however, expected to behave as we discussed in Section 2.6. That is, the starch molecules will associate and give up the water molecules it holds as the concentration is increased beyond the semi-dilute concentration. In ultrafiltration of the starch solution, this may be true at the membrane surface, where the concentration is much higher than that of the bulk. The associated starch is retained by the membrane and increases the resistance layer thickness and obstructs of the pores of the membrane. Therefore, the effect of concentration increase on the viscosity behavior beyond semi-dilute concentration is negligible. Because, in this range, small solutes that are not involved in the association determines the viscosity of the solution permeating through the membrane and layer of deposit during ultrafiltration of degraded starch solution.

During ultrafiltration of a starch solution, it is also worth remembering that the starch could be degraded by shear force and could result in a decrease in viscosity [Tanford, 1961; Bayazeed and Trauter, 1991]. This causes an increase in flux when ultrafiltration is run at constant concentration. The flux could even increase as the solution is concentrated over a certain range of concentration as a result of shear thinning macromolecular solution [Howell et al., 1996]. Potato starch shows a shear thinning behavior [Heitman et al., 1997] and it may also have such concentration range in which the flux could increase with concentration. The concentration range may also depend on the applied shear force.

2.8. Diffusion coefficient

In a dilute solution, the diffusion coefficient can be determined from the Stokes-Einstein relation and given by:

$$D = \frac{k_B T}{6 p h R_h} \qquad 2.18$$

where k_B is the Boltzman's constant, T is the temperature and h is the solvent viscosity and R_h is the hydrodynamic radius. From the equation, we can see that the diffusion coefficient decreases as the concentration [Gaddis, 1999] and the molar mass increase. In semi-dilute solutions, the association of the starch will also affect the diffusion coefficient and make it much smaller, because the starch forms entanglement networks that act as infinitely large molecules.

Chapter 3

Membrane filtration processes

In this chapter, general membrane filtration processes are discussed with particular emphasis on ultrafiltration. Further, the fouling mechanisms, basic models that are used to account for the effect of the mechanisms on the flux decline, the principles used in the evaluation of the contributions of the mechanisms for the flux decline are also reviewed.

3.1. Introduction to membrane filtration

Membrane filtration processes are the most applied membrane separation processes in the industry [Mulder, 1996; Cardew & Le, 1998]. The filtration processes include microfiltration, ultrafiltration, nanofiltration and reverse osmosis. Microfiltration deals with particles at the boundary of visibility i.e. the particle is less than 500 nm. At the other end of the scale there is reverse osmosis which deals with the separation of ions and small molecules from water. In between, we have ultrafiltration and nanofiltration processes. Ultrafiltration is principally concerned with separation of macromolecules with molar mass ranging from 1000 to 1000000 g/mol. Nanofiltration is used to separate small low molar mass non-volatile organic molecules from water.

Membrane filtration processes are all pressure-driven processes. The transmembrane pressure forces the liquid to pass through the membrane. The performance of the membrane is described by the flux of the liquid through the membrane and the retention or the selectivity of the membrane for species in the treated liquid. The operating pressure and the recovery (the extent of concentrating) varies from process to process. The nature of the solution and the size of the solute to be treated dictate the type of membrane material and process to be used. Table 3.1 shows a summary of operating pressure ranges, the membrane material used and the recovery of each process.

Membrane filtration processes use mainly sieving as separation mechanism. In addition, there are also some other mechanisms that play a significant role in the separation depending on the characteristics of the membrane and the feed. They include the effect of charge and the affinity between the membrane and the feed. For instance, if there are similar charges on the solute in the solution and on the membrane, there will be a tendency for solutes to be excluded. If the conformation of the large macromolecules is very flexible, the macromolecule could slip through the pores. The diffusion rate of particles through the membrane may also affect the separation efficiency of the membrane. The rejections of the membrane are differently characterized for different processes. Table 3.2 shows the range of pore size of the membrane used, the separation principles and the rejection characteristics of each process.

Table 3.1 Typical operating parameters and membrane materials used for pressure driven processes [Mulder, 1996; Toyomoto and Higuchi, 1992; Thorsen, 2000].

Process	Membrane		Typical operating ranges	
	Material	Structure	Pressure	Recovery
Microfiltration	Polymers Ceramics Metals	Porous	0.5 – 2 bar	90 – 99.9
Ultrafiltration	Polymers Ceramics	Asymmetric	1 – 10 bar	80 – 98
Nanofiltration	Polymers	Asymmetric	10 – 40 bar	50 – 95
Reverse osmosis	Polymers	Asymmetric Composite	30 – 70 bar	30 – 90

Table 3.2 Characteristics of separation processes [Cardew & Le, 1998].

Process	Separation principle	Pore size range (nm)	MWCO	Retention characteristics
Microfiltration	Size	50 – 1000	Absolute, nominal	Absolute, nominal
Ultrafiltration	Size, charge	1 – 50	>1000	MWCO
Nanofiltration	Size, charge affinity	0.6 – 1	200 –1000	Rejection, MWCO
Reverse osmosis	Size, charge affinity diffusion	< 0.6	< 200	Rejection

3.1.1. Principle of ultrafiltration

Ultrafiltration is commonly run in cross flow configuration. In a cross flow filtration, a feed stream flows across a membrane, tangent to the membrane surface. While the liquid flows across the membrane, a small fraction of the liquid passes through the membrane. This stream is known as the permeate. The portion that is passed over the membrane is referred to as the retentate or the concentrate. During ultrafiltration, the retentate is enriched in the solutes or suspended solids that are retained by the membrane. By maintaining cross flow along the membrane surface, the material retained by the membrane is swept off its surface. Figure 3.1 shows a schematic representation of cross flow filtration.

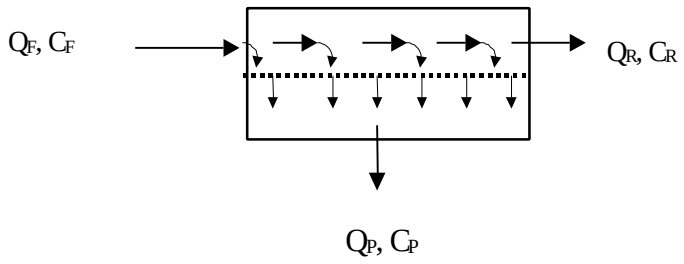

Figure 3.1: Schematic representation of cross flow filtration.

A simple mass balance for the cross flow filtration process is given as

$$Q_F \cdot C_F = Q_R \cdot C_R + Q_P \cdot C_P \qquad 3.1$$

where Q_F is the feed flow rate, Q_R is the retantate flow rate and Q_P is the permeate flow rate with the corresponding solute concentrations C_F, C_R and C_P in the streams, respectively.

The separation efficiency of the membrane is given by the retention coefficient defined as:

$$R = \frac{C_F - C_P}{C_F} = 1 - \frac{C_P}{C_F} \qquad 3.2$$

Since the retention of the solute by the membrane increases the concentration of solute at the membrane surface, the theoretical (intrinsic) retention coefficient would be higher. If the membrane surface solute concentration is C_m, the intrinsic retention of the membrane will be given by:

$$R_{\text{int}} = \frac{C_m - C_P}{C_m} = 1 - \frac{C_P}{C_m} \qquad 3.3$$

3.1.2. Characteristics of ultrafiltration membrane performance

The characteristic parameters for ultrafiltration membrane performance include permeability, rejection (retention), diffusion and separation. All the parameters depend on the membrane morphological parameters (e.g.pore size, pore size distribution, membrane thickness: skin thickness for an asymmetric membrane), pore shape and various chemical and physical properties (e.g. absorptive properties and charge density). Any phenomena that change the morphological parameters and the physico-chemical properties may affect membrane performance characteristics.

Membrane manufacturers use specifications set by a nominal molecular weight cut-off (MWCO) for their products for use in process design. MWCO is defined as the molar mass that is 90 % rejected by the membrane. The MWCO values of the membrane are used in absolute term. For

instance, if the membrane is gauged to be 25, 000 MWCO, it means that more than 90 % of the solutes with a molar mass larger than 25,000 g/mol are rejected. This does not tell the distribution of the molar mass retained by the membrane. The MWCO depends on the heterogeneity of the pores of the membrane. For a membrane with a narrow molar mass distribution, the membrane may have a so-called sharp MWCO. When the membrane has a broad pore size distribution, the membrane may have a diffuse MWCO. The conformation of the molecules also affects the cut-off of the membrane. For instance, despite their size, linear flexible macromolecules can pass through the smaller pores and make the cut-off diffuse. Figure 3.2 shows two membranes, one with a sharp MWCO and an other with a diffuse MWCO.

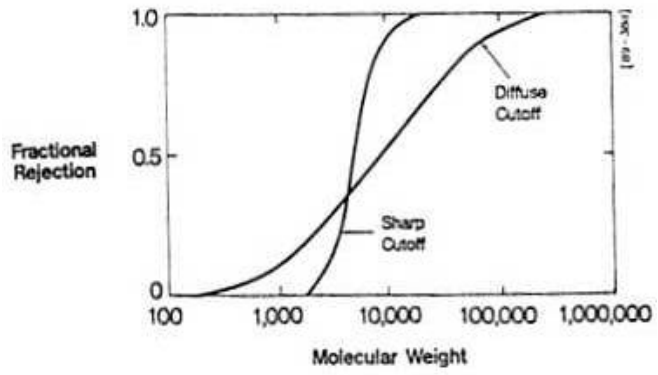

Figure 3.2. Sharp and diffuse molecular weight cut off in UF membranes [reproduced from Porter, 1972].

The MWCO is usually determined using a single solute (e.g. protein or dextran). Generally, however, the MWCO depends on the solute shape (e.g., linear or globular proteins) and the operating conditions (e.g. pressure, pH, temperature, and the condition of the membrane surface, i.e., the history of operation). The effect of operating conditions is related to different phenomena (e.g. concentration polarization, adsorption and pore blocking). Abaticchio et al. (1990) and Hanemaaijer et al. (1988) studied the effect of these operating conditions on the performance of ultrafiltration of macromolecules. The result of their studies are summarized as follows:

- Linear and flexible macromolecules are less retained than a rigid globular one of the same molecular mass.

- When there is interaction between the membrane and the macromolecules (e.g. adsorption), it will reduce the size of the pores and particles smaller than the pores of the membrane will not pass. Hence the retention of the membrane increases.
- The accumulation of the retained species at the membrane surface (concentration polarization) decreases the retention due to an increase of concentration gradient across the membrane. This effect is strongly dependent on the operating pressure and the cross flow velocity (see Figure 3.3). This phenomenon and the operating parameters also affect the selectivity of the membrane. For instance, an increase of cross flow velocity is observed to improve the selectivity while an increase of the pressure has an opposite effect.
- There is fouling due to precipitation or gelification of macromolecules taking place at the membrane surface, which tends to have irreversible tendency. This results in a partial or total formation of another layer on the membrane having characteristics that may be completely different from those of the initial membrane, usually with the effect of increased retention and decreased hydraulic permeability of the membrane.
- As the operating time is increased, both retention and membrane selectivity are increased. This can be seen from the cumulative molar mass distribution of dextran in two permeates collected after two different operating times and the feed, see Figure 3.4. This difference is attributed to the effect of the increased fouling with time.

Morphological characteristics

Ultrafiltration membranes have wide ranges of pore sizes which are usually approximated by lognormal distributions [Zeman, 1996]. In addition, the surface of the membrane is rough and the shapes of the pores are very irregular and have features that are vulnerable to pore constriction. The roughness ranges from 1 nm to 20 nm (the difference between the "valley" and the 'hill') [Cuperus and Smolders, 1991]. Usually, the pores are found in the "valleys".

The wide pore size distribution makes the membrane susceptible to pore blocking [Belfort et al., 1993]. The effect of this depends, of course, on the nature of the solute size distribution and its conformation. The fouling of the membrane also depends on the membrane surface roughness. An increase in the roughness of the surface enhances fouling [Cuperus and Smolders, 1991] due to an increase in the adsorption of solute because of a larger surface area and the resistance to the movement of the macromolecules along the membrane surface. In addition, the presence of pores in the "valley"

increases the velocity of solvent near the surface which promotes the effects of concentration polarization [Zydney, 1996; Nguyen and Neel, 1983].

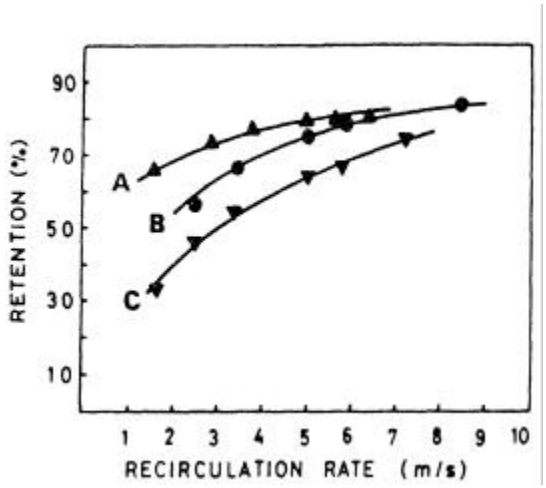

Figure 3.3. Effect of pressure on the retention of a Kalle membrane. Pressure (A) 1 bar; (B) 2 bar; (C) 3 bar [reproduced from Abaticchio et al. (1990)].

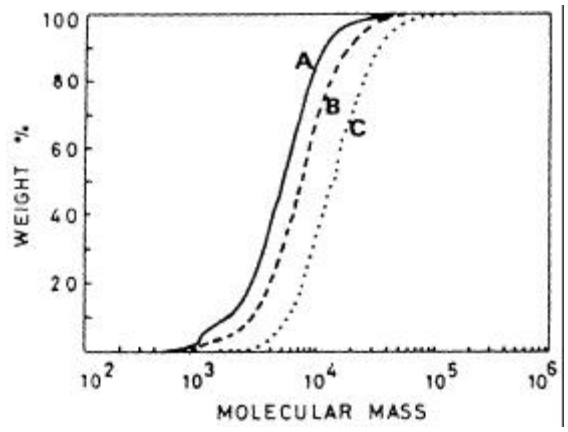

Figure 3.4. The effect of operating time on Dextran molecular mass distribution in the permeate of UF using a Kalle 420 membrane. Operating time: (A) 170 min; (B) 10 min; (C) feed, dextran T40 [reproduced from Abaticchio et al. (1990)]

Physico-chemical characteristics

Physico-chemical characteristics are also very important for understanding the behavior of the membrane during ultrafiltration. These characteristics include the hydrophilicity or hydrophobicity, the charge density and the specific affinity of the membrane.

Generally, the hydrophobic membrane is susceptible to adsorptive fouling of organic solute in ultrafiltration. As to our knowledge, there is no literature that discusses the adsorption of starch on a membrane. For other macromolecules like protein, however, the fouling was observed to be worse on hydrophobic membranes than on hydrophilic [Lee andRuckenstien, 1988; Persson et al., 1993; Pitt, 1987]. The thermodynamic reason for why hydrophobicity favors adsorption of any macromolecules is discussed in section 2.5.

The effect of macromolecule adsorption on membrane transport depends critically on the relative size of the macromolecules and the pore sizes. Zydney (1996) reviewed the effect of protein adsorption on fully permeable membranes (microfiltration), semi-permeable and totally retentive membranes on permeate flux. The microfiltration membranes freely allow the passage of the protein and forms a similar adsorption pattern in the pore as on a non-porous surface, a monolayer [Persson et al, 1993; Belfort et al., 1994]. The observed effect of protein adsorption on the solvent flux is quite small. When the pore of the membrane is slightly larger than the sizes of the protein, adsorption in the pores is affected bysteric interactions. The steric effect results in a loss of accessible surface area due to simple geometric exclusion. The adsorption of protein on fully retentive ultrafiltration membranes is primarily a surface phenomenon, since the pores are virtually inaccessible to the proteins. The effect of adsorption on flux decline is due to its pore blocking and the resistance added by the adsorbed layer [Zydney, 1996]. As earlier discussed, adsorption can also have a significant effect on the sieving characteristics of semi-permeable and fully retentive ultrafiltration membranes. It increases the selectivity and retention of the membrane [Zeman, 1983; Abaticchio et al., 1990; Mochizuki & Zydney, 1992].

Another physico-chemical property is membrane surface charge. Depending on their molecular structure, membrane surfaces can contain different types of charged spots, which may be due to the dissociation of the intrinsic membrane polymer groups. Even without such special entities, a neutral membrane pore surface could carry a definite charge [Cuperus and Smolders, 1991]. In aqueous solution, neutral membranes have negative

charges as all the other neutral particles. Hence, this is also true for starch in aqueous solution. If the species in the solution, e.g. aprotein, that is to be separated has a charge, the performance of the membrane will be strongly affected by the interaction between membrane and solute. If the membrane and the solute are oppositely charged, the membrane fouling will be a serious problem.

Therefore, in ultrafiltration of degraded starch solution, we expect that adsorption, pore blocking and constriction may affect the performance of the membrane as a result of the characteristics of the ultrafiltration membrane and the starch solution properties. It is one of the objectives of this study to uncover the significance of the contribution of each mechanism through experimental investigation. However, it is important knowing the physical phenomena behind each mechanism and the models that can be used to account for them in order to predict the performance of ultrafiltration membranes. This will be discussed in the following subsections.

3.2. Fouling mechanisms

In general, flux decline during the ultrafiltration is a result of the superposition of different fouling mechanisms. These mechanisms cause the flux decline by decreasing the driving force and/or by increasing the resistance to the flow through the membrane. The flux is expressed as a function of driving force, resistance and viscosity of the fluid as follows:

$$J = \frac{driving\_force}{vis\cos ity * total\_resist.} \qquad 3.4$$

For ultrafiltration, the driving force is the applied transmembrane pressure drop. For pure water flux, the resistance is only the membrane resistance, which is an intrinsic membrane property. During the ultrafiltration of a solution of macromolecules, the fouling mechanisms generate additional resistances due to the presence of solute and its distribution near the membrane surface. As mentioned earlier, the main mechanisms are concentration polarization and gel-layer, adsorption, and deposition (pore plugging, blocking and cake formation). A schematic representation of the resistances due to the mechanisms is shown inFigure 3.5. All the fouling mechanisms that cause flux decline could also affect the retention.

A good understanding of these mechanisms is helpful to design the membrane process that is least affected by the fouling mechanisms. In the next subsection, we will discuss how such mechanisms develop and are affected by the operating parameters.

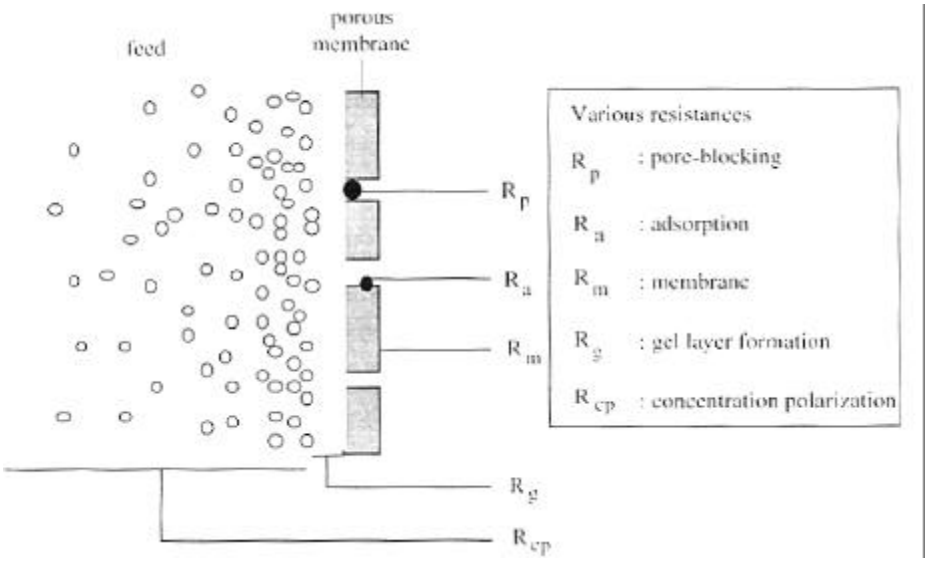

Figure 3.5 Overview of various types of resistance towards mass transport in ultrafiltration

3.2.1. Concentration polarization

During ultrafiltration of the solution, the semi-permeable membrane retains the solute and accumulates at the membrane surface while the solvent is passing. This creates a concentration boundary layer. The phenomenon is called concentration polarization. Concentration polarization is reversible. The presence of concentrated layer near the membrane wall would increase the resistance of the membrane for the fluid flowing through it. Commonly, it is referred to as reversible fouling. Concentration polarization increases as the convective flow of the solvent toward the membrane is increased. When the concentration of the macromolecule reaches a certain value, a layer of gel/precipitates of aggregated starch could also be formed, see Figure 3.6. This layer adds more resistance and also limits further increase of the flux

with pressure. When gel starts to form, further increase in pressure is presumed to add on more gel. The gel is usually assumed to be incompressible. In such a case, the thickness of the gel increases proportionally with the applied transmembrane pressure drop beyond the start of the gel formation. But it is worth remembering that some polymeric solute gel formed may also be compressible. For instance, Gaddis et al. (1999) observed that gelatinized starch gel is compressible. Thus, we may have the same behavior for the gel of degraded starch, which we are going to study in this thesis.

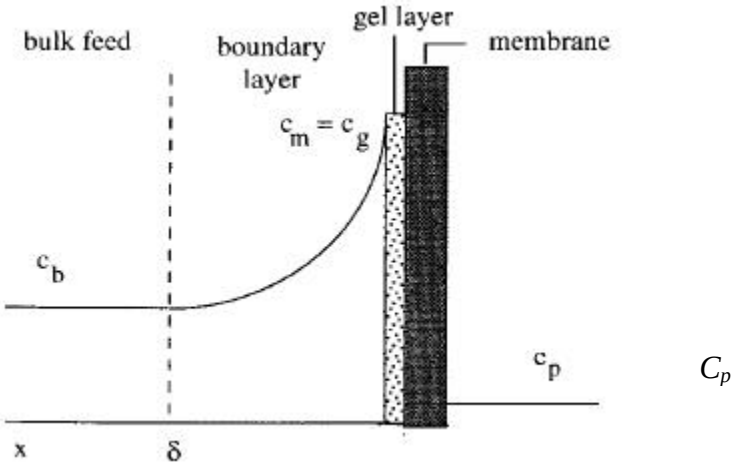

Figure 3.6. Profile of concentration polarization and gel layer.

The effect of concentration polarization on the flux decline varies with the value of the operating parameters. For example, an increase in transmembrane pressure drop increases any concentration polarization as a result of an increased flux. On the other hand, for a given device design, by increasing the cross flow velocity, one can reduce concentration polarization. This is because of an increase in the shearing stress at/near the membrane surface that redistributes the solute at the membrane surface. An increase in temperature could also affect the degree of concentration polarization. This is a result of its effect on viscosity; the viscosity decreases as the temperature is increased. This results in an increase in the diffusion coefficient (increases diffusion of the solute away from the membrane surface) and convective flow toward the membrane. If there is a net

increase of the flux as a result, there will be an increase in concentration polarization.

3.2.2. Adsorption

In ultrafiltration of macromolecules, the adsorption may start as soon as the surface of the membrane is in contact with a macromolecular solution. The adsorption even occurs before there is any transmembrane pressure drop across the membrane. Since adsorption takes some time to reach equilibrium, it could also be responsible for the flux decline with time from the early stage of ultrafiltration. In addition, other mechanisms may also contribute to the initial flux decline with time. For a given membrane-solute system, adsorption may be affected by a change in the concentration, the molar mass of the solute or the pH. As discussed in Section 2.5, until the adsorption plateau is reached, the equilibrium concentration increases with concentration. Thus, the operating parameters that affect the concentration near the membrane surface may also affect the adsorption rate. For example, a transmembrane pressure drop increases the solute concentration at the membrane surface while cross flow velocity reduces the concentration.

3.2.3. Deposition

Macromolecule deposition on the membrane is a non-equilibrium phenomenon that is governed by the hydrodynamics and body forces acting upon the macromolecules in the membrane module. These include the viscous drag force exerted on the particle by the flowing liquid, the hydrodynamic lift force, Brownian diffusion and shear-induced diffusion forces. For degraded starch, which is expected to be on an average of a particle size less than 500 nm, viscous drag force and Brownian diffusion are the only important forces that determine the deposition phenomenon. Particle deposition will occur when the drag force associated with flux velocity is larger than the diffusion force.

The extent of flux decline depends on the amount of deposit and the phenomena involved in the deposition. Generally speaking, deposit causes obstruction to permeate flow due to mechanical blocking of the pores. A reason could be through pore blockage (by reducing the number of accessible pores), pore constriction (by reducing the effective pore size) and cake formation (by increasing resistance to fluid flowing towards the pores).

Pore constriction is only possible for membranes with relatively large pores that are easily accessible to the macromolecules/particles while the pore blockage and cake formation will dominate when the pores are smaller than the size of the particles.

In cross flow filtration, the extent of pore blocking and the contribution of the deposition mechanisms depend largely on the membrane morphology and the size of the macromolecules in the feed solution. Membranes with straight-through pores are susceptible for pore blockage that will effectively eliminate filtrate flow through blocked pores. The contribution of this mechanism depends on the pore size. Membranes with very small pores are expected to trap fewer particles than membranes with pores of the same size as the macromolecules [Howell andNystrom, 1993]. On the other hand, for a membrane with a random and network-like pore structure, deposition may disturb the fluid flow through the membrane by mainly increasing the penetration distance [Zydney, 1996]. In this case, the resistance is mainly added to that of the membrane due to cake formation, rather than pore blocking.

The contribution of the mechanism depends on the operating conditions and the nature of the macromolecules. The size of deposition may increase with an increase in the transmembrane pressure drop and the feed concentration. In addition to the hydrodynamics, in ultrafiltration of degraded starch, starch molecules are expected to associate and precipitate at concentrations higher than the semi-dilute concentration. The associated starch will be retained and will form gel at the membrane surface where there is little mixing. The deposit and the gel of the starch at the membrane surface can be tied to the adsorbed layer and within itself by hydrogen bonding between hydroxyl groups on the macromolecules. Herein the deposit usually refers to the individual solutes brought to the membrane, retained and forced into the pores and on the membrane surface as a result of net hydrodynamic force (on the solute) toward the membrane. On the other hand, the gel layer is a network of solute formed as a result of attraction or association due to high solute concentration at the membrane surface. However, since both the deposit and the gel are formed as a result of the hydrodynamic force, both of them can be considered as a deposit. If the starch deposit/gel has a certain degree of compressibility, an increase in transmembrane pressure drop may increase the density of the deposit, which may induce a higher resistance. The relation of this resistance to the applied pressure is discussed in Section 3.3.

On the other hand, by increasing the cross-flow, one may reduce the resistance due to deposition [Ousman and Bennasar, 1995]. Yet the contribution of pore plugging and constriction can still increase due to an increase in the hydrodynamic force (or increases of permeate flux). Moreover, the cross flow velocity also determines the steady state deposit thickness [Suki et al., 1984; Green and Belfort, 1980].

3.2.4. Osmotic pressure across the membrane

In ultrafiltration, the difference in concentration across the membrane generates an osmotic pressure. This reduces the effective operating pressure. As we discussed in section 2.3.4, the magnitude of the osmotic pressure depends on the molar mass, the concentration of solute at the membrane surface, the interaction of solutes with each other and with the solvent (water in our case). The effect of operating pressure and cross flow velocity on osmotic pressure is related through their effect on solute concentration at the membrane surface. As discussed in Section 2.6, the effect of concentration depends on thehydrophilicity of the solute. For an intensely hydrophilic solute, the osmotic pressure increases exponentially with concentration. For a hydrophobic solute like starch, however, an increase in concentration beyond the semi-dilute concentration does not have a significant effect on the osmotic pressure. However, it can be said that an increase in concentration gradient across the membrane will increase the osmotic pressure.

3.2.5. Viscosity of the starch solution

In addition to the other mechanisms, according to Equation 3.4, the permeate flux is also affected by the viscosity of the solution. An increase in viscosity reduces the flux. The reason is an increase in the friction coefficient between the permeate and the membrane. Viscosity also affects concentration polarization through its effect on the diffusion coefficient. Generally, viscosity increases with concentration. As discussed in Section 2.7, beyond the semi-dilute concentration, the dependence of viscosity on concentration seems to be related to the dependence of the starch solubility on concentration. For an intensely hydrophilic solute, the solute remains in solution and the viscosity increases exponentially with concentration [Clifton et al., 1984]. In such a case, the viscosity of the solution largely influences the performance of the membrane. When the concentration of

hydrophobic macromolecules (e.g. starch) increases, however, they associate and release the water on their surface so that the viscosity of the liquid will not change or decrease as the concentration is increased further. At the semi-dilute concentration, the viscosity is 2 to 4 fold that of pure water at ambient temperature. Since the permeate has smaller molecules and a lower concentration than in the feed, in order to simplify the evaluation, its viscosity is approximated as water.

3.3. Ultrafiltration models

For pure water flux through the clean membrane, Equation 3.4 can be written as :

$$J_V = \frac{\Delta P}{\eta R_m} \qquad 3.5$$

where J_V is the flux, ΔP is the transmembrane pressure drop, R_m is the pure membrane resistance and η is the viscosity of the solution.

In ultrafiltration of a solution, however, the effects of other flux decline mechanisms discussed in section 3.2 add to this resistance and reduce the effective driving force. There are several models developed to predict the performance of ultrafiltration, but most of them are developed to predict the effect of concentration polarization. Examples are the film/polarization model, the gel-layer model, the gel-polarization model, the boundary layer resistance model and the osmotic pressure model. In some cases these models can be modified to account for the effect of other fouling mechanisms, for example adsorption and deposition [Wijmans et al., 1984; Ma et al., 1985; Nabetani et al., 1990; Zydney, 1996]. The only one model that accounts for all flux decline mechanisms is known as the resistances-in-series model [Chiang and Cheryan, 1986].

The most commonly used models in the ultrafiltration of macromolecules are the gel-polarization model, the osmotic pressure model, and the resistance in series model. In the following sections, the weakness and strength of these three models are discussed. Modifications of the models are also presented to account for the effect of other mechanisms so that they may give better prediction of the permeate flux.

3.3.1. Polarization and gel- polarization model

Polarization/film model

The model is developed based on the film theory and using the mass balance principle about the membrane. At steady state, theconvective flow to the membrane surface will be balanced by the solute flux through the membrane plus the diffusive flow from the membrane. Figure 3.6 shows the concentration profile near the membrane surface at steady state from the feed side. The following equation expresses the material balance:

$$J_V C + D\frac{dC}{dx} = J_V C_P \qquad 3.6$$

where C is the concentration at distance$x$ from the membrane surface, C_p is the permeate concentration and$D$ is the diffusion coefficient of the solute.

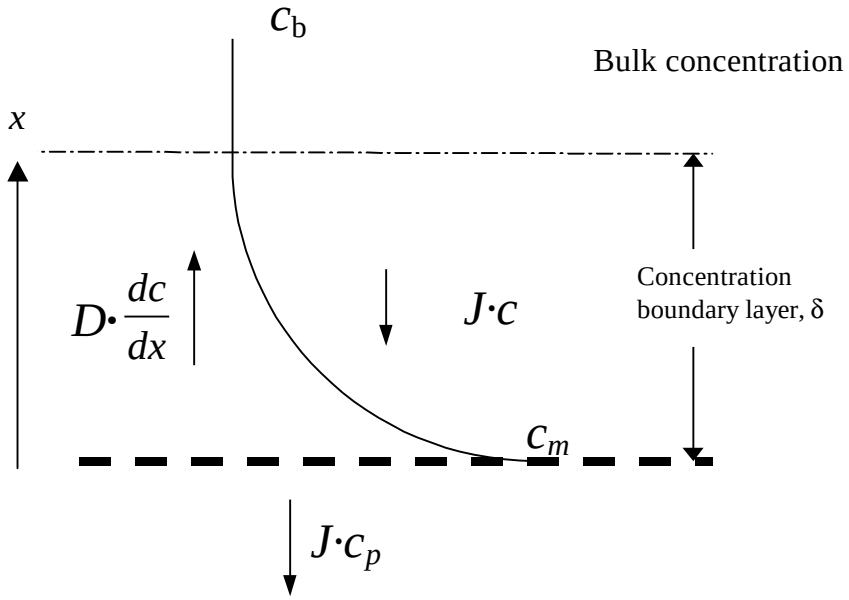

Figure 3.7. Concentration profile near the membrane surface during steady state ultrafiltration.

The boundary conditions are:

x = 0 $\Rightarrow$ $C=C_m$

x = d $\Rightarrow$ $C=C_b$

where d is the boundary layer thickness (the distance from the membrane surface to where there is complete mixing of the solute, the bulk concentration c_b) and c_m is the maximum value of the boundary layer concentration, which is the concentration at the membrane surface. Integrating Equation 3.6 gives the relation:

$$J_V = k \ln \frac{C_m - C_P}{C_b - C_P} \qquad 3.7$$

where $k = D / d$ is called the mass transfer coefficient. This model is called the film model/polarization model. The mass transfer coefficient depends strongly on the hydrodynamics of the system.

The mass transfer coefficient is usually defined from the Sherwood number (Sh) as described below:

$$Sh = \frac{kd_h}{D} = a \,\mathrm{Re}^b \, Sc^c \left(\frac{d_h}{L} \right)^d \qquad 3.8$$

where Re is the Reynolds number equal to $d_h v r / h$, Sc is the Schmidt number equal to h / rD, d_h is the hydraulic diameter, h is the dynamic viscosity, v is the flow velocity, L is the length of the tube and a, b, c and d are constants. This equation shows that the mass transfer coefficient is mainly a function of the feed flow velocity, the diffusion coefficient of the solute, viscosity, density and module shape and dimensions.

Gekas and Hallstrøm (1987) reviewed the mass transfer coefficient correlation for the turbulent flow regime, discussed the effect of viscosity and diffusion coefficient change on the correlation as a result of changes in concentration polarization, membrane surface roughness and flux through the membrane. They also suggested a modification to be made to the correlation when they are used in membrane filtration processes. However, in the present study, we decided that the correlation given by Mulder (1996) is enough in order to estimate the mass transfer coefficient where it is necessary.

For a tubular membrane, the hydraulic diameter d_h (= the inner diameter of the tube, d) and the mass transfer in the laminar and turbulent flow regimes are given by

$$Sh = kd_h \frac{kd_h}{D} = 1.62 (\mathrm{Re}\, Sc \frac{d_h}{L})^{0.33} \quad \text{(for laminar flow)} \qquad 3.9a$$

$$Sh = \frac{kd_h}{D} = 0.04\,\mathrm{Re}^{0.75}\,Sc^{0.33} \qquad \text{(for turbulent flow)} \qquad 3.9b$$

where the variables are as described for Equation 3.8. The mass transfer coefficient k, is strongly dependent on the cross flow velocity and the diffusion coefficient D, for a given module configuration. An increase in the cross flow velocity and the diffusion coefficient improves the k value. On the other hand, D decreases as the concentration increases due to an increase in viscosity. Hence, any operating conditions that change the concentration profile in the system also affect k.

Gel-layer model

As the pressure increases, the membrane surface concentration also increases and at high pressure, it can even reach to the point of incipient gel precipitation; and hence a gel layer is formed, to which the model is referring. This model assumes that the incipient gel precipitation concentration is the maximum concentration ever achieved during ultrafiltration. A further increase in the pressure does not add to the flux but increases the gel layer thickness. This flux is called the limiting flux, J_∞. In this case, the membrane surface concentration c_m in Equation 3.7 is substituted by the gel layer concentration C_g. Hence, J_∞ is given by the expression:

$$J_\infty = k \ln \frac{C_g - C_P}{C_b - C_P} \qquad 3.10$$

It can be seen from Equation 3.10 that J_∞ becomes zero as C_b approaches C_g.

C_g depends on the size, shape, chemical structure and degree of solvation but is independent of the bulk concentration [Mulder, 1996]. It is mostly assumed to be independent of experimental conditions like cross flow velocity and pressure [Nabetani et al, 1990]. The common practice to determine C_g is experimental. Plotting J_∞ vs $ln\ (C_b\text{-}C_p)$, the intercept of the straight line on the abscissa ($J_\infty=0$) will give the value of $ln\ (C_g\text{-}C_p)$. For starch solution at ambient temperature, the maximum gel concentration should not exceed 0.75 g/mL [Galinsky and Burchard, 1996]. Wiljmans et al. (1984 & 1985) found that C_g depends on the bulk concentration and the cross flow velocity and varies from experiment to experiment. In this light, the values of C_g estimated from this relation are uncertain and, in some cases, the estimate may not be physically meaningful. That is, C_g can be a pseudo concentration determined in order to predict the limiting flux [Howell et al., 1996]. C_g is commonly determined using D calculated for

dilute concentration assuming it is independent of the concentration. In reality, D is concentration dependent as discussed in section 2.8. This also affects the estimate of k and could also contribute to the uncertainty of C_g.

Gel-polarization model

The polarization model is limited to the prediction of the flux for any membrane surface concentration less than the gel concentration. On the other hand, the gel layer model is limited to determine the limiting flux. Besides, in both models, the dependence of flux on transmembrane pressure is implicit. In order to predict the flux for the whole range of applied transmembrane pressure drops, for flux limited by concentration polarization and for gel formation at the membrane surface, Yeh (1996) formulated the relation based on the following assumptions:

- When the applied pressure is very small (nearly zero), the effect of concentration polarization and gel is negligible. In this case, the relation between the flux and pressure depends only on membrane resistance.
- When the applied pressure is high (nearly limiting flux), the resistance due to the membrane is negligible. Thus, the resistance is approximated by $\Delta P / J_\infty$.

$$J_V = \frac{\Delta P}{R_m + \Delta P / J_\infty} \qquad 3.11$$

where R_m is the intrinsic membrane resistance. R_m can be substituted with R that includes resistance due to adsorption, etc., provided it is independent of pressure. Actually, this is an other expression of the resistances-in-series model (given in section 3.3.3) with only one mechanism (concentration polarization) involved. Equation 3.11 can be rewritten as:

$$\frac{1}{J_V} = \frac{1}{J_\infty} + \frac{R_m}{\Delta P} \qquad 3.12$$

This modified gel-polarization model will be good enough for prediction if a straight line from $1/J_V$ vs. $1/\Delta P$ relation can be constructed on linear scale from the experimental data at a given flow velocity and feed concentration (using the least-square method). If the effect of other phenomena are significant and they contribute strongly pressure dependent resistance that is not accounted for by the given relation, the prediction will not produce a good fit for the data obtained from ultrafiltration experiments.

According to Gaddis et al. (1999), the fouled layer (of gelatinized starch) of the membrane is compressible. In addition, according toGeissler et al. (1991) and Masashi et al. (1999), polymer gel and deposits have a certain degree of compressibility. Thus, this may also be true for starch polymer gel and deposit. In that case, the model should also account for the pressure dependence of the resistance due to the deposit. The resistance added by the gel/deposit could make the relation between the resistance and the pressure a power function with a power larger than one. In such a case, the flux will decrease as the pressure is increased further. In fact, a decrease of the flux after the maximum flux is quite often observed in ultrafiltration of macromolecules [Jonsson, 1984; Ousman and Bennasar, 1995; Gomez-Gotor et al., 1996]. Thus, a broad discussion on the possible effect of pressure on this resistance is presented in section 3.3.3. In addition, it is worth noting that the contribution of other fouling mechanisms should be accounted for by modifying the model if the contribution of the mechanism is significant.

3.3.2. Osmotic pressure model

The osmotic pressure model is developed on the assumption that it can explain the flux decline mechanism that limits the flux. A concentration difference between two solutions, which are separated by a membrane, will cause an osmotic pressure difference. In order to create osmotic equilibrium, water is induced to flow from the low concentration region to the high concentration region. This reduces the convective flux generated by the operating transmembrane pressure. As any other flows in nature, the permeate flow across the membrane is governed by the free energy difference across the membrane. In addition, the coupling effect between water and solute may reduce this energy difference, and the effective transmembrane pressure may drop.

Originally, Kedem and Katchalsky (1958), using irreversible thermodynamics, derived the relation:

$$J_V = L_P(\Delta P - s\Delta p) \qquad 3.13$$

where J_V is the permeate flux, L_P is the membrane permeability, Δp is the osmotic pressure across the membrane [$\Delta p = p(C_m) - p(C_P)$] and s is the reflection coefficient of solute across the membrane. The osmotic pressure effect on the permeate flux decline is scaled by the parameter s . The

parameter measures the relative restriction of the membrane to transmit the solute compared to the solvent, and varies between 0 for a freely permeable to 1 for a completely impermeable solute. C_m is determined from Equation 3.7.

The Kedem and Katchalsky solute flux across the membrane J_s, is broken into convective and diffusive fluxes as expressed by:

$$J_s = B\Delta p + J_V(1-s)\bar{C} \qquad 3.14$$

where B is the solute permeability of the membrane and $\bar{C}$ is the log mean concentration difference across the membrane. The first part of Equation 3.14 is the solute diffusive flux while the second part is the solute flux due to the drag effect of the net solvent flux. Since there is friction between the solute and the solvent, the second part shows also that the solute has a slowing effect on the flow of the solvent towards the membrane. This effect is proportional to the friction coefficient of the solute and the rejection of the membrane. Thus, in the osmotic pressure model, the behavior of the system is governed by the three phenomenological parameters: the membrane permeability L_P, the solute permeability of membrane B, and the reflection coefficient s .

The model we discussed in this section is similar to Equation 3.5 except that the effective transmembrane pressure drop is used instead of the applied pressure. The L_p is equal to the inverse of hR_m. This model may also describe the limiting flux behavior as in the gel polarization model. An example for this is given by Bhattacharjee et al. (1994) an intensely hydrophilic macromolecules. For such macromolecules, the osmotic pressure increases exponentially with concentration for concentrations larger than the semi-dilute concentration. For starch solutions, however, the relation between the osmotic pressure and concentration seems to be quite the opposite. This is discussed in Section 2.6. In such a case, the osmotic pressure is far from being a limiting factor for the permeate flux in ultrafiltration of degraded starch solution. However, the osmotic pressure model can be used to account for the effect of concentration polarization provided the model is modified to include the effect of the mechanisms that limit the permeate flux. In Nabetani et al. (1990) and Zydney (1996) the osmotic pressure model is modified by introducing the fouling resistance R_f to account for the resistance added by mechanisms other than concentration polarization. This is given as:

$$J_V = \frac{\Delta P - s\Delta p}{h(R_m + R_f)} \qquad 3.15$$

In their papers, R_f is assumed to be independent of pressure and stands to account for the effect of adsorption. However, where the osmotic pressure difference fails to be the limiting factor and R_f is the limiting factor, R_f should have some incremental relation with pressure in order for a model to predict the limiting flux. Thus, R_f may also include resistance added to the system due to gel formation, precipitation and deposition of the solute. This resistance may be pressure dependent.

3.3.3. Resistances-in-series model

The third model is the resistances-in-series model. The model has been used to predict the performance of ultrafiltration of different macromolecule solutions. It is expressed as:

$$J_V = \frac{\Delta P}{h \cdot (R_m + \sum_{i=1}^{n} R_i)} \qquad 3.16$$

where R_i is attributed to resistance due to i fouling mechanism. This model takes into account all fouling mechanisms including concentration polarization as serial resistances. When the flux decline is a result of adsorptive fouling R_a, depositional fouling R_d and concentration polarization R_{cp} or gel layer formation, the resistances-in-series model is written as:

$$J_V = \frac{\Delta P}{h \cdot (R_m + R_a + R_d + R_{cp})} \qquad 3.17$$

This model is insensitive to the actual mechanism. That is, the model does not differentiate between the mechanisms but accounts for all as additive resistances. For instance, the osmotic pressure and the gel layers are accounted for, in the same manner, as additive resistances. However, the former reduces the driving force while the latter adds to the hydraulic resistance to flow. Yet the model predicts well the performance of ultrafiltration membranes. The contribution of resistance by each mechanism depends on the procedure used for determination of the resistance due to each mechanism.Dal-Cin et al. (1996) suggested a method

that gives realistic contribution of each mechanism. This will be discussed in Section 3.4.

The relation of each resistance or lumped resistances with operating pressure can be approximated from physical relations found in the literature while the coefficients and constants used for the model fitting are estimated from experimental data. R_m is intrinsic property of the membrane, and it depends only on the physical property of water and membrane. Thus, it is independent of the pressure provided the membrane and the water is incompressible. Assuming a linear relationship between R_{cp} and ΔP, one may express R_{cp} as follows:

$$R_{cp} = a\Delta P \qquad 3.18$$

where a is a constant. According to Yeh (1996), R_{cp} includes the gel resistance since the increase in resistance due to gel is assumed to be a result of only the increase in the thickness of the gel layer. But, as we discussed earlier, the polymer gel could have a certain compressibility, and hence, the effect of the gel may not be accounted for well by the relation given for R_{cp}. In such cases, R_{cp} should be modified to include the effect of compressibility or the fouling resistance R_f should account for the effect. In this study, we chose to take it into the fouling resistance. This is discussed in the following paragraphs.

In ultrafiltration of macromolecules where other mechanisms such as adsorption and deposition are at work, the effect of gel is indispensable. The adsorbed macromolecules enhance the gel formation (aggregation) and the material brought to the surface by hydrodynamic force is deposited or fills in the network formed by the gel at the surface of the membrane. In order to simplify the model, we may lump all resistances added by these mechanisms into a fouling resistance R_f. When adsorption and deposition is significant and polymer deposit or gel layer is formed, there would be some kind of dependence of R_f on pressure because of the compressibility of the layer [Geissler et al., 1991; Masashi et al., 1999].

The permeability of the polymer sediment, network and gel up to about 6 % cross linking density and supported by the membrane is related to the volume fraction of polymer by the power function as described by the relation (White, 1960; de Gennes, 1979; Tokita and Tanaka, 1991; Tokita, 1993):

$$p = a_o (f)^{-n} \qquad 3.19$$

where p is the permeability of the polymer gel, f is the volume fraction of the polymer, a_o is a constant that depends on the nature of the polymer and n is a power constant that has a value that ranges from 1.4 to 1.5 for low pressures (less than 0.01 bar) (de Gennes, 1979; Tokita and Tanaka, 1991; Tokita, 1993) and is about 1.0 for pressures from 0.45 to 2.05 bar (White, 1960). On the other hand, the elastic and compressive behavior of a polymer gel is related to the volume fraction of the polymer by the relation [Geissler et al., 1991; Masashi et al., 1999]:

$$E = E_O f^m = f\frac{\partial P}{\partial f} \qquad 3.20$$

where E is elastic module of the polymer gel.

E_O is a constant that depends on the given network of polymer and m is a power that has a value of 1/3 [Geissler et al., 1991]. From Equations 3.21 and 3.22, one can get a relation between the resistance of the polymer layer (gel and deposit) and the applied pressure across the layer, which is given by a power function

$$R_f = b \cdot \Delta P^C \qquad 3.21$$

where b is the constant that depends on the polymer system and the thickness of the layer and c is about 3 for ΔP less than 0.01 bar and about to 2 for ΔP from 0.45 to 2 bar at room temperature. For a higher pressure, the value of c could be less than 2. Thus, this relation can be used to predict the dependence of the fouling resistance R_f on the transmembrane pressure ΔP provided the operating pressure corresponds to the pressure range for which the value of c is given above.

3.4. Evaluations of the contribution of fouling mechanisms

In ultrafiltration of macromolecular solutions, all the fouling mechanisms are expected to affect the permeate flux to certain extent. Resistances-in-series model has been used to estimate the magnitude of the contribution of each mechanism [Belfort et al., 1993; Pouliot et al., 1994]. In order to

determine the contributions, the following flux data should be available or determined experimentally:

1. J_i - pure water flux for new or clean membrane,
2. J_a - pure water flux for a membrane which is fouled by static adsorption of partially degraded starch solution,
3. J_f - pure water flux for a membrane which is fouled by partially degraded starch solution,
4. J_v - permeate flux of ultrafiltration of partially degraded starch solution under a given set of operating conditions.

There are two ways to determine the resistances from the flux data. The first and most common method is the one that uses Equation 3.17 and determines the resistances starting with clean membrane pure water resistance R_m and by adding sequentially the resistance(s) in the equation related to the flux used for the calculation. The steps are given in [Ousman and Bennasar, 1995; Dal-Cin et al., 1996]. This method gives unrealistic contribution of the fouling mechanisms, in particular where adsorption is significant [Dal-Cin et al., 1996]. The other is the one proposed by Dal-Cin et al. (1996). This method uses the relative flux loss due to each mechanism to the overall flux decline to calculate the fraction of the resistance contributed by the mechanism to the overall fouling resistance during the ultrafiltration of the solution. Dal-Cin et al. (1996) made a comparison between the two methods. They found that the second method gives a more realistic information on the contribution of the fouling mechanisms. For detail refers to [Dal-Cin et al., 1996]. Thus, in our study, the second method, the flux loss ration principle, is used to determine of the contribution of each fouling mechanism. The flux loss ratio principle assumes that the resistance contributed by each mechanism is proportional to the relative flux loss due to the mechanism.

The clean membrane resistance R_m is determined from Equation 3.5 and pure water flux (J_i) at a given pressure and temperature. Assuming equal viscosity for the permeate and pure water, the additive resistance due to overall fouling R_f can be determined from the ratio of J_i to J_v.

$$\frac{J_i}{J_v} = \frac{R_t}{R_m} = \frac{R_m + R_f}{R_m} \qquad 3.22$$

where R_t is overall resistance (= R_m + R_f) and R_f is the overall fouling resistance that also includes the effect of concentration polarization. The

following relations would give the contribution of each fouling mechanism based on the flux loss ratios (FLRs):

For adsorptive FLR resistance (r_a):

$$r_a = R_f \frac{J_i - J_a}{J_i - J_v} \qquad 3.23a$$

For pore plugging FLR resistance (r_d):

$$r_d = R_f \frac{J_a - J_f}{J_i - J_v} \qquad 3.23b$$

For concentration polarization FLR resistance (r_{cp}):

$$r_{cp} = R_f \frac{J_f - J_v}{J_i - J_v} \qquad 3.23c$$

That is, the sum of r_a, r_d and r_{cp} gives R_f. Note, in order to differentiate between the resistances in resistance-in-series model (Section 3.3.3), small case r is used to represent the resistance calculated according to the FLR method. The detailed discussion of the method is found in Dal-Cin et al. (1996).

Chapter 4

Experimental

4.1. Laboratory experimental unit

The UF experiments were carried out on laboratory scale PCI membrane pilot plant rig with a tubular module (Paterson Candy International, Hants, UK). The module can operate with one or two tubular membranes, each with a diameter of 12 mm and a length of 120 cm. The rig is equipped with a 25 liter feed tank, a heat exchanger (that was regulated by a thermostat and cooling water), a plunger pump (Cat pump, model 5CP6121, Minneapolis, USA), a back pressure valve (Tescom) to control the main line pressure and needle value to control a by-pass line. Figure 4.1 shows a schematic representation of the test unit.

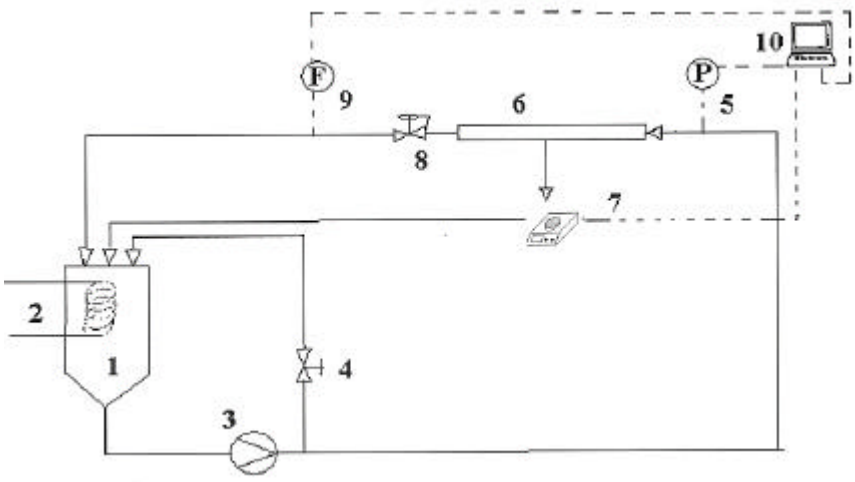

Figure 4.1. Ultrafiltration experimental unit. (1) Feed tank, (2) heat exchanger, (3) pump, (4) by-pass control valve (needle valve), (5) pressure transmitter, (6) membrane module, (7) balance, (8) backpressure valve, (9) flow meter and (10) computer.

The pressure transmitter (Keller type PR21, 0-24 bar, current output 4-20 mA), accuracy ± 1 kPa, was placed upstream the membrane module while the flow meter (Yokogawa, model SE 115MJ, Tokyo, Japan), accuracy ± 1 l/h, was placed downstream. The temperature of the heat exchanger was controlled by a thermostatic bath and a manually adjusted cooling water flow rate. The accumulated permeate mass was weighed on a balance (Presica Instrument AG, Model Precisa 6200, Ditikon, Switzerland).

The inlet pressure, the volumetric flow rate of the feed, and the permeate flux were automatically measured and the data were stored in a computer. The Field Point data acquisition system (from National Instruments) with a Labview program was used to record and store the data. The process variables were sampled six times per minute.

4.2. Feed solution preparation

The native potato starch (from Norske potetindustrier) was degraded by α-amylase (Bactosol MTN Liquid, from Clariant). The degradation was made to get a degraded starch with molar mass in the order of 40 000, 200 000 and 2 000 000 g/mol. The procedure used for the preparation of the degraded starch is given in Appendix-A. The reproducibility of the degraded starch obtained using the procedure is also reported in the appendix. The degradation was limited to 2 % due to the limitation of the reactor used (due to difficulties to get reproducible degradation). Therefore, in this study, the maximum feed concentration used was 2 wt %. The reproducibility of the three model degraded starches used as a feed is also reported in the same appendix. The average molar mass distributions of all three model starches are plotted in Figure 4.2. Their average molar mass, radius of gyration and polydispersity are given in Table 4.2. The polydispersity values we found are comparable while the radius of gyration are about three folds smaller than those of partially degraded potato starch by acid hydrolysis [Galinsky and Burchard, 1995] at a corresponding molar mass. The difference in the radius gyration could be a result of different analysis conditions used. Therefore, we have assumed that the other physical properties of the partially degraded starch by acid hydrolysis [Galinsky and Burchard, 1995 & 1996], given in Chapter 2, can be used to approximate the physical properties of our partially degraded potato starch at a corresponding molar mass and at ambient temperature. In the ultrafiltration experiments, the 2 wt

% partially degraded starch solution was used as it was and/or diluted to 0.1, 0.5, 1.0 wt %.

Table 4.2. The average molar mass, radius of gyration and polydispersity for solution I (MWI), solution II (MWII) and solution III (MWIII).

Model Solution	Average molar mass (g/mol)	Radius of gyration (nm)	Polydispersity (MWm/MWn)[1]
MWI	40000	8.3	5.5
MWII	170000	13.1	12.4
MWIII	1500000	23.4	35.3

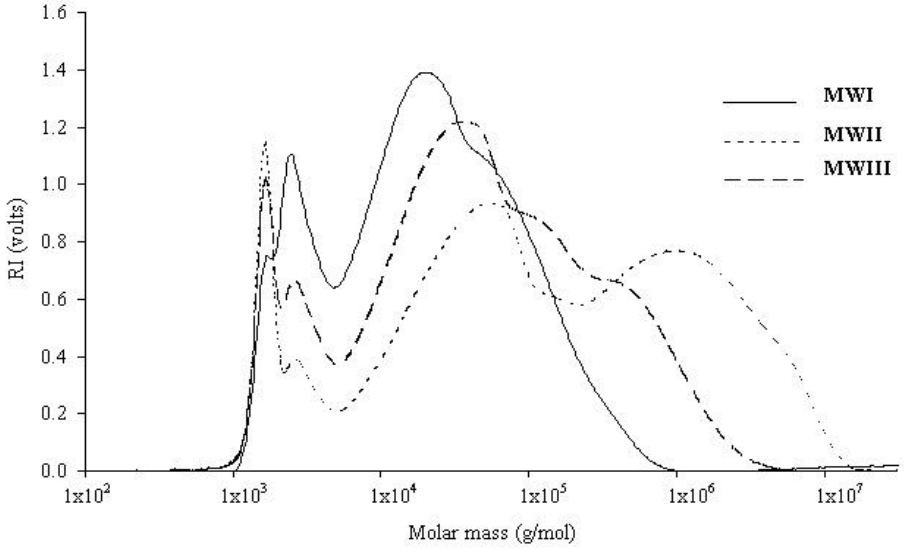

Figure 4.2. The molar mass distribution of model solutions: MWI, MWII and MWIII.

[1] MWm/MWn – the ratio of the weight average molecular weight to number average molecular weight.

4.3. Characteristics of tubular membranes used

Two types of membranes were used in this study. One was an ES625 membrane procured from PCI membrane systems and the other was a MPT-U-20 membrane from KOCH membrane systems. According to the manufacturers, the ES625 membrane was made of polyethersulphone, while the MPT-U20 membrane was made from modified polyethersulphone in order to give a much better hydrophilicity than the polyethersulphone membrane. Both of them were claimed to have a 25000 MWCO and equal pure water flux. The ES625 membrane is a hydrophobic membrane and is indicated to have about 95 l/(m^2h) pure water flux at 16^{o}C and 2.0 bar operating condition. The MPT-U20 membrane is said to have a 70 l/(m^2h) pure water flux at 30^{o}C and 1.0 bar transmembrane pressure. When these fluxes are corrected to 25^{o}C and 2 bar operating condition, they are equal to 121 l/(m^2h) and 125 l/(m^2h), respectively. That means, they have almost equal pure water flux. For other MPT-U20 membrane surface properties, there was no literature available, except the expectation by the manufacturer for its better hydrophilicity, and neither did we study the properties due to lack of facilities. Thus, we used the pure water flux, retention and contribution of adsorptive fouling as indicator of performance and the properties of the two membranes. The pure water used in this study is a deionized water with conductivity less than 2*mS/cm* and a pH of 7.

The water permeability of the membrane L_p was determined from the familiar relation given by Equation (3.5). This is rewritten as:

$$J_w = L_p \Delta P \qquad 4.1$$

where $L_p = 1/hR_m$. In this study five ES625 and one MPT-U20 membranes were used several times for the investigation of the contribution of the fouling mechanisms on the flux decline and the performance of the membranes after each cleaning. The pure water permeability of a new and cleaned membrane was determined. The pure water flux and the corresponding transmembrane pressure drop are presented and discussed in section 5.1.

4.4. Ultrafiltration experimental procedures

4.4.1. New membrane pretreatment and cleaning procedures

New tubular membrane was first cleaned with caustic soda solution at a pH of 12 and temperature of 50°C and then flushed with deionized (pure) water as prescribed by the manufacturer. In order to stabilize the membrane (or remove the effect of compaction of the membrane, if there is any) before the membrane was used for generating test data, the pure water was ultrafiltered through the new membrane at a transmembrane pressure drop of 4 bar and at 25°C for 2 hours [Persson et al., 1995]. Then, pure water fluxes for series of lower pressures were taken.

To clean the membrane, the cleaning procedure suggested by [Razavi et al., 1996] for membranes fouled with lipids-protein-polysaccharides matrix was used. But, only two of the cleaning reagents (NaOH solution and oxidizing agent, in our case – H_2O_2 solution) were applied. In brief, the procedure can be summarized as follow:

$$Flushing \Rightarrow NaOH\ solution \Rightarrow Flushing \Rightarrow H_2O_2\ solution \Rightarrow Flushing$$

The cleaning procedure was tested to check whether it could enable us to recover the flux of the membrane that was fouled during ultrafiltration of a 0.5 wt % partially degraded starch solution. The cleaning agent and conditions used: caustic soda solution at pH 12 and 350 ppm H_2O_2 solution at 50°C for 20 min with 250 l/h circulation rate. In between, the membrane was flushed with pure water at room temperature and then the pure water flux of the membrane was determined. After each cleaning process, the pure water flux of the membrane was determined at a transmembrane pressure equal to 2.0 bar, a cross flow velocity equal to 1.0 m/s and a temperature of 25°C. The membranes were reused until the membrane was damaged and had more than 10 % percent deviation from the new membrane pure water flux [Dal-Cin et al., 1996]. Flux data generated only from one membrane were used to study the effect of one operating variable at time. One membrane could be used to study the effect of more than one operating variable as long as the membrane was not damaged.

4.4.2. Evaluation of the contribution of fouling mechanisms

In the evaluation of the contribution of the fouling mechanismsDal-Cin et al. (1996) procedure was used. According to this procedure, four fluxes were determined for each set of operating variables. How these fluxes were acquired is presented below.

1. J_i: clean membrane pure water flux was measured for 30 min and the average of the last ten flux measurements was taken for evaluation.

2. J_a: first, partially degraded starch solution was adsorbed on the clean membrane at a zero transmembrane pressure drop (ΔP) and with a 50 l/h circulation flow rate, to supply gentle mixing, for 2 h. Then the solution was drained and the membrane was flushed at 350 l/h three times, each time with about 15 liter of pure water. Then the feed tank was filled with pure water, and the pure flux of the adsorbed membrane was determined.

3. J_v: first, partially degraded starch solution was ultrafiltered for 2 h. The flux was measured at selected times: after 10 min, 30 min, 1 h, 1.5 hr and 2 h. J_v at 2 h was used for flux loss ratio calculation.

4. J_f: the membrane was drained from the solution of the previous run and flushed as in procedure 2. Then the feed tank was filled with pure water, and then the pure water flux for the fouled membrane was determined.

The contribution of the fouling mechanisms was studied for both ES625 and MTP-U20 membranes.

In order to determine the contributions of the fouling mechanism on the flux decline at a given condition, one complete experimental run took about 7-8 h. This is relatively short when it is compared to that of Dal-Cin et al. (1996), which took more than 24 h. In our case, we assumed that the compaction of the membrane was negligible. In order to make the time used on the experiment manageable, the effect of operating variables was studied at 2 or 3 levels except for the transmembrane pressure drop, which had four levels. The effect of operating variables on the contribution of the fouling mechanisms was studied. The operating variables that have an effect on the contribution of the fouling mechanisms which depend on the membrane materials, the investigation was made on both ES625 and MPT-U20 membranes. These variables are feed concentration, molar mass and pH of

the starch solution. The effect of other operating parameters, such as transmembrane pressure drop, cross flow velocity and temperature, on the contribution of the fouling mechanisms were studied using ES625 membranes. For other operating variables, concentration, molar mass and pH, both types of membranes were used. The values of the operating variables used are given in Section 5.2, Table 5.2.

4.4.3. Ultrafiltration performance

4.4.3.1. Complete recycling mode

In order to study the performance of the ultrafiltration of degraded starch solution, ES625 membrane was used. The process was run under complete recycling mode (constant concentration mode), i.e. the feed concentration is constant through out the run. Because the solution and the permeate were recycled into the feed tank. The flux measurements were made at fixed time intervals until steady state was reached. For a given set of concentration, cross flow velocity and molar mass: ultrafiltration was started with the lowest ΔP. When the steady state was reached, ΔP was increased to the next selected operating pressure level and run until a new steady state was reached. This was done for all selected higher pressures. For each pressure, a permeate sample was taken at the corresponding steady state. The experiments were carried out for two model solutions: MWI (40000 g/l) and MWII (170000 g/mol) partially degraded starch solutions. The values of the operating variables used are given in Section 5.4.

4.4.3.2. Concentrating mode

In this mode, MWI degraded starch solution with an initial concentration of 0.5 wt % was ultrafiltered continuously in concentrating mode at a transmembrane pressure of 1.5 bar, a temperature of 25^{o}C and a cross flow velocity of 1.0 m/s. The permeate was withdrawn from the system and the concentrate was recycled in the system until the volume was reduced by a factor of 4. The flux was measured continuously and the permeate samples were taken at 10 min and every hour after the ultrafiltration started.

4.5. Analytical methods

Concentration: The concentration of starch in the samples was measured using the phenol-sulfuric acid (PS) analysis. The full procedure is given in Dubois (1956). First, a calibration curve for a blank, and 10, 20, 50, 100 µg/ml solutions prepared by diluting the standard glucose solution (from Sigma) was established. The absorbance was measured using a Shimadzu UV-260 (CME101-264) at 485 nm wavelength. The samples were diluted to a concentration in the calibration range and were later calculated back by multiplying by the dilution factor. For the first few samples, the concentrations were also measured in terms of COD using a colorimeter method (by LASA Photometer – Cuvette Test LCK 114), [Eaton et al., 1995] in order to evaluate the retention determined by the former method. For each sample, four replicates were made. The retention determined by both methods were almost equal, see Table D-3, in Appendix D.1.

pH was measured by a pH meter (Metrohm, model 744), accuracy $\pm$ 0.05 pH units. The measurement was done by directly dipping the electrode in the sample.

Molar mass and size distribution: Molar mass and size distribution were determined using high pressure liquid size exclusion chromatography HPLSEC, Perkin Elmer (series 2000). The samples were adjusted to 5 mg/ml with DMAc/Na_2SO_4. HPLSEC was performed at 40^{o}C using a HPLC pump operating at a flow rate of 1.0 ml/min and with an autosampler. The injected samples contained 50-200µg of dissolved degraded starch per ml in the flowing stream (eluate). The elution was monitored by a refractive index detector (Shimadzu RID-10A) and a multi angle laser light scattering detector (MALLS, Wyatt Dawn DSP, 633 nm). For each sample analyzed, two or three replicates of the SEC analysis were made.

Chapter 5

Results and discussion

In this study, five ES625 membranes and one MPT-U20 membrane were used. The ES625 membranes are named according to their order of use as M-I, M-II, M-III, M-IV and M-V. Some of these membranes were used to investigate the contribution of the fouling mechanisms during ultrafiltration. Others were used to generate flux data to evaluate the performance of ultrafiltration of the starch solution. In the first section, we discuss the pure water fluxes obtained for new membranes, the cleaning performance of the cleaning agents for fouled membrane, the variation of pure water flux of the cleaned membranes. In the next section, we discuss the time required to reach steady state during ultrafiltration of starch solution. Then, we will present contributions of the fouling mechanisms on flux decline and the effect of operating variables on the contributions, and on the performance of ultrafiltration and the models that might be used to account for all mechanisms. The discussion on the models fitted for the flux data is also presented. At last, we will see how the flux and retention/rejection of the membrane were developed as the feed was concentrated. All flux, pressure and concentration data are reported in $l/(m^2h)$, bar and wt %, respectively.

5.1. Pure water flux of new and cleaned membrane

In this discussion, "new membrane" stands for the virgin membrane that had undergone pretreatment in order to use it in the ultrafiltration of the starch solution. On the other hand, "cleaned membrane" stands for the cleaned fouled membrane after it had been used in ultrafiltration of the solution. The pure water flux of new and cleaned membranes are discussed in the following two subsections.

5.1.1. Membrane treatment

New membranes were treated as prescribed in section 4.3. Pure water flux was determined for pressures lower than or equal to the stabilization pressure (4.0 bar). The flux vs. pressure relationship was plotted for each membrane (see Appendix-B). They are all straight lines, almost passing through the origin with a very good correlation ($R^2 \approx 0.999$). This is in a good agreement with what is expected for incompressible membranes. The pure water fluxs obtained for both types of membranes is larger than the ones given by the manufacturer. For example, we obtained on average 165 l/(m^2h) and 210 l/(m^2h) for the ES625 and the MPT-U20 membranes, respectively, while according to the manufacturer the flux of both membranes is about 120 l/(m^2h). The difference might be a result of the difference in pretreatment of the virgin membrane, the quality of the pure water used and the variation among the virgin membranes. As we can see in the following section (Section 5.1.2), the variation among virgin membranes could make a significant contribution to the observed pure water flux variation among the membranes.

5.1.2. Pure water flux of cleaned membrane

In order to check the effectiveness of the cleaning procedure suggested in section 4.4.1, two ultrafiltration test runs were carried out using ES625 membrane (M-I). The test was carried out for MWI (40000 g/mol) starch solution at a transmembrane pressure drop of 2.0 bar. Due to an irreversible fouling of the membrane, the membrane lost about 35 % of its initial (new membrane) pure water flux. See Table D-1 in Appendix D.1 for pure water flux before and after fouling of the membrane. The fouled membrane was cleaned as prescribed in Section 4.3 in two stages: by NaOH solution and by H_2O_2 solution. During cleaning by NaOH solution, about 50 % of the pure water flux was recovered. Further treatment by H_2O_2 solution gave almost the initial pure water flux of the new membrane with about ± 4 % variation. Although the foulants are somehow different, the results agree with that of Razavi et al. (1996).

These two stage cleaning procedure was used throughout our experimental work in order to clean the fouled membrane after running each ultrafiltration experiment. The pure water flux of the membrane was measured after each cleaning. In order to show the variation of the pure water flux of the cleaned membrane, we plotted the pure water flux vs. the number of cleanings for

one of the ES625 membranes (M-V) and for the MPT-U20 membrane in Figure 5.1. The average fluxes and their corresponding standard deviations for all membranes used are given in Table 5.1. The retention of these membranes for MWI starch solution was also determined and the result will be discussed in Section 5.4.

Table 5.1. Average pure water flux of cleaned ES625 and MPT-U20 membranes at ΔP =2.0 bar, CFV=1.0 m/s, T=25^{o}C, Conc.=0.5 wt % and pH=6.5.

Type	Membrane used	Number of cleaning	ΔP (bar)	Pure water flux (ℓ/m^2h)	Percent of deviation (%)
ES625	M-I	12	2.11 ± 0.02	143.6 ± 9.4	6.54
	M-II	16	2.09 ± 0.03	172.9 ± 9.1	5.26
	M-III	20	2.10 ± 0.02	163.5 ± 5.9	3.61
	M-IV	7	2.04 ± 0.02	159.4 ± 9.5	5.96
	M-V	36	2.05 ± 0.03	172.7 ± 4.6	2.66
MPT-U20	I	17	2.05 ± 0.03	210.2 ± 9.1	4.33

Statistically, the observed variation of pure water flux among ES625 membranes and between ES625 membranes and MPT-U20 membrane was significant (p-value was almost zero) at a 95 % confidence level. The result of the analysis of variance computed by MINITAB is given in Appendix-C. Thus, the assumption made that the variation of fluxes between the membranes would be significant is reasonable. In addition, the use of only one membrane to study the effect of a given operating parameter on the subject of interest avoided the interferenceof the possible variation of the flux between membranes (as a result of possible variation of membrane properties) on the evaluation of the result.

The observed variation in ΔP and other parameters during the experiments could not account for the observed variation in the pure water flux. Thus, as Dal-Cin et al. (1996) suggested, the variation should be attributed to the very nature of the permeation experiment (which is susceptible to variation from experiment to experiment) and (slight) variation of the morphological properties of the membranes one from other. In addition, MPT-U20 membrane may also have differences in hydrophilicity (in membrane material property) from that of the ES625 membranes.

The correlation of the retention and the flux showed in Section 5.4 supports that there is at least a morphological variation among ES625 membranes and between the two types of membranes.

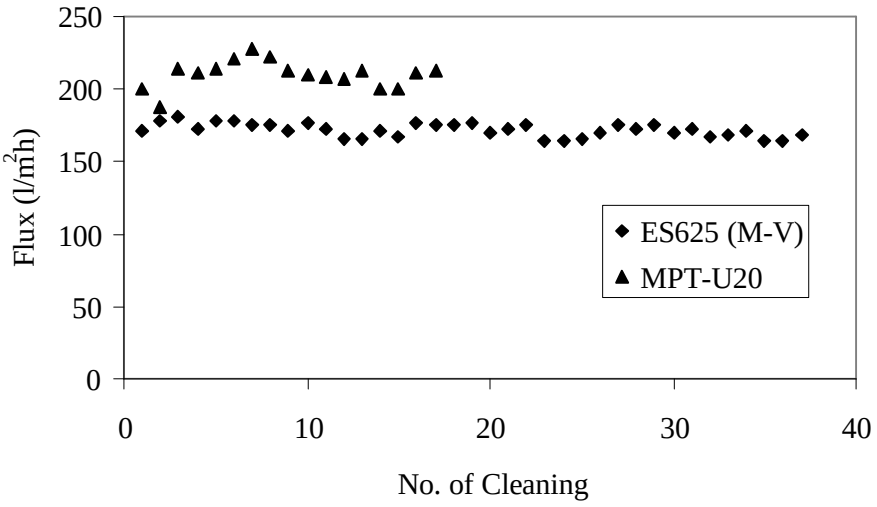

Figure 5.1. Variation of pure water flux for cleaned ES625 (M-V) and MPT-U20 membranes at ΔP =2.0 bar, CFV=1.0 m/s, T=25°C, Conc. = 0.5 wt. % and pH=6.5.

5.2. Steady state and limiting flux of ultrafiltration of starch solution

Permeate fluxes were measured for over 2 hours using ES625 membrane (M-I) for the first two experiments. These are plotted in Figure 5.2. The plot shows that the steady state was obtained very quickly, on an average in less than 15 min. In Gomez-Gotor et al. (1996) work we find almost the same steady state time for ultrafiltration of soluble starch solution, though the feed concentration used was somewhat smaller than ours. In addition, the steady state times were observed to vary with transmembrane pressure and cross flow velocity in our later experiments as the concentration and molar mass of the solute in the solution were increased. It increased with an increase in transmembrane pressure drop, feed concentration and molar mass, and decreased as the cross flow velocity was increased. For instance, we

observed that during ultrafiltration of MWIII (1500000 g/mol) starch solution with 2.0 wt % concentration, at T=25°C, ΔP =4.0 bar and CFV=0.5 m/s, the system took almost an hour to reach steady state. This might be because of the association and deformation of macromolecules at the membrane surface takes larger time to stabilize as the concentration and molar mass of the macromolecules are increased [Tager, 1971, Tanford, 1961].

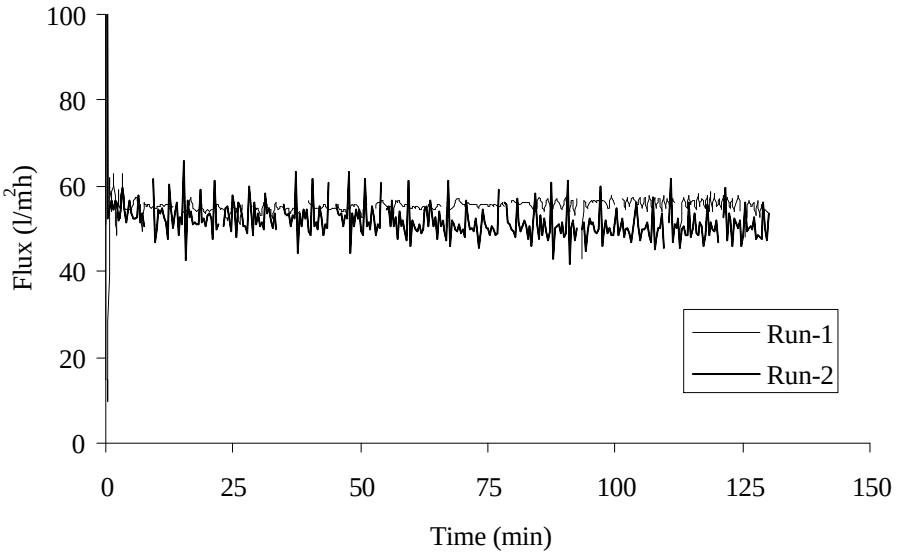

Figure 5.2. Permeate flux profile of ultrafiltration of MWI (40000 g/mol)degraded starch solution using ES625 membrane (M-I) at ΔP =2.0 bar, CFV=1.0 m/s, T=25°C and conc.= 0.5 wt % and pH=6.5.

In addition, we determined permeate flux vs. pressure for a given operating condition using the same membrane. The average permeate flux vs. pressure is plotted in Figure 5.3. As we can see from the plot, the limiting flux was reached at a pressure less or equal to about 2.0 bar. An increase of pressure beyond 2.0 bar rather reduced the permeate flux. The same phenomenon of decrease in permeate flux beyond the limiting flux was also observed in the literature [Jonsson, 1993; Ousman and Bennasar, 1996; Gomez-Gotoret al., 1996]. The reason might be that the gel/deposit of starch polymers was compacted as the pressure was increased. The existence and effect of this phenomenon during ultrafiltration of the starch solution is discussed in Section 5.3.1.

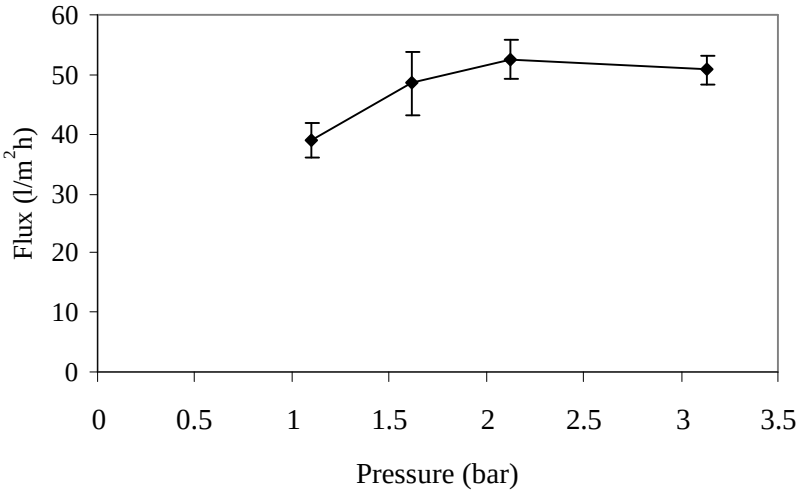

Figure 5.3. Flux vs. pressure in ultrafiltration of MWI (40000 g/mol) starch solution at CFV=1.0 m/s, T=25°C, conc.= 0.5 wt % and pH=6.5.

5.3. Contribution of the fouling mechanisms

In the forthcoming discussion, a transmembrane pressure drop of 1.5 bar and 2.0 bar were used as a reference and a maximum pressure, respectively, in the evaluation of the effect of pressure on the contribution of fouling mechanisms. The other parameters were chosen arbitrarily within the limit of the equipment and the feed solution. The values of the parameters are given in Table 5.2. The experimental results discussed hereafter were obtained by running the test for 2 h. Although the steady state of the system was observed to be reached in a shorter time, the run time was chosen assuming that the effect of different fouling mechanisms could take longer to stabilize.

Table 5.2. The value of operating variables used for the evaluation.

Membrane	CFV (m/s)	Conc. (wt. %)	pH	Pressure (bar)	Temp (^{o}C)	Model solution
ES625	0.25 1.0	0.1 0.5 1.0	4 6.5 10	0.5 1 1.5 2	25 50	MWI MWII MWIII
MPT-U20	1.0	0.1 0.5 1.0	4 6.5 10	1.5	25	MWI, MWII, MWIII

Note: the underlined values are the reference values for each variable. The variables were kept at their reference when the effect of one of the variables on the contributions of flux decline mechanisms was tested.

ES625 and MPT-U20 membranes were used for the evaluation of the significance and contribution of the fouling mechanisms. The contributions of the fouling mechanisms to the flux decline during the ultrafiltration were determined based on the flux loss ratio (FLR) principle at a given operating condition. The evaluation of how the fouling mechanisms affected the flux decline when the operating variables were varied was made using normalized[1] flux loss to avoid the effect of interdependence of the mechanisms and to make the comparison easier. Otherwise, even if only one mechanism is affected by a change of a given operating variable, the other two may also change because of their interdependence.

5.3.1. Contributions of the fouling mechanisms for ES625 membrane

5.3.1.1. Effect of pressure and cross flow velocity

The average flux data generated for four transmembrane pressure drop and two cross flow velocity values for the MWI (40000 g/mol) starch solution with 0.5 wt % concentration and a temperature of 25^{o}C using the M-II membrane are given in Table 5.3. From the table, the resistance contributed by each fouling mechanism was calculated for both cross flow velocity levels (laminar and turbulant flow regimes) at the reference operating

[1] Normalized flux loss is defined here as the flux loss due to the mechanism divide by J_i initial flux: for example, $(J_i-J_a)/J_i$, $(J_a-J_d)/J_i$, etc.

pressure (ΔP≈1.5 bar), see Figure 5.4. The flux loss caused by each fouling mechanism was also calculated and plotted in Figure 5.5 as a function of transmembrane pressure drop for both cross flow velocities.

Table 5.3. Average pure water fluxes of clean, adsorbed and fouled membranes and permeate flux vs. ΔP for MWI degraded starch solution for two levels of cross flow velocity (condition: conc. 0.5 %, temp. 25°C and pH 6.5) using membrane (M-II).

CFV (m/s) [Re]	ΔP (bar)	J_i (l/m^{2}h)	J_a (l/m^{2}h)	J_f (l/m^{2}h)	J_v (l/m^{2}h)
0.25 [3000]	0.52 ± 0.06	47.57 ± 2.7	29.4 ± 2.8	20.3 ± 0.3	13.8 ± 1.84
	1.04 ± 0.04	91.00 ± 3.8	59.5 ± 2.6	36.9 ± 2.2	18.7 ± 1.27
	1.55 ± 0.03	135.30 ± 10.0	89.6 ± 2.6	44.7 ± 5.2	21.2 ± 0.7
	2.06 ± 0.03	183.16 ± 1.8	116.1 ± 3.0	46.6 ± 6.2	21.8 ± 0.13
1.00 [12000]	0.59 ± 0.00	51.81 ± 0.1	27.9 ± 5.7	20.7 ± 1.6	19.3 ± 0.8
	1.08 ± 0.01	89.22 ± 2.5	53.7 ± 9.4	37.4 ± 0.6	31.9 ± 1.5
	1.59 ± 0.00	132.60 ± 0.2	83.2 ± 12.3	56. 8 ± 3.9	45.3 ± 3.2
	2.09 ± 0.01	177.46 ± 1.2	110.1 ± 17.9	66.5 ± 5.7	47.0 ± 2.3

Adsorption: At reference operating condition, in the turbulant flow regime, adsorption gave the largest fouling resistance (see Figure 5.4). This is expected for hydrophobic membranes [Dal-Cin et al., 1996]. The magnitude of the resistance contributed by the mechanism was observed to depend on the operating condition. According to the experimental procedure, adsorption is independent of pressure and cross flow velocity. The observed change is however due to interdependence of the contributions of all fouling mechanisms and a change in the overall fouling resistance (as a result of the change in the permeate flux due to the effect of the other two mechanisms). In order to see the effect of the parameters on the contribution made by the mechanisms to the flux loss, we calculated the normalized (relative) flux loss as a result of the mechanism. See Figure 5.5. The figure shows a larger relative flux loss due to the adsorption in the turbulent flow regime than in the laminar regime in the lower pressure range. According to the experimental procedure, this was not expected, because the adsorption was made at low and the same cross flow velocity for both flow regimes. But the cross flow velocities at which the pure water flux of the adsorbed membrane was determined were in accordance with respective flow regime at which the ultrafiltration experiments were conducted. Thus, the observed higher flux loss for turbulent flow regime might be a result of the washing off the

adsorbed solute from the membrane surface by the turbulence of the flow when the pure water flux of the adsorbed membrane was determined. The washed solute will make the water in the system less pure and hence it will give a lower flux than what is expected if the water is pure (no dissolved starch in it). As we can see from the figure, the flux loss in the turbulent flow regime decreased and approached that of the laminar flow regime as the pressure was increased. Because, as the transmembrane pressure drop is increased, the pressure holding the adsorbed solute against the membrane increases. As a result the removal of solute from the membrane surface by the shearing effect of the turbulent flow is reduced.

Concentration polarization: In the turbulence flow regime, the contribution of the concentration polarization to the flux decline was the least contributor (see Figure 5.4). As the cross flow velocity was reduced to the laminar regime, its contribution was increased. This is in agreement with ultrafiltration theory [Mulder, 1996]. The effect of the transmembrane pressure drop on the relative contribution of the concentration polarization for flux decline is shown in Figure 5.5. The figure shows that the effect of the pressure of depends on the flow regime. In the turbulent flow regime, the relative flux loss due to concentration polarization was increasing with pressure. In the laminar flow regime, however, the relative flux loss due to concentration polarization increased in the lower pressure range and decreased in the upper pressure range used in this study. This might be explained by two phenomena. One is the effect of the flux and the other is the effect of the compaction of the gel/deposit. The former is due to the fact that the pressure dependence of the flux decreased as the pressure was increased. Because, as the flux increases, more mass of the solute is brought to the membrane surface, which increases pore plugging and resistance to flow. The later might be a result of the gel/deposit getting more compact with an increase in transmembrane pressure drop. As a result of the latter phenomenon the amount of gel removed by flushing only during the cleaning of the membrane decreases with an increase in transmembrane pressure. Hence, this will be reflected in a decrease of the contribution of the concentration polarization and an increase of the contribution of the deposition as the transmembrane pressure is increased.

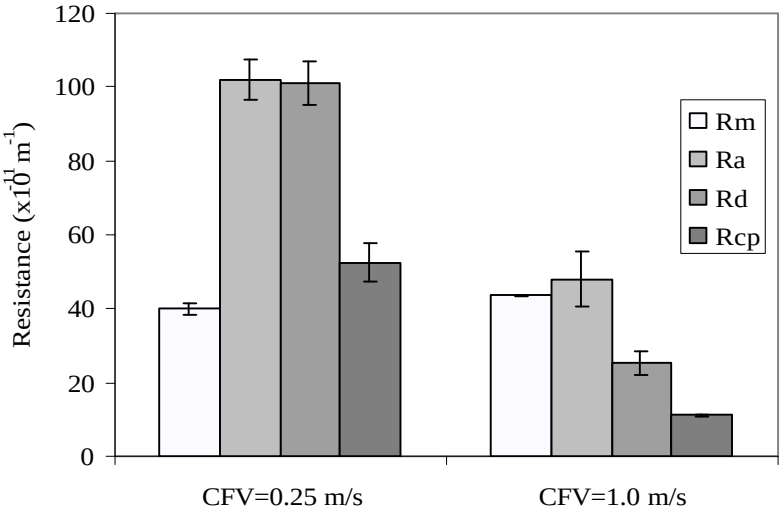

Figure 5.4. The resistance added by adsorption (R_a), deposition (R_d) and concentration polarization (R_{cp}) to the intrinsic membrane resistance (R_m) at ΔP=1.6 bar when MWI (40000 g/mol) starch solution with T=25°C, conc. = 0.5 % and pH=6.5 was ultrafiltered.

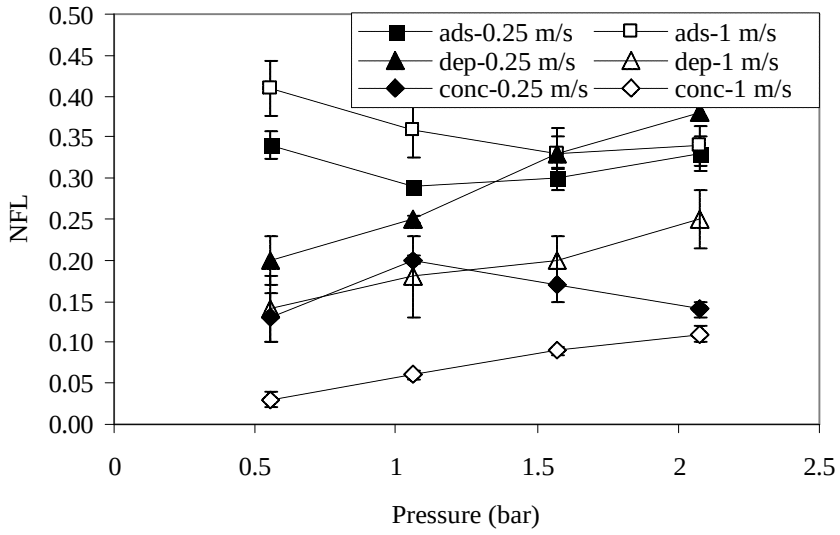

Figure 5.5. Normalized flux loss due to adsorption (ads), deposition (dep), concentration polarization (con) as a function of pressure for laminar (CFV=0.25 m/s) and turbulent (CFV=1.0 m/s) flow regimes with MWI (40000 g/mol) starch solution ultrafiltered at T=25°C, conc. 0.5 % and pH=6.5.

Deposition: Depositional fouling was the second contributor to the overall fouling resistance in the turbulent flow regime (see Figure 5.4). In the laminar flow regime, the contribution of depositional fouling was almost equal to that of the adsorptive fouling. This might be attributed to a lower shearing effect of the cross flow velocity that results in a thicker gel/deposit layer [Suki et al., 1984]. The lower the cross flow velocity, the more concentrated and thicker the gel layer would be. The effect of pressure on the relative contribution of this mechanism can also be seen in Figure 5.5. From the figure, the contribution of the mechanism to the flux decline was increasing with pressure for both levels of cross flow velocities. Ousman and Bennasar (1995) observed the same trend. This is probably due to (1) an increase gel/deposit and pore plugging when the permeate flux increases with pressure, and (2) an increase in the compaction and thickness of the gel/deposit with pressure when the flux increase with pressure is negligible.

The overall magnitude of the resistance added by the mechanisms under the laminar flow regime was much larger than that of the turbulent flow regime, see Figure 5.4. As we can see from Table 5.3 and Figure 5.5, the severity of the fouling was pressure dependent. Thus, one could conclude from this that the contribution of the fouling mechanisms to the flux decline and the severity of the fouling depends strongly on the cross flow velocity and the pressure at which the ultrafiltration experiment was run.

5.3.1.2. Effect of concentration

To see the effect of feed concentration on the relative flux loss due to the fouling mechanisms and their resistance contributions to the flux decline, the experiments were run for three concentrations (0.1, 0.5 and 1 wt %) using membrane (M-III). The results are given in Table 5.4. The normalized flux loss caused and the resistance added by each mechanism were calculated from the data and plotted in Figures 5.6 and 5.7, respectively.

Table 5.4. Average pure water fluxes of clean, adsorbed and fouled membrane and the permeate flux of MWI starch solution for three different concentrations at ΔP=1.6 bar, T=25^{o}C, CFV=1.0 m/s using membrane (M-III).

Concentration (wt %)	J_i (l/m^{2}h)	J_a (l/m^{2}h)	J_f (l/m^{2}h)	J_v (l/m^{2}h)
0.1	113.8 ± 2.7	82.8 ± 3.6	55.2 ± 4.4	51.2 ± 5.5
0.5	109.8 ± 7.9	58.8 ± 8.0	46.5 ± 6.9	39.5 ± 5.0
1.0	100.1 ± 12.4	54.5 ± 8.5	40.2 ± 3.3	33.1 ± 1.9

Adsorption: The relative flux loss caused by and the resistance added by the adsorption were the largest contributors to fouling resistance for all the three feed concentrations (see Figure 5.6). When the flux loss for the three feed concentrations are compared, the flux loss due to adsorption was the least at a concentration of 0.1 wt % and almost the same at 0.5 wt % and 1.0 wt %. The absence of flux loss difference for the last two concentrations might be because the adsorption plateau was attained at a concentration less than or equal to 0.5 wt %.

Concentration polarization: The flux loss caused by the resistance added by concentration polarization was the least for all the three feed concentrations (see Figure 5.6). The flux loss due to concentration polarization was increasing with feed concentration. This is in agreement with the literature [Mulder, 1996]. The reason is due to an increase in the osmotic pressure gradient across the membrane and the viscosity of the feed solution as a result of an increase in concentration.

Deposition: The relative flux loss caused by deposition was the second to adsorption for all the three feed concentrations (see Figure 5.6). The relative flux loss due to deposition was the largest at 0.1 wt % and the smallest 0.5 wt %. The highest flux loss at 0.1 wt % might be the result of severe depositional fouling due to pore plugging and constriction as a result of the observed higher flux compared to the fluxes for the other two concentrations. On the other hand, the cake formation increases as the concentration is increased. In addition, when the concentration is increased beyond semi-dilute concentration, the starch macromolecules in the solution start to associate and form a gel/network on the surface of the membrane. The thickness and the compaction of the gel/network also increase as the feed concentration is increased. However, since the test was conducted in a very low concentration range it does not seem to cause serious cake-deposit and gel that may surpass the contribution of pore plugging to the overall depositional fouling as a result of highest flux observed for the lowest feed concentration used. Therefore, this could lead to the observed largest flux loss due to deposition at 0.1 wt % feed concentration.

The overall fouling resistance was larger than the membrane resistance (see Figure 5.7). For the highest concentration we used, it is almost two folds of that of the membrane resistance. It was observed to increase with feed concentration. The largest portion of the resistance comes from adsorptive fouling. However, we presume that the fouling of the membrane will be severe as a result of the contribution of concentration polarization and

depositional fouling as the feed concentration is increased beyond semi-dilute concentration.

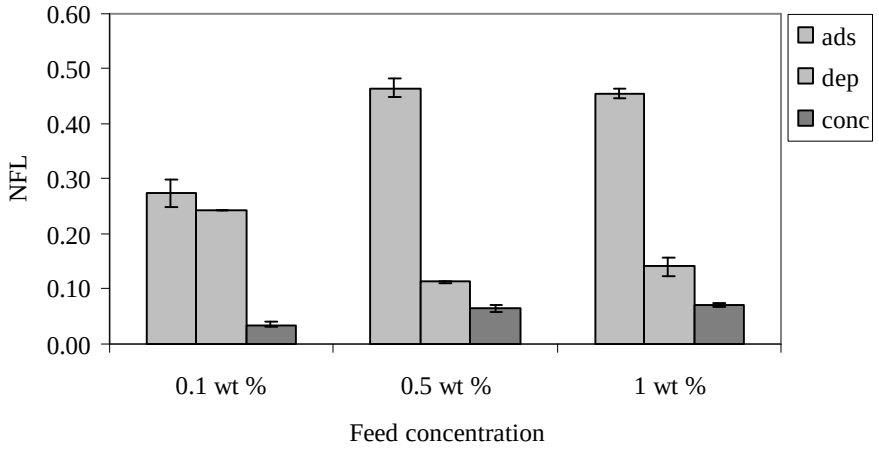

Figure 5.6. Normalized flux loss (NFL) due to adsorption (ads), deposition (dep) and concentration polarization (conc) for three different feed concentrations during ultrafiltration of MWI (40000 g/mol) starch solution at ΔP=1.6 bar, CVF=1.0 m/s, T=25^{o}C and pH=6.5.

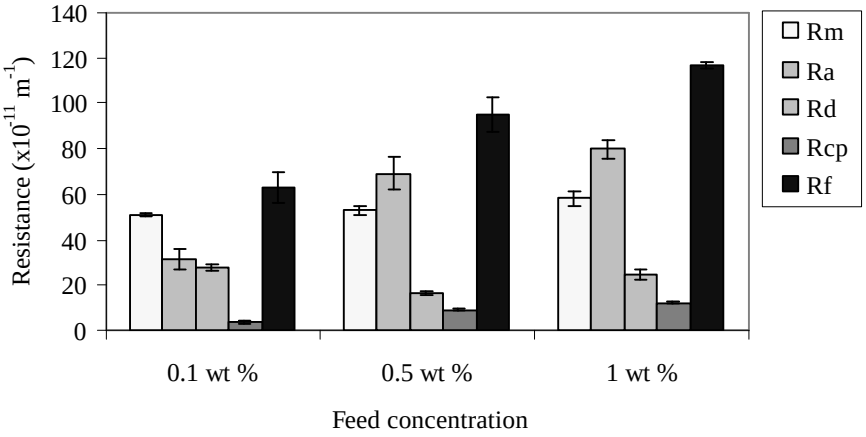

Figure 5.7. The overall fouling resistance (R_f) and the resistance contributed by adsorption (R_a), deposition (R_d) and concentration polarization (R_{cp}) and added to the intrinsic membrane resistance (R_m) during ultrafiltration of MWI (40000 g/mol) starch solution for three different concentrations at ΔP=1.6 bar, CFV=1.0 m/s, T=25^{o}C and pH=6.5.

5.3.1.3. Effect of molar mass and molar mass distribution

For the three starch solutions, the flux data generated for the evaluation of the effect of molar mass are given in Table 5.5. From the data, the relative flux loss caused by and the fouling resistance added by each fouling mechanism was calculated from the data. The result is plotted in Figures 5.8 and 5.9, respectively.

Table 5.5. Average pure water fluxes of clean, adsorbed, fouled and permeate flux determined for MWI (40000 g/mol), MWII (170000 g/mol) and MWIII (1500000 g/mol) starch solutions at ΔP=1.6, CFV=1.0 m/s, T=25^{o}C, conc. 0.5 wt. % and pH=6.5 using membrane (M-III).

Molar Mass	J_i (l/m^{2}h)	J_a (l/m^{2}h)	J_f (l/m^{2}h)	J_v (l/m^{2}h)
MWI	109.8 ± 3.9	58.8 ± 4.0	46.5 ± 3.4	39.5 ± 2.5
MWII	104.0 ± 0.4	60.0 ± 1.7	39.5 ± 0.5	35.7 ± 0.6
MWIII	111.0 ± 0.2	79.2 ± 2.9	37.2 ± 0.7	34.4 ± 0.4

Adsorption: The relative flux loss as a result of adsorption of the starch solute was decreasing, as the average molar mass of the starch in the solution was increased (see Figure 5.8). We know from the discussion in section 2.5 that the adsorption increases with molar mass for linear polymer with the same conformation. The solution of partially degraded starch is, however, composed of linear and branched molecules with a broad molar mass distribution. Accordingly, the conformation of the molecules in the solution is broad. Depending on the degree of degradation, the solution can be dominated by linear and smaller or branched and large molecules. The branched starch has a star like shape (see Figure 2.8) and is more hydrophilic than linear starch due to steric effects. Thus, when the molecules are more branched, the number of molecules adsorbed will be less, and the adsorbed network of starch layer on the membrane surface will be more loose and open. In addition, as discussed in Section 2.3, when the degraded starch is dominated by linear molecular components and an average molar mass close to about 350 DP, it has a higher tendency to reassociate and/or precipitates from the solution than other molar mass [Pfannemüller, 1971]. Since MWI starch is much closer to 350 DP, this may also favor its better adsorption on the membrane surface (solid) [Jönsson, 1998] than the other two starch solutions. In the light of this, the observed adsorption decrease with an increase in the average molar mass can be explained.

Concentration polarization: The relative flux loss due to concentration polarization was also observed to decrease with an increase in molar mass (see Figure 5.8). Theoretically, there are two opposing phenomena that affect concentration polarization. One is an increase in the concentration polarization as a result of an increase in retention with molar mass. The other is a decrease of the osmotic pressure as the molar mass is increased. That is, for a given mass concentration, the molar concentration in the solution decreases with an increase in the molar mass. In the light of the discussion in section 2.6, an increase in the osmotic pressure with concentration is not significant beyond the semi-dilute concentration. The osmotic pressure is increasing proportional to molar mass according to the relation $\pi \propto 1/M_W$. Thus, as the experimental result shows, the relative flux loss due to concentration polarization (i.e. osmotic pressure gradient across the membrane) can decrease with an increase in the molar mass of the starch.

Deposition: The relative flux loss due to depositional fouling was observed to increase with molar mass (see Figure 5.8). This could be an effect of an increase in larger macromolecules and a broader molar mass distribution as the solution was chnaged from MWI to MWIII starch solutions. The more we have larger macromolecules in the solution, the thicker the deposit will be. The broader the molecular weight distribution, the more likely the flux declines are due to all depositional phenomena: pore blocking, constriction and cake formation. Thus, these might be the explanations to why we had the fouling more severe for the larger starch molecules.

The overall fouling resistance was larger than the membrane resistance (see Figure 5.7). For the highest concentration we used, it is almost two folds of that of the membrane resistance. It was observed to increase with feed concentration. The largest portion of the resistance comes from adsorptive fouling. However, we presume that the fouling of the membrane will be severe as a result of the contribution of concentration polarization and depositional fouling as the feed concentration is increased beyond semi-dilute concentration.

As we can see from Figure 5.9, in this case, the overall fouling resistance was larger than the membrane resistance, too. For the starch with largest molar mass used in the experiments, it is more than two folds of that of the membrane resistance. It was observed to increase with an increase in molar mass. Its increase with molar mass is largely a result of an increase in depositional fouling with molar mass. Hence, one can presume that the fouling of the membrane will get severe as a result of an increase in the

depositional fouling when the molar mass of the starch in the solution is increased.

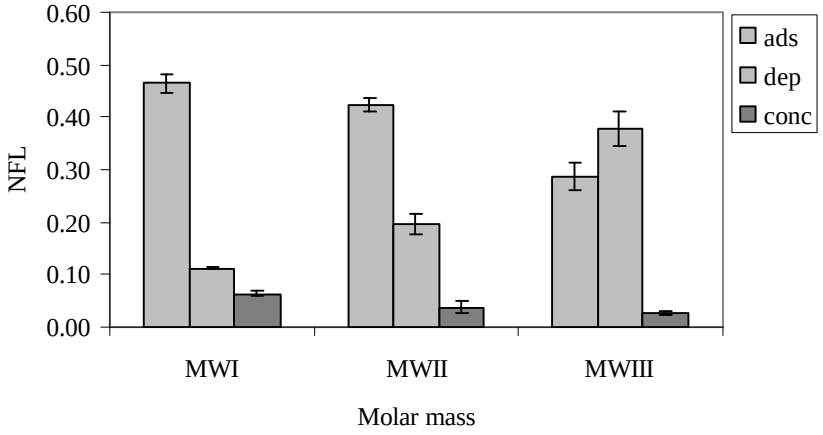

Figure 5.8. Normalized flux loss (NFL) due to adsorption (ads), deposition (dep) and concentration polarization (conc) during ultrafiltration of starch solutions with three different molar masses: MWI (40000 g/mol), MWII (170000 g/mol) and MWIII (1500000 g/mol) at ΔP =1.6 bar, CFV=1.0 m/s, T=25^{o}C, conc.= 0.5 wt % and pH=6.5.

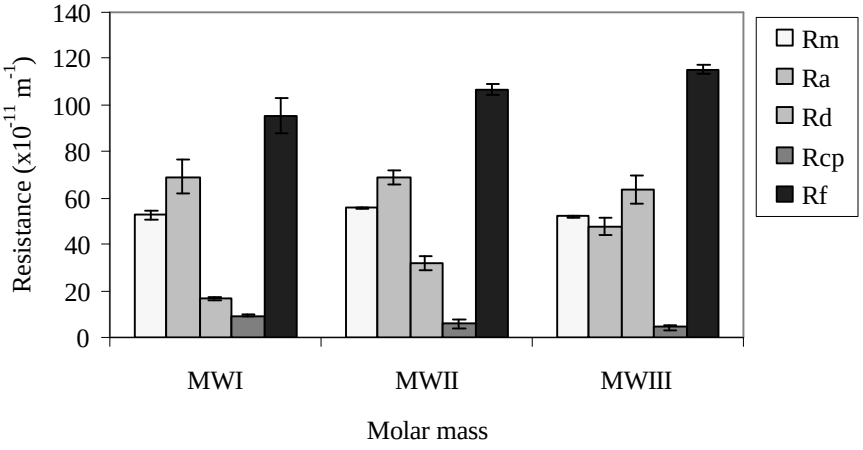

Figure 5.9. The overall fouling resistance (R_f) and the resistance contributed by adsorption (R_a), deposition (R_d) and concentration polarization (R_{cp}) and added to the intrinsic membrane resistance (R_m) during ultrafiltration of starch solution with three different molar masses: MWI (40000 g/mol), MWII (170000 g/mol) and MWIII (1500000 g/mol) at ΔP =1.6 bar, CFV=1.0 m/s, T=25^{o}C, conc.= 0.5 wt % and pH=6.5.

5.3.1.4. Effect of temperature

In order to see the effect of temperature on the contribution of the fouling mechanisms, experiments were carried out for an other level of temperature, 50°C, using membrane (M-III). The average measured fluxes with their corresponding standard deviations are given in Table 5.6. From this table, the relative flux loss caused and the resistance contributed by each mechanism are plotted in Figures 5.10 and 5.11, respectively. The table shows that the flux data obtained at 50°C are almost two fold of those at 25°C. For the clean membrane, an increase in pure water flux was due to a decrease in the viscosity of the water as the temperature was increased. In addition to this, other phenomena also affected the pure water flux of adsorbed and fouled membranes, and the permeate of the solution. This is discussed below in relation to each fouling mechanism.

Table 5.6. Average pure water fluxes of clean, adsorbed and fouled membrane and permeate flux of ultrafiltration of MWI (40000 g/mol) degraded starch solution with conc=0.5 %, pH=6.5, ΔP=1.6 bar and CFV=1.0 m/s using membrane (M-III).

Temperature (°C)	J_i (l/m^{2}h)	J_a (l/m^{2}h)	J_f (l/m^{2}h)	J_v (l/m^{2}h)
25	109.8 ± 3.9	76.8 ± 4.0	60.9 ± 3.4	50.3 ± 2.5
50	180.1 ± 10.0	170.2 ± 9.1	111.0 ± 2.0	88.1 ± 1.7

Adsorption: The flux loss due to adsorption decreased very much when the temperature was increased from 25°C to 50°C (Figure 5.10). At 50°C, its contribution to the flux decline was the least as compared to the other mechanisms. The decrease of the adsorption effect as the temperature was increased was in agreement with literature [Jönsson et al., 1998]. The most likely explanation is that the solubility of the starch in water increases with an increase in temperature. This implies, of course, that the starch has a lower adsorption isotherm at 50°C than at 25°C.

Concentration polarization: The relative flux loss due to concentration polarization was increased, as the temperature was increased (see Figure 5.10). This was attributed to the higher flux at 50°C, which increased the amount of the starch brought towards the surface of the membrane. The concentration polarization was also observed to be the second largest contributor for the overall flux decline at 50°C, though it was not much larger than that of adsorption.

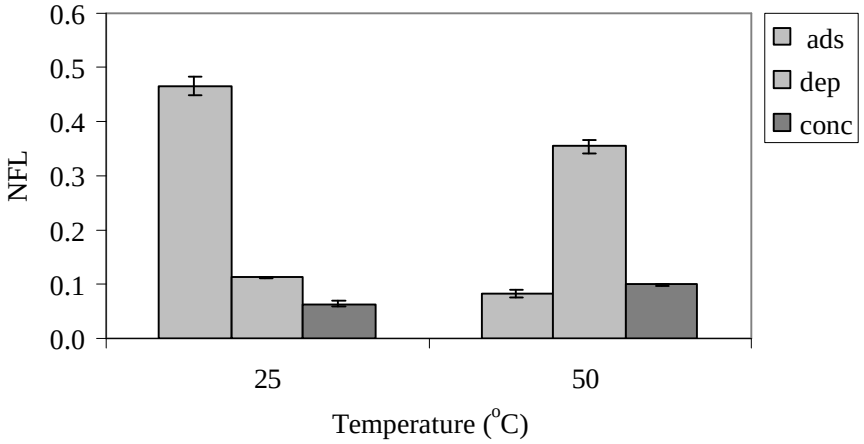

Figure 5.10. Normalized flux loss (NFL) due to adsorption (ads), deposition (dep) and concentration polarization (conc) during ultrafiltration of MWI (40000 g/mol) starch solution at two temperatures at ΔP =1.6 bar, CFV=1.0 m/s, conc=0.5 wt % and pH=6.5.

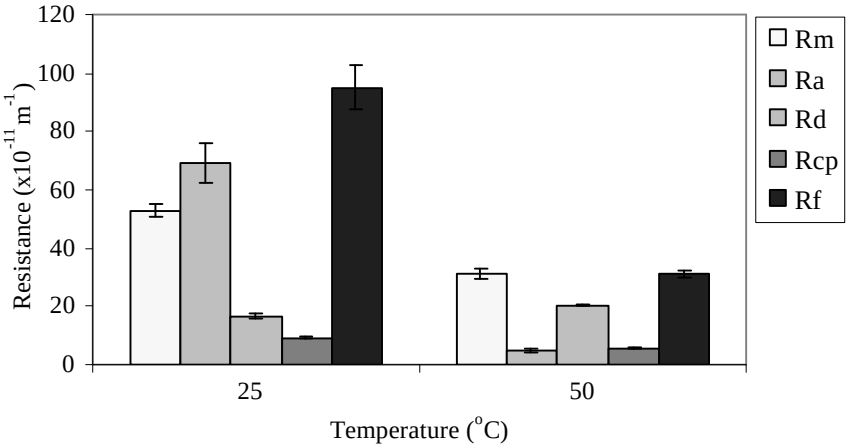

Figure 5.11. The overall fouling resistance (R_f) and the resistance contributed by adsorption (R_a), deposition (R_d) and concentration polarization (R_{cp}) and added to the intrinsic membrane resistance (R_m) during the ultrafiltration of MWI (40000 g/mol) starch solution at two temperatures at ΔP =1.6 bar, CFV=1.0 m/s, conc=0.5 wt % and pH=6.5.

Deposition

When we compare the relative flux loss due to the depositional fouling for the two temperature levels, the loss at 50°C was much higher than at 25°C (see Figure 5.10). Deposition was also the largest contributor to the overall flux decline at 50°C. The relative flux caused more severe fouling due to pore plugging, constriction and deposit.

Overall, we see that the fouling resistance was reduced by a factor of four as the temperature was increased from 25°C to 50°C, which can be seen in Figure 5.11. As said before, it was largely because of a decrease in the viscosity of the solvent, in our case, water. In addition, an increase in the solubility of starch in the water (a decrease in the adsorption of the starch) might also have a significant effect. At 50°C, the effect of adsorption on the flux decline was almost removed. At this temperature the flux decline was largely due to depositional fouling. Therefore, we can say that operating at the higher temperature reduces the adsorptive fouling and the overall fouling resistance during ultrafiltration of partially degraded starch solution. Of course, all these results were expected.

5.3.1.5. Effect of pH on the adsorption

The experiments were carried out to evaluate the flux decline due to adsorption for three different pH levels: acidic, neutral (reference pH) and alkaline, using membrane (M-III). The pure water fluxes of the membrane measured before and after adsorption are given in Appendix D.3, Table D-5. The calculated flux loss data due to adsorptive fouling for the three pH levels are plotted in Figure 5.12.

As it can be seen from the figure, the flux loss due to adsorption was slightly decreasing as the pH was increasing. But, the change of the flux loss with pH was within the range of experimental error. This makes it difficult to draw a conclusion on the effect of pH on the adsorption of starch on the membrane. However, if there is any such effect, there are two phenomena that might be responsible for the observed behavior. One is the shielding effect of the excess hydrogen ion at lower pH and the repulsion effect of hydroxyl ion at higher pH. Although it is small, a neutral membrane surface (i.e. hydrophobic membrane) and starch molecules have a negative surface charge in aqueous solution. Thus, this could cause the repulsive force of certain magnitude acting against the adsorptive force when the starch molecules approach the membrane. The presence of excess hydrogen ions could shield and take away or reduce this repulsive force while the presence of excess hydroxyl ions could increase the magnitude of this force. Another

possible reason might be that alkaline environments are better in dissolving carbohydrate, protein, etc than acidic ones [Bartlett et al, 1995; Razavi et al., 1996] in water. Eckner and Zottala (1992) also found in their work that flux increases as the pH is increased from acidic to alkaline conditions, though their result was obtained from ultrafiltration of skimmed milk. Therefore, theoretically, one can conclude that adsorption of starch decreases as the pH of the solution is increasing. This supports the result obtained from our experimental data.

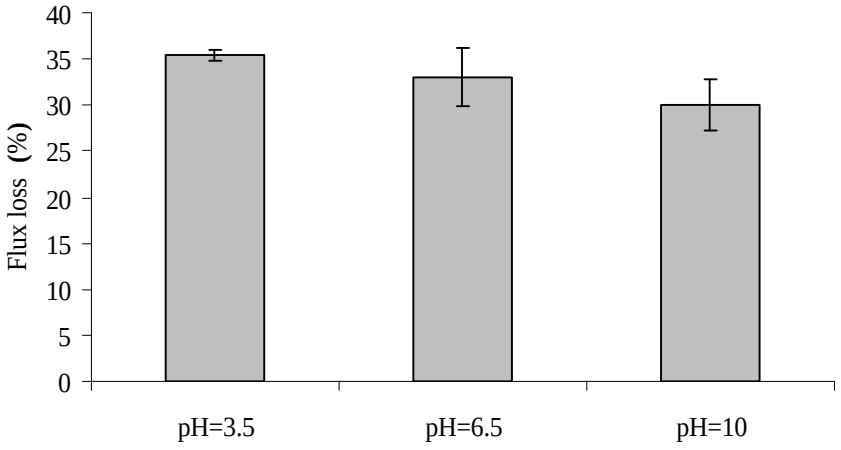

Figure 5.12. Flux loss due to adsorption of MWI (40000 g/mol) starch in solution with 0.5 wt % conc. on ES625 membrane M-III at three different pH levels and ΔP=1.6 bar, CFV=1.0 m/s and T=25^{o}C.

5.3.2. Contribution of flux decline mechanisms for MPT-U20 membrane

In this section, we discuss the effect of three operating parameters: feed concentration, molar mass and pH on the relative flux loss due to each of the fouling mechanisms and their contribution to the overall fouling resistance for MPT-U20 membrane.

5.3.2.1. The effect of feed concentration

The flux data generated from ultrafiltration experiments for three feed concentration levels are given in Table 5.7. The relative flux loss caused and the resistance contributed by each mechanism are calculated from the data in the table and plotted in Figures 5.13 and 5.14, respectively.

Table 5.7. Average pure water fluxes of clean, adsorbed and fouled membrane, and the permeate flux for three different concentrations of MWI starch solution at ΔP=1.6 bar, T=25°C, CFV=1.0 m/s and pH=6.5.

Concentration (wt %)	J_i (l/m^{2}h)	J_a (l/m^{2}h)	J_f (l/m^{2}h)	J_v (l/m^{2}h)
0.10	166.0 ± 1.8	115.4 ± 3.4	86.4 ± 1.3	70.7 ± 1.1
0.50	155.3 ± 8.9	101.0 ± 3.9	69.6 ± 2.6	50.8 ± 1.7
1.00	169.6 ± 0.3	107.6 ± 1.3	60.7 ± 0.1	35.9 ± 1.0

Adsorption: At the reference operating conditions, the relative flux loss due to adsorption was the largest (see Figure 5.13). When we compare the relative flux loss due to adsorption for the three feed concentrations, we get the lowest at 0.1 wt % and almost equal for the other two concentration levels. This trend is similar to what is observed for ES625 membrane. For MPT-U20 membrane, however, the magnitude of the relative flux loss is smaller for the two higher feed concentrations. The experimental error was too small to account for the difference between the two membranes. Thus, the difference may be a result of the larger pores of the MPT-U20 membrane. That means, some of the adsorbed starch can be washed away during flushing of the membrane after the membrane is contacted with starch solution for adsorption and during the determination of the pure water flux of the adsorbed membrane. This may result in a larger pure water flux through the adsorbed membrane J_a, and hence, the flux loss due to adsorption (J_i-J_a) will be smaller.

Concentration polarization: The relative flux loss due to the concentration polarization was the least for this membrane (see Figure 5.13). Its trend with an increase in concentration is also similar way as the ES625 membrane. But its magnitude is larger for the MPT-U20 membrane than for the ES625 membrane because of its larger permeate flux, which increases the mass brought (concentration polarization) to the membrane surface.

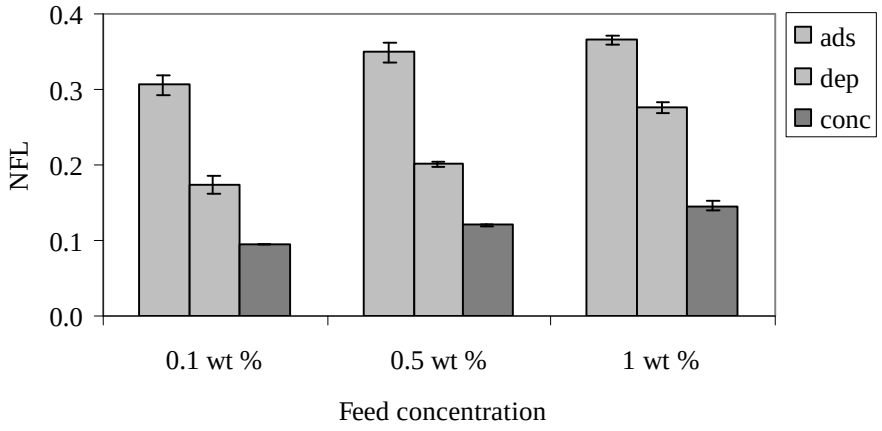

Figure 5.14. Normalized flux loss (NFL) due to adsorption (ads), deposition (dep) and concentration polarization (conc) during ultrafiltration of MWI (40000 g/mol) starch solution for three different concentrations at ΔP =1.6 bar, CFV=1.0 m/s, T=25^{o}C and pH=6.5.

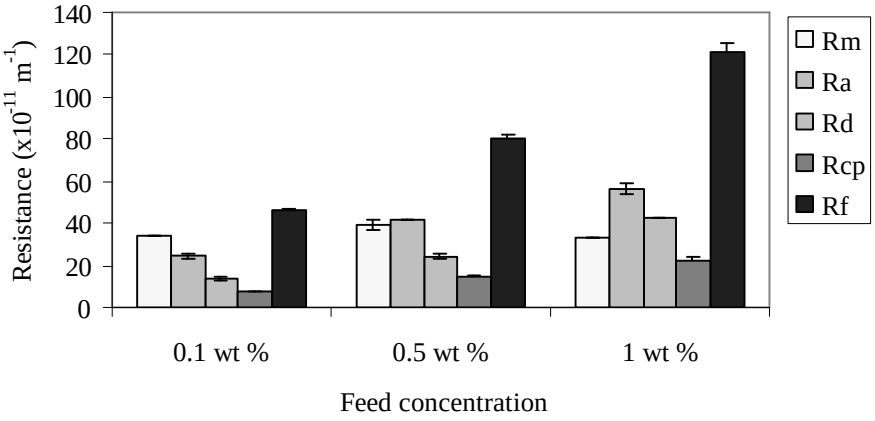

Figure 5.15. The overall fouling resistance (R_f) and the resistance contributed by adsorption (R_a), deposition (R_d) and concentration polarization (R_{cp}) and added to the intrinsic membrane resistance (R_m) during ultrafiltration of MWI (40000 g/mol) starch solution for three different concentrations at ΔP=1.6 bar, CFV=1.0 m/s, T=25^{o}C, and pH=6.5.

Deposition: For the MPT-U20 membrane, the deposition was also the second largest contributor to the flux decline observed. The relative flux loss due to the mechanism increased with the feed concentration. This trend is different from what was observed for the ES625 membrane, which can be seen by comparing Figures 5.6 and 5.14. The difference might also be attributed to the larger pores of the MPT-U20 membrane. One reason might be the decrease in the contribution of adsorption to the flux loss as a result of washing of the adsorbed starch from the pores of the membrane. The larger J_a as a result of the washing of the adsorbed starch is, the larger the flux loss due to deposition (J_a-J_f) will be. In addition, if the pore size gets larger than the size of the macromolecules, fouling of the membrane due to pore plugging and constriction decreases. On the other hand, the deposition fouling due to deposit/cake formation on the membrane surface increases always with concentration. Thus, the net effect could be an increase in overall depositional fouling as the feed concentration is increased.

As we can see in Figure 5.15, for this membrane, the overall fouling resistance is larger than the membrane resistance. For the highest concentration, the fouling resistance is about three fold of the membrane resistance. This is larger than that of ES625 membrane (compare Figures 5.7 and 5.15). The difference is an effect of the larger pore of the MPT-U20 membrane. The overall fouling resistance is however comparable to that of the ES625 membrane and is increasing with the feed concentration. All fouling mechanisms have a significant contribution at all levels of feed concentration. As said for ES625 membrane, it seems also that the depositional fouling and concentration polarization would be responsible for the severity of the fouling as the feed concentration is increased.

5.3.2.2. Effect of molar mass and molar mass distribution

The flux measured with respect to molar mass for the same MTU-U20 membrane is given in Table 5.8. From the table, we calculated the contribution of each mechanism and its relative resistance and plotted the results in Figures 5. 16 and 5.17, respectively.

Table 5.8. Average pure water flux of clean, adsorbed and fouled membrane, and the permeate flux of ultrafiltration of starch solution for three different molar masses: MWI (40000 g/mol), MWII (170000 g/mol) and MWIII (1500000 g/mol) at ΔP=1.6 bar, CFV=1.0 m/s, conc=0.5 % and pH=6.5.

Molar mass	J_i (l/m^{2}h)	J_a (l/m^{2}h)	J_f (l/m^{2}h)	J_v (l/m^{2}h)
MWI	155.3 ± 8.9	1010.0 ± 3.9	69.6 ± 2.6	50.8 ± 1.7
MWII	162.5 ± 0.3	115.6 ± 1.1	79.5 ± 0.6	46.6 ± 0.8
MWIII	159.0 ± 0.6	107.9 ± 1.9	67.6 ± 0.5	35.1 ± 0.2

Adsorption: The relative flux loss due to adsorption was found to be the largest for MWI starch solution and the least for MWII starch solution (see Figure 5.16). This is also different from the trend of the flux loss vs. molar mass observed for the ES625 membrane (see Figures 5.10 and 5.16). The magnitude of the flux loss was also smaller for the MPT-U20 membrane than for the ES625 membrane. One might attribute the observed difference to the morphological and the hydrophilicity difference between the two membranes. However, even if MPT-U20 membrane were more hydrophilic than ES625 membrane, the trend of flux loss would not be different from that of ES625 membrane. Because, the amount of the degraded starch adsorbed on a given membrane (irrespective of its hydrophilicity) decreases as the hydrophilicity of the degraded starch decreases with an increase in the molar mass. But the difference in the hydrophilicity between the membranes affects the degree of adsorption. The smaller relative flux loss observed for the MPT-U20 membrane may be partly attributed to that it is more hydrophilic (as expected by the manufacturer). For the observed difference in trend of relative flux loss the higher pore size of the MPT-U20 membrane could be responsible. For instance, assuming that the two membranes have no difference in hydrophilicity, at the same operating condition the adsorbed mass on both types of membranes could be equal for each model starch. However, when the pure water flux of the adsorbed membrane was determined, the larger amount of adsorbed starch around and in the pores of the MPT-U20 membrane than in the ES625 membrane could be washed away. This seems to be due to the larger pore size and higher flux through the pores of the MPT-U20 membrane. The amount of adsorbed starch washed from the membrane decreases as the average molecular weight is increased. Thus, the overall effect could be: (1) the relative flux loss due to adsorption is lower for the MPT-U20 membrane as compared to that of the ES625 membrane, and (2) for the MPT-U20 membrane, the relative flux loss due to adsorption is the least for the MWIIstarch solution.

Concentration polarization: The relative flux loss due to concentration polarization was increased, as the molar mass was increased (see Figure 5.16). The trend of the flux loss due to concentration polarization is also opposite to that of the ES625 membrane (see Figures 5.8 and 5.16). The magnitude of relative flux was also larger than what was observed for the ES625 membrane. As discussed earlier, theoretically, the contribution of concentration polarization to the flux decline decreases as the molar mass is increased. The reason for the deviation from this may be attributed to the larger pores of the MPT-U20 membrane and the experimental procedures used to determine the fluxes that were used in the evaluation of the contribution of the fouling mechanisms. For MWI starch solution, MPT-U20 membrane might be fouled largely as a result of pore plugging and constriction. For MWIII starch, the depositional fouling might come largely from deposit or gel formed on the surface of the membrane. In addition, the deposit/gel compaction decreases and the thickness increases as the molar mass is increased. Hence, when the fouled membrane is flushed right after it is used for ultrafiltration of the solution, some deposit will be washed away. The amount of the washed starch increases with the thickness and the looseness of the deposit. That means, it increases with molar mass of the starch in the solution. As a result this may give largest J_f-J_v (flux loss due to concentration polarization) for MWIII and the least for MWI starch, as shown in Figure5.16. Thus, it seems that the interaction of the pore size of the membrane and experimental procedure is largely responsible for the observed difference between the two membranes. That means if these effects were removed, we might have end up with a trend similar to that of the ES625 membrane.

Deposition: The relative flux loss due to deposition was also increased with molar mass. The trend was similar to what was observed for the ES625 membrane but the contribution with this membrane was larger. That might be the effect of the higher flux and the larger pores of the MPT-U20 membrane. As a result the membrane had severe overall depositional fouling due to more severe pore plugging and constriction, and a thicker and more compact deposit/gel. There may also be the effect of the flushing process of the fouled membrane on the deposit/gel thickness we considered earlier (under concentration polarization), and yet the result could assume the observed trend. That means, the actual depositional fouling could be larger than what was observed.

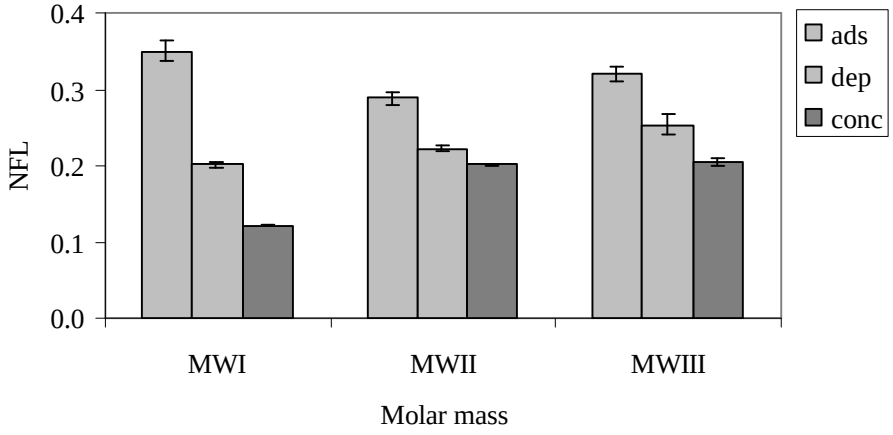

Figure 5.16. Normalized flux loss (NFL) due to adsorption (ads), deposition (dep) and concentration polarization (conc) during ultrafiltration of MWI (40000 g/mol), MWII (170000 g/mol), and MWIII (1500000 g/mol) starch solutions with 0.5 wt % concentrations at ΔP =1.6 bar, CFV=1.0 m/s, T=25^{o}C and pH=6.5.

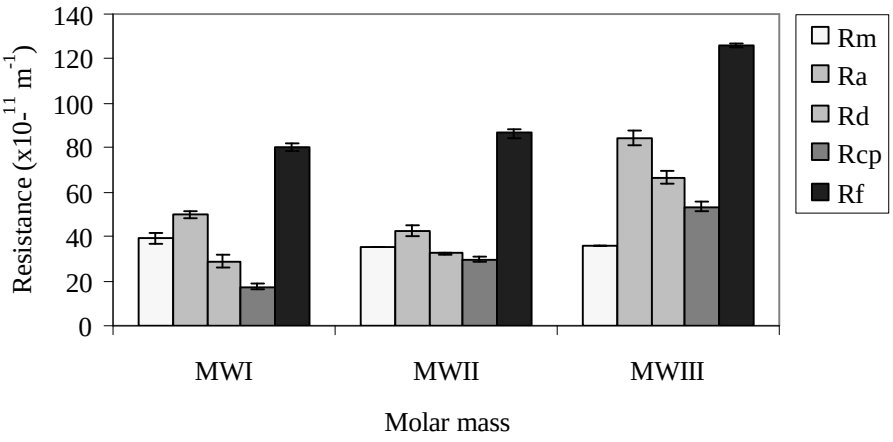

Figure 5.17. The overall fouling resistance (R_f) and the resistance contributed by adsorption (R_a), deposition (R_d) and concentration polarization (R_{cp}) and added to the intrinsic membrane resistance (R_m) during ultrafiltration of MWI (40000 g/mol), MWII (170000 g/mol), and MWIII (1500000 g/mol) starch solutions with 0.5 wt % concentrations at ΔP=1.6 bar, T=25^{o}C, and pH=6.5.

The overall fouling resistance is larger than the membrane resistance (see Figure 5.17). For the larger molar mass used in the experiments, it is about three folds of the membrane resistance. This is also larger that of the ES625 membrane (compare Figures 5.9 and 5.17). The difference is due to the larger pore of the MPT-U20 membrane. The overall fouling resistance is however comparable with that of ES625 membrane and was increasing with an increase in molar mass. Each mechanism has a significant contribution to the overall resistance at all model starch levels. In addition, as said for ES625 membrane, the depositional fouling seems to dominant limiting fouling mechanisms as the molar mass increases.

5.3.2.3. Effect of pH on the adsorption

The effect of pH on the adsorption of MWI starch solution on MPT-U20 membrane was evaluated by measuring pure water fluxes before and after cleaning the membrane. The flux was measured before and after starch was adsorbed on the membrane at a concentration of 0.5 wt %, a temperature of 25^{o}C and a pressure of 1.6 bar for three different pH levels. The measured data is given in Appendix D.6, Table D-10. The flux loss due to adsorption calculated from the flux data is plotted in Figure 5.18.

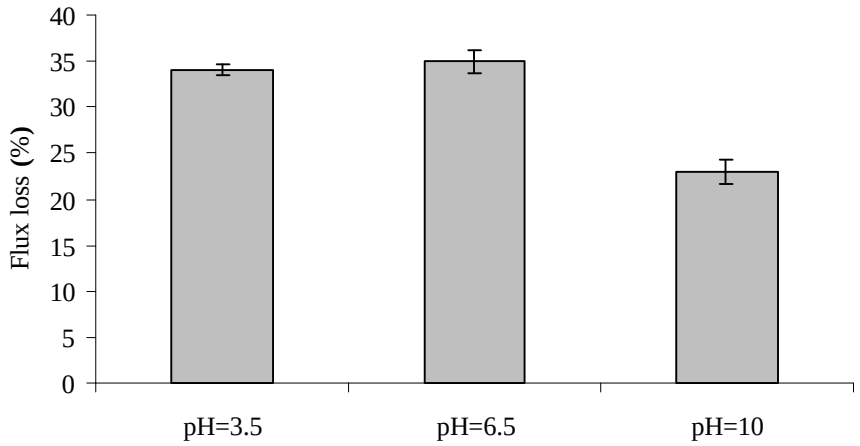

Figure 5.18: Flux loss due to adsorption of MWI (40000 g/mol) starch in solution with 0.5 wt % conc. on MPT-U20 membrane at three different pH levels and ΔP=1.6 bar, CFV=1.0 m/s and T=25^{o}C.

The result shows almost equal flux losses in acidic and neutral environments. For an alkaline environment, however, the flux loss due to adsorption is much less than for the other two pH levels. For the observed result of this membrane, the discussion given in section 5.3.1.5 might also be applied. Thus, an alkaline environment of the solution seems to give the least adsorption of starch on the membrane.

5.3.3. Summarizing remarks

In ultrafiltration of partially degraded starch solution, all fouling mechanisms (adsorption, concentration polarization and deposition) were responsible for the flux. The major contributors were however adsorption and deposition. Their severity was dependent on the operating conditions. Adsorption is largely responsible at low-pressure operation while the deposition effect increased with pressure and became dominant at higher pressures (near or the beyond limiting flux). The effect of deposition at higher pressure seems to come mainly as result of the compaction of the gel/deposit of starch formed on the membrane surface. The depositional fouling resistance seems to have more than linear relationship (e.g. a power function with power larger than 1) with the transmembrane pressure drop. Although the concentration polarization effect is relatively small, it is also observed to increase linearly with pressure in the turbulent flow regime. In the laminar flow regime, the fouling due to concentration polarization is much larger than that in the turbulent flow regime. However, its contribution increases for the lower pressure and decreases for the higher-pressure range used in this study. An increase in cross flow velocity also reduces the resistance contributed by deposition. An increase in the operating temperature is observed to reduce largely the flux loss due to adsorption and increase deposition and concentration polarization. However, the overall fouling resistance added is reduced when the temperature is increased.

The two membranes showed somehow different patterns of flux loss due to adsorption and concentration polarization with an increase in feed concentration and molar mass. The cause of the difference in the contribution of the flux decline mechanisms for the two membranes are most likely due to the difference in the morphology between the two membranes and the experimental procedure. There might also be some difference in the hydrophilicity that might be partly responsible for the lower flux loss to each of the mechanisms. This should be checked in a future study. In any case, during the ultrafiltration of the model starch

solutions, for both types of membranes the overall fouling resistance increased with concentration and molar mass. In addition, adsorption of starch on both membrane types was observed to be the least in an alkaline environment.

5.4. Ultrafiltration membrane performance

5.4.1. Retention

5.4.1.1. Comparison between retention of ES625 and MPT-U20 membranes

The retention of four ES625 membranes (M-I, M-II, M-III and M-V) and one MPT-U20 membrane was determined. The samples used for the analysis were the feed and permeate samples collected from the first two runs for each membrane. For comparison, the average retention at the reference operating condition was plotted in Figure 5.18. As it was for the pure water flux of cleaned membranes, statistically, the variation of the retention from membrane to membrane was significant (p-value was less than 0.032) for a 95 % confidence interval, see Appendix-C.2. At the given operating condition, from the ES625 membrane group, membrane (M-V) had the lowest retention while membrane (M-III) had the highest. On the other hand, the MPT-U20 membrane had a lower retention than all the ES625 membranes. This result seemed to be related to the discussion on the membrane pure water flux in Section 5.2. The membrane with the lowest flux also showed the largest retention. As said earlier in Section 5.1, this supports that the variation of the flux between the membranes is due to the difference in their morphology: their pore size and pore size distribution.

However, we can approximate the retention of the ES625 membranes by the average retention of all the four sample membranes, which was found to be 64.85 ± 5.58 %. For the MPT-U20 membrane, in order to get the average retention of the membrane, tests should be done on more membranes. As a preliminary information, however, we can use the retention of the only MPT-U20 membrane used, which is53.82 ± 3.88 %.

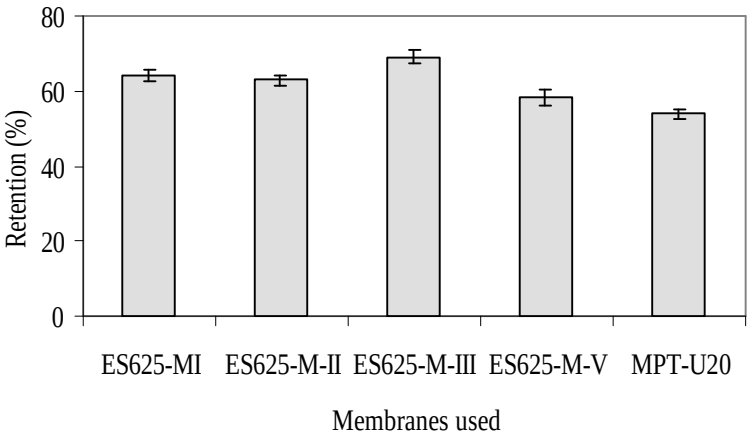

Figure 5.18. Comparison of the retention of the different ES625 membranes and MPT-U20 membrane for MWI (40000 g/mol) starch in solution with conc=0.5 wt % at ΔP=1.6 bar, CFV=1.0 m/s, T=25^{o}C and pH=6.5.

5.4.1.2. Effect of operating parameters on retention

The dependence of retention on three operating parameters was investigated for the ES625 membrane (M-V). The parameters were the transmembrane pressure drop, cross flow velocity and the molar mass of the model starch. The result was plotted in Figure 5.19 as retention vs. transmembrane pressure drop for a given cross flow velocity and molar mass. The plots show similar trends but are quantitatively different. This difference was dependent on the values of the cross flow velocity and molar mass of starch in the solution.

As seen in the figure, the retention curves tend to be concave upward. For CFV ≈ 1.0 m/s, the retention decreased until it attained a constant value for pressures between 0.6 and 3.0 bar. One can presume that even for CFV≈ 1.0 m/s, the curve might tend to concave upward if the ultrafiltration was also run for a larger transmembrane pressure drop. This behavior may be explained by the effect of pressure on concentration polarization and depositional fouling. As discussed in Sections 3.2 and 5.2, concentration polarization increases with pressure where the flux increases with pressure (until the limiting flux is attained). On the other hand, the deposition fouling increases with pressure over the whole range of pressures used. In the lower pressure range the depositional fouling is largely due to pore plugging and constriction while for the higher pressure range the deposit/gel compaction

seems to make the fouling severe. This is due to pore blocking, constriction and/or deposit, or compaction of deposit. Thus, the former might lead to a decrease in retention as the pressure was increased in the lower range of pressures while the latter could lead to an increase in retention as pressure was increased in a higher range of pressure.

The effect of cross flow velocity on retention was observed to depend on molar mass. For the MWI (40000 g/mol) starch solution, retention increased as the cross flow velocity was increased from 0.5 to 1.0 m/s and decreased as the cross flow velocity was increased from 1.0 to 1.5 m/s. For the MWII (170000 g/mol) starch solution, the retention increased with cross flow velocity. This could be a result of two opposing effects an increase in cross flow velocity generates. When the cross flow velocity is increased, the concentration polarization (the concentration gradient across the membrane) is reduced and the flux is increased. The reduction in concentration polarization may improve retention. On the other hand, an increase in the flux increases the drag force on the solute, which may result in a decrease in the retention for a relatively smaller and flexible solute. Because, the smaller and the more flexible the solute is, the easier it can be deformed and squeezed through the pores when the drag forces on the solute is high. When the size of the molecule gets larger and more branched (larger than the pore of the membrane), the effect of the drag force will be less, or may cause rather an increase in pore blocking, which results in an increase in retention. Hence, the effect of the drag force (the flux) might be cancelled out due to an increase in flux when the cross flow velocity is increased. In light of this, the former may be the cause for the retention profile obtained for the MWI starch solution and the latter for the retention of the MWII starch solution.

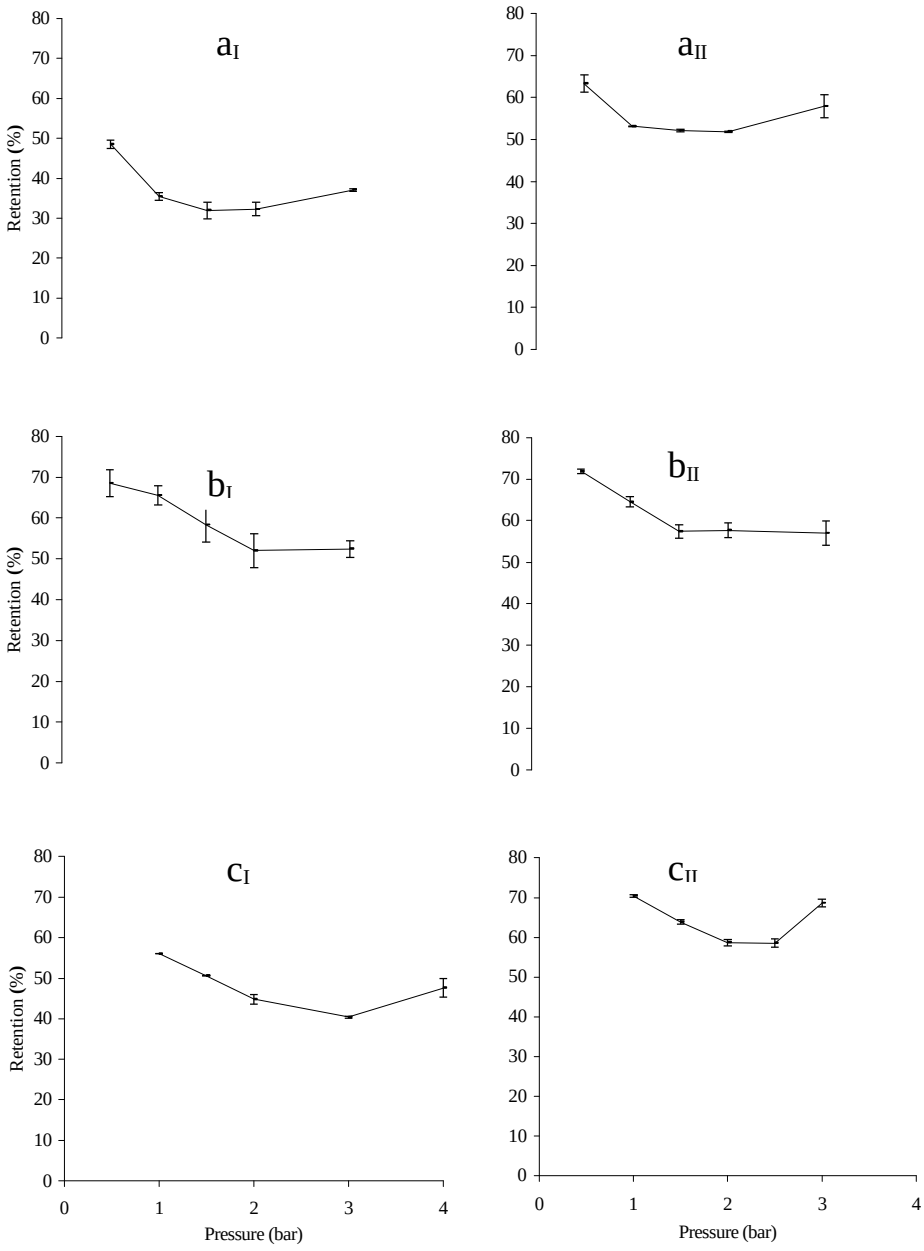

Figure 5.19. Retention vs. pressure at (a) CVF=0.5 m/s, (b) CFV=1.0 m/s, and (c) CFV=1.5 m/s, conc=0.5 %, T=25^{o}C and pH=6.5. The subscript I and II indicate MWI (40000 g/mol) and MWII (170000 g/mol) starch solutions used during the ultrafiltration, respectively.

5.4.2. Permeate flux and the effect of operating parameters

The permeate flux was measured in ultrafiltration of two starch solutions with different molar masses, MWI (40000 g/mol) and MWII (170000 g/mol), for five transmembrane pressures for each level of cross flow velocity and feed concentration at 25°C and pH 6.5. The experiments were conducted for three cross flow velocities and feed concentration levels. The values used were: for the cross flow velocities 0.5, 1.0 and 2.0 m/s, for the transmembrane pressure drop 0.5, 1.0, 1.5, 2.0, 2.5, 3.0 and 4.0 bar, and for the feed concentration 0.5, 1.0 and 2.0 wt %. The values of the fluxes measured for each set of operating conditions is given in Appendix–D, Table D-8.

The average flux vs. transmembrane pressure drop with their corresponding standard deviation is plotted in Figure 5.20 for MWI starch solution and in Figure 5.21 for MWII starch solution for each set of cross flow velocity and feed concentration. From the figures the following observation can be made. The flux and the limiting (maximum) flux were increased with cross flow velocity. The limiting flux was decreased as the concentration and the molar mass was increased. As the applied transmembrane pressure drop was increased beyond the limiting flux, the flux was observed to decrease. In the light of the theoretical background in Section 3.2 and the discussion in Section 5.3, the observed effect of cross flow velocity, concentration and molar mass was expected. Flux decline beyond the limiting value was also observed in previously cited works. The reason can be summarized as follows. As discussed earlier, the flux decreased as concentration was increased. This was a result of an increase in viscosity and in the osmotic pressure gradient across the membrane. As the cross flow velocity was increased, the flux was improved as a result of the reduction in concentration polarization. The flux was decreased as the molar mass was increased due to an increase in the amount of particles retained by the membrane, which increases the resistance to liquid flow toward and through the membrane. Flux decline beyond the limiting pressure was largely due to an increased compaction of the deposit/gel layer on the membrane as the transmembrane pressure drop was increased.

For both model solutions at the lowest feed concentration used, the limiting (maximum) flux was reached at about $\Delta P \leq 2.0$ bar. As the concentration was increased, the limiting flux and the pressure corresponding to the limiting flux decreased. At higher concentrations, it was observed that the lowest transmembrane pressure that can be used in the pilot plant was larger

than the limiting pressure. For instance, for both mode starch solutions with a feed concentration of 2.0 wt %, the plots of flux vs. pressure were almost flat; rather, they seemed somehow to decrease as the operating pressure was increased further. Running ultrafiltration above the limiting pressure is inefficient. Therefore, for optimum operation, the operating pressure should be reduced as the concentration is increased to get better flux and/or to make the process more energy efficient as far as the pressure drop in the apparatus allows.

4.4.3. Summarizing remarks

The ES625 membrane had about 63 % retention for degraded MWI starch solution of 0.5 % concentration, pH 6.5 and temperature 25°C when it was used for ultrafiltration with a 1.5 bar transmembrane pressure drop and a 1.0 m/s cross flow velocity. The retention of the MPT-U20 membrane was even smaller (53.9 %). Retention has a trend opposite to that of the flux. Retention of the membrane decreases for the lower range of pressure where the flux is increased with the pressure and increased for the upper range of pressure where flux is constant or is decreasing as the pressure is increased. The decrease of the observed retention in the lower pressure range seems to be due to an increase in the drag force on the solute that squeezes through the pores and the concentration gradient across the membrane. An increase in retention in the upper pressure range was due to an increase in pores blocked by pore plugging and the compaction of the deposit/gel. The effect of cross flow velocity was dependent on the molar mass of the starch solution. For MWI (40000 g/mol) starch retention decreases with an increased cross flow velocity while for MWII (170000 g/mol) retention increases with an increase in the cross flow velocity.

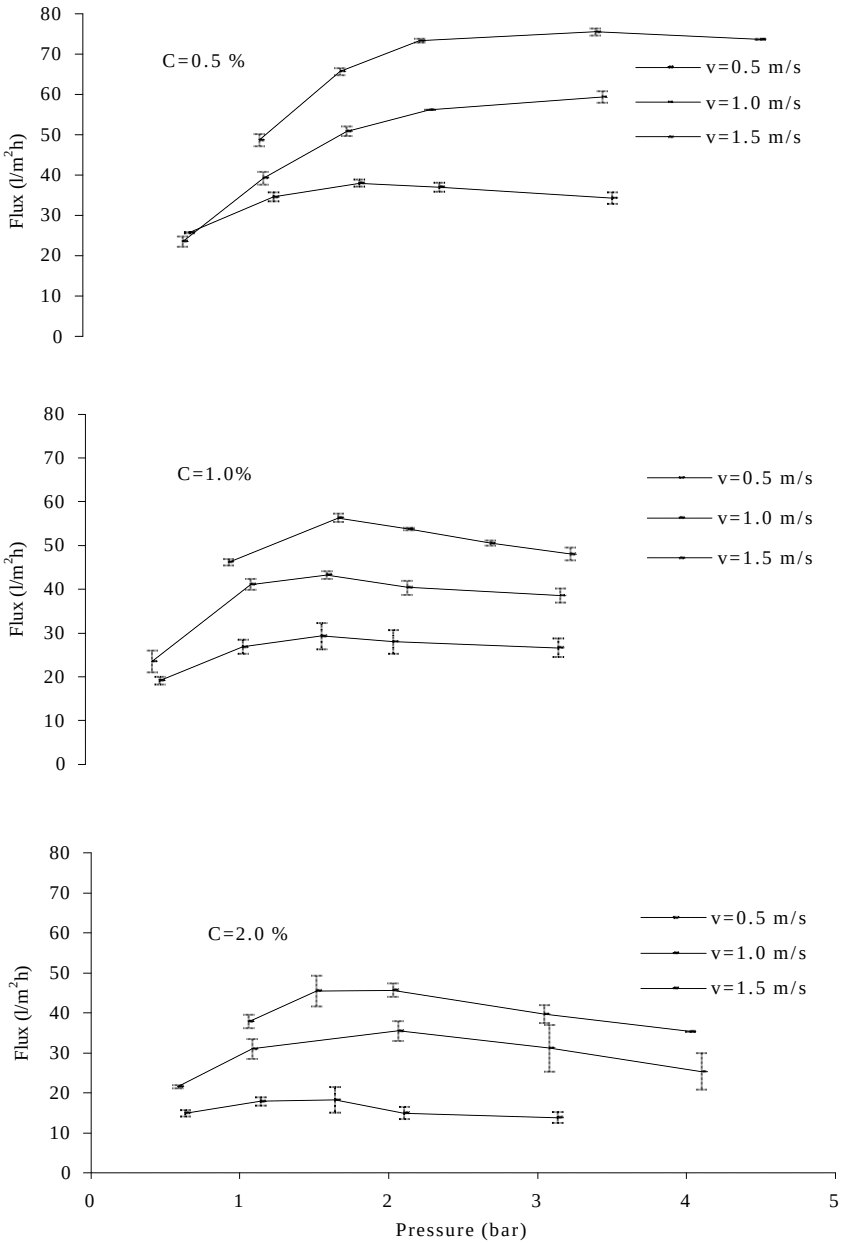

Figure 5.20. Permeate flux vs. transmembrane pressure drop for ultrafiltration of MWI (40000 g/mol) starch solution for three cross flow velocities and concentrations at T=25°C and pH=6.5.

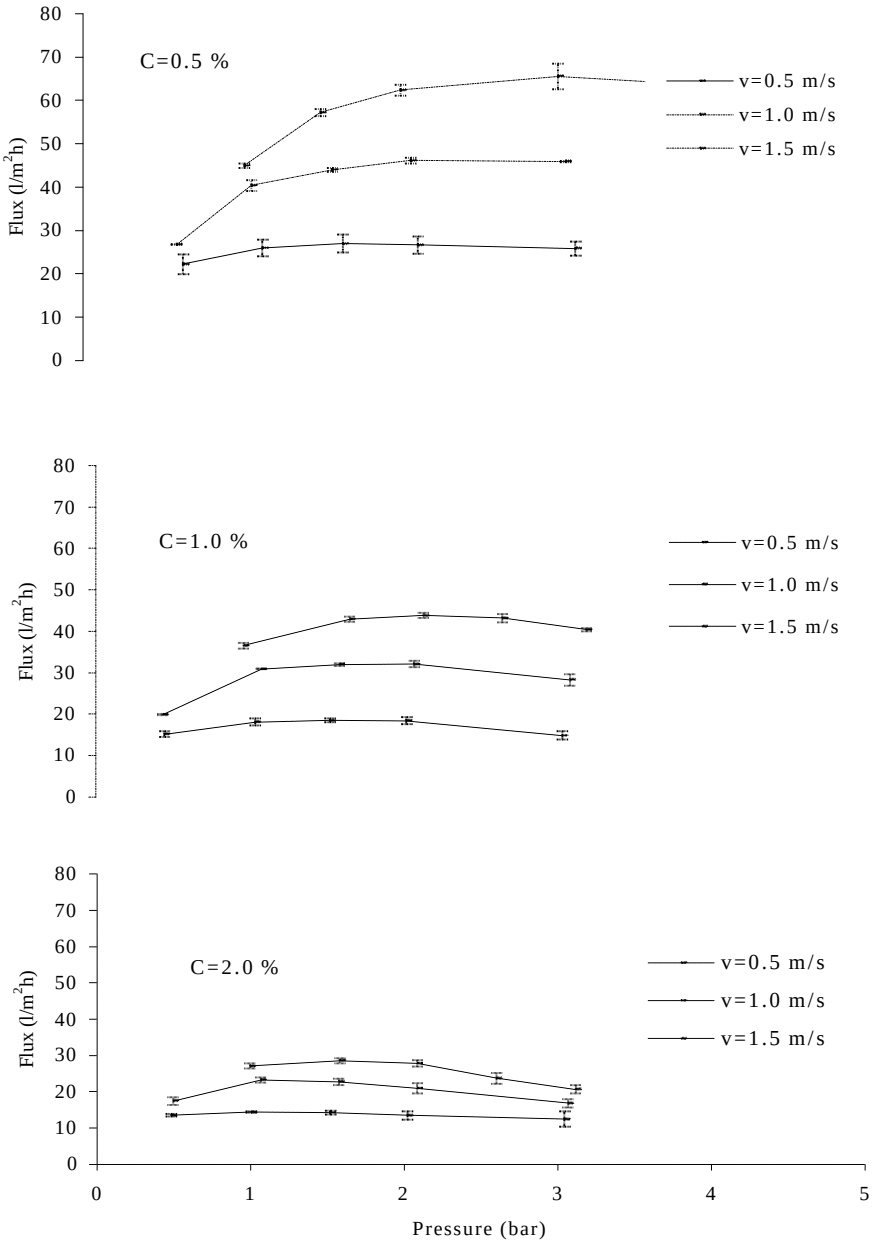

Figure 5.21. Permeate flux vs. transmembrane pressure drop for ultrafiltration of MWII (170000 g/mol) starch solution for three cross flow velocities and concentrations at T=25°C and pH=6.5.

5.5. Fitting selected ultrafiltration models

Our discussion in Sections 5.2 and 5.3 showed that the flux and retention were strongly affected by all three fouling mechanisms, which are adsorption, deposition and concentration polarization. Adsorption and deposition were responsible for a large portion of the flux decline. In the light of this, though the gel-polarization model could approximate the flux behavior to a certain extent, it would give little physical meaning. Because, it is developed to predict a flux decline due to the concentration polarization. The same is true with the osmotic pressure model, since it is also developed to predict the limiting flux as a result of concentration polarization. This is because the starch molecules associate above a certain concentration (semi-dilute concentration) and act as a network with infinite molar mass (see Section 2.6). Besides, the contribution of concentration polarization (osmotic pressure) for the flux decline is very small so that it can not be limiting factor (see Section 5.3.1). Therefore, the only model that accounts for all the fouling mechanisms is the resistances-in-series model. However, this model has also a weakness in that it is insensitive to the mechanisms. It gives flux as a function of the over all resistance added by the mechanisms. But it is the only model that somehow physically makes sense. Therefore, the resistances-in-series model is used in order to fit experimental data obtained from the experiment and then to predict the permeate flux of degraded starch solution. In order to make better estimation of the contribution of the fouling mechanisms, the model is also somehow modified and compare with unmodified one.

On the other hand, in order to predict the retention of starch molecules during ultrafiltration, to our knowledge, there is no model that accounts for the effect of the two dominant fouling mechanisms. The only relations we know from literature that relates flux and retention are Equations 3.2 and 3.7. Equation 3.7 is developed based on a concentration polarization model, assuming negligible fouling due to the other mechanisms. In this study, therefore, model fitting for retention is not included.

5.5.1. Resistances-in-series model

As we saw in Section 5.3, depositional resistance has higher than linear relationship (e.g. a power function with power larger than one) with pressure. The relationship of the resistance due to concentration polarization and deposition fouling with transmembrane pressure drop given in Section

3.3.4 seemed to be supported by the result in Section 5.3. In order to simplify the regression, however, we assumed that depositional fouling resistance is proportional to the square of the transmembrane pressure drop. Hence, the equation used for the resistances-in-series model is written as:

$$J = \frac{\Delta P}{R_m + a\Delta P + b\Delta P^2} \qquad 5.1$$

where a and b are functions of CFV and the concentration of the polymer in the solution.

The prediction of the parameters a and b at a given cross flow velocity and concentration is given by Equation 5.2.

$$a, b = aV^b C^c \qquad 5.2$$

The parameters of the model are determined by a nonlinear regression procedure using S-plus statistical software. The confidence level used was 95 % (i.e. p value < 0.05). The estimates of the constant coefficients determined are given in Table 5.9. The correlation coefficient (R^2) found was 0.95 and 0.97 for MWI (40000 g/mol) and MWII (170000 g/mol) starch solutions, respectively. The fitting of the model for the two solutions are shown in Figures 5.22 and 5.23, respectively.

Table 5.9. The estimates of the parameters from the regression analysis

Model solution	Parameters	a	b	c
MWI	α	0.0058 ± 0.0012	0.396 ± 0.096	-1.176 ± 0.148
	β	0.0004 ± 0.0002	0.865 ± 0.256	-0.744 ± 0.255
MWII	α	0.0062 ± 0.0002	0.448 ± 0.013	-0.974 ± 0.018
	β	0.0005 ± 0.0003	0.927 ± 0.190	-0.404 ± 0.167

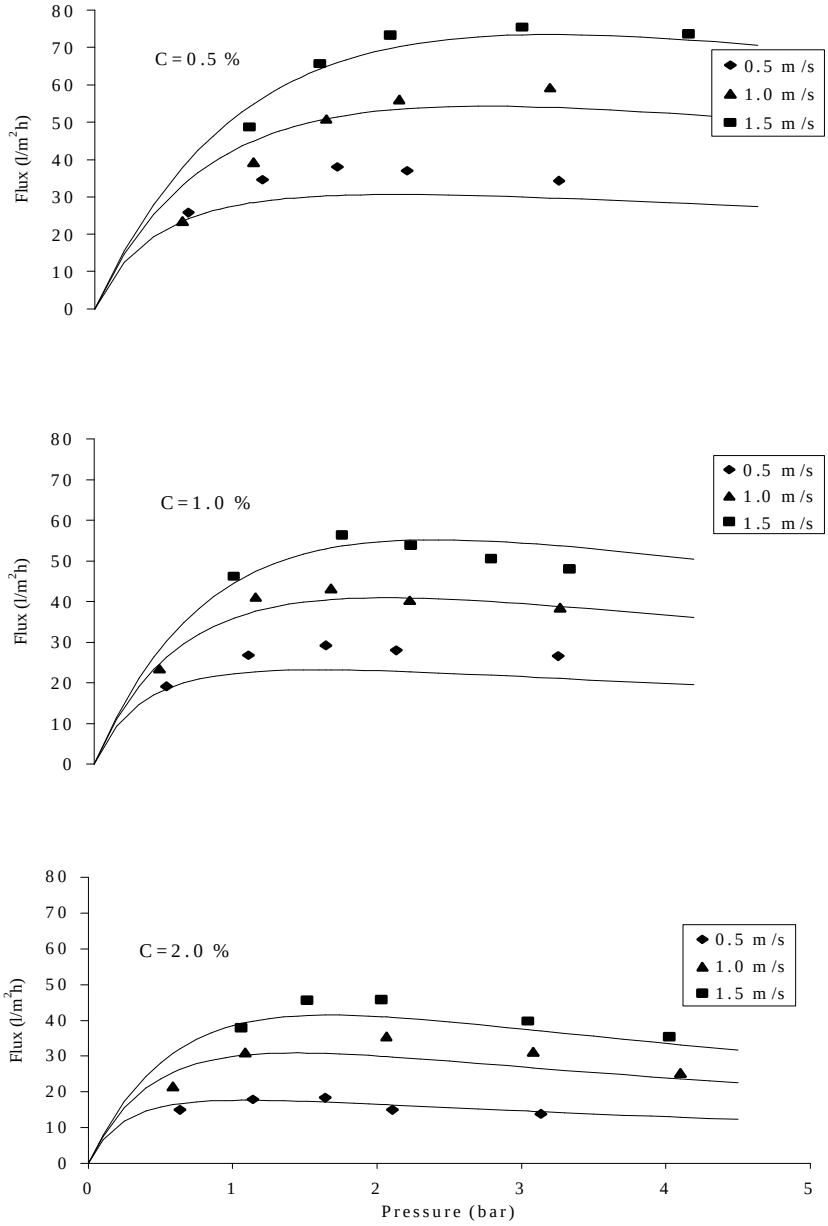

Figure 5.22. Prediction of the effect of process variables on the permeate flux from ultrafiltration of MWI (40000 g/mol) starch solution using ES625 membrane (M-V). The dots are experimental points and the solid lines are fitting of the resistances-in-series model (Equation 5.1) where a and b are predicted from Equation 5.2.

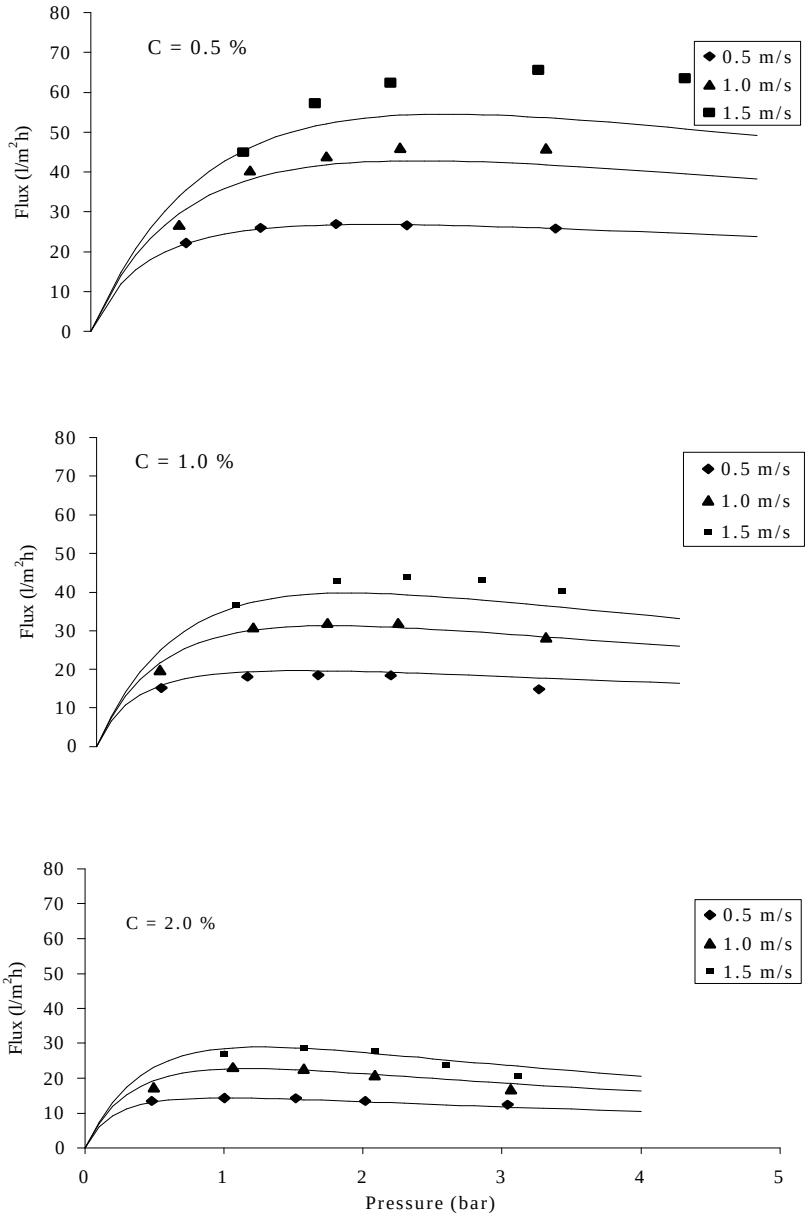

Figure 5.23. Prediction of the effect of process variables on the permeate from ultrafiltration of MWII (170000 g/mol) starch solution using ES625 membrane (M-V). The dots are experimental points and the solid lines are fitting of the resistances-in-series model (Equation 5.1) where a and b are predicted from Equation 5.2.

5.5.2. Modification of the resistances-in-series model

From the discussion in Section 5.2, we know that concentration polarization is the least contributor to fouling resistance. But when the resistance is calculated from the resistance-pressure relations given for each mechanism using the coefficient in Table 5.9, the resistance due to concentration polarization is much larger than for the other mechanisms. See Figure 5.24. This is because the relation given for each resistance in the model does not represent an independent relation of each resistance with pressure. That is, the linear portion of the contribution of deposition will be added to R_{cp} while the square contribution of concentration polarization to the flux decline (if there is any) will be added to R_d. This does not affect the overall fouling resistance, but gives unrealistic values when the contribution of each mechanism is determined from the model. In order to represent better the contribution of each individual resistance in the model, the resistance due to each of the mechanisms should be determined experimentally as we did for the evaluation of the contributions of the fouling mechanisms to the flux decline in section 5.3. But this procedure is costly and tedious. However, by introducing the osmotic pressure in Equation 5.1 we can remove the resistance due to concentration polarization (reversible fouling) from the resistances in the series and account for it separately. The remaining resistance is the sum of adsorptive fouling, gel (aggregate of the starch molecules), and depositional fouling resistances, which is commonly referred to as irreversible fouling resistance. Thus, this modified model can show the significance of the resistance contributed by the irreversible fouling as compared to the reversible one.

Since the hydrodynamic phenomena are responsible for the formation of both gel and deposit, one can consider both as a deposit or gel layer. In the light of this, the model can be modified as described below:

$$J = \frac{\Delta P - s\Delta p}{R_m + R_a + a\Delta P^n} \qquad 5.3$$

where R_a is the adsorptive fouling resistance which is assumed to be independent of pressure.

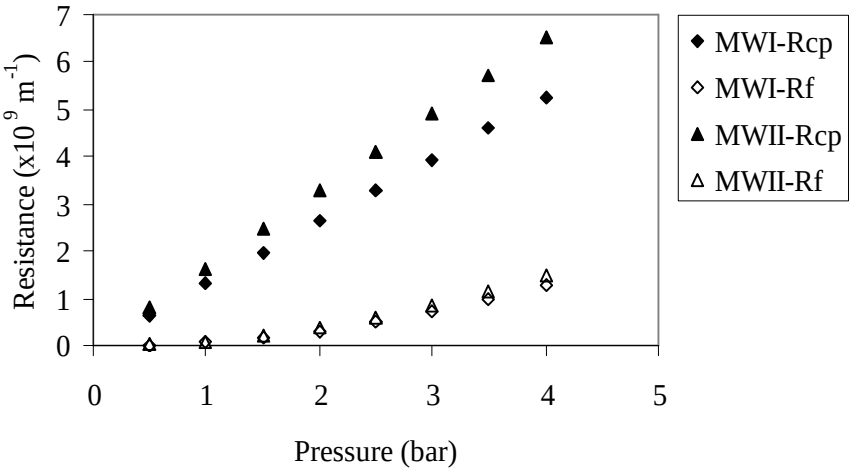

Figure 5.24. Estimation of the resistance due to the concentration polarization (R_{cp}) and the fouling (R_f) from Equations 3.18 and 3.21, respectively, for ultrafiltration of 0.5 wt % MWI (40000 g/mol) and MWII (170000 g/mol) starch solution at CFV=1.0 m/s and pH=6.5

The reflection coefficient *s* of the average starch molecules is assumed to be one since the intrinsic retention of the membrane is almost 100 %. The coefficient *a* and the power *n* are functions of concentration and cross-flow velocity as given by Equation 5.4. The resistance in the denominator shows the sum of irreversible fouling resistances: adsorptive fouling which is independent of pressure and deposition /gel which is pressure dependent

$$R_a,\ a,\ n = aC^b V^c \qquad 5.4$$

In order to find a better approximation for the osmotic pressure used in the model, an experimental determination of the osmotic pressure of degraded starch gel/precipitates would be necessary. In this study, however, we assume that the van 't Hoff's relation gives good enough approximate of osmotic pressure. When the concentration of the starch is slightly over the semi-dilute concentration, as discussed in Section 2.4, the osmotic pressure is largely due to the tails of the starch molecules forming the gel/deposit. The molar concentration of the tails can be approximated by an average molar concentration of the starch macromolecules at the membrane surface. The concentration at the membrane surface is approximated by the estimate

from the concentration polarization model (Equation 3.7) assuming C_P (permeate concentration) to be zero and the diffusion coefficient to be independent of concentration. The constants in Equation 5.3 were determined solving simultaneously Equation 2.4 (van't Hoff's equation), Equation 3.7 (the mass transfer equation) and Equation 5.3. The physical constants and dimensions used in the calculation are given in Appendix-E. The S-Plus statistical software was used for the analysis.

From the values of R_a, a and n obtained for each set of concentration and cross flow velocity, the values of a, b and c can be determined from Equation 5.4 by regression analysis. The values obtained from the analysis are given in Table 5.10. The fitting of the model into the data generated for the two starch solutions are given in Figures 5.25 and 5.26. The permeate flux and the transmembrane pressure drop are highly correlated (R^2 = 0.96 for MWI and 0.98 for MWII starch solutions). The figures are very similar to Figures 5.22 and 5.23. In addition, the calculated estimate of resistance due to the irreversible fouling from the modified model is shown in Figure 5.27. This figure shows that the modified model gives better information on the contribution of the irreversible fouling mechanisms, i.e. the irreversible fouling is responsible to the much larger portion of the flux decline. Besides, if the contribution of all the fouling mechanisms are known/determined at one chosen operating condition, the contribution of all fouling mechanisms can be known provided the assumption that adsorptive fouling is independent of transmembrane pressure is true.

Table 5.10. The estimates of the parameters from the regression analysis.

Starch solution	Parameters	*a*	*b*	*c*
MWI	R_a	0.0032 ± 0.0024	0.383 ± 0.293	-0.444 ± 0.343
	a	0.0009 ± 0.0004	0.764 ± 0.138	-1.429 ± 0.208
	n	2.1754 ± 0.2586	-0.035 ± 0.051	0.132 ± 0.065
MWII	R_a	0.0022 ± 0.0014	0.489 ± 0.244	0.881 ± 0.377
	a	0.0026 ± 0.0003	0.669 ± 0.038	-1.464 ± +0.062
	n	1.3802 ± 0.1836	0.096 ± 0.055	0.308 ± 0.073

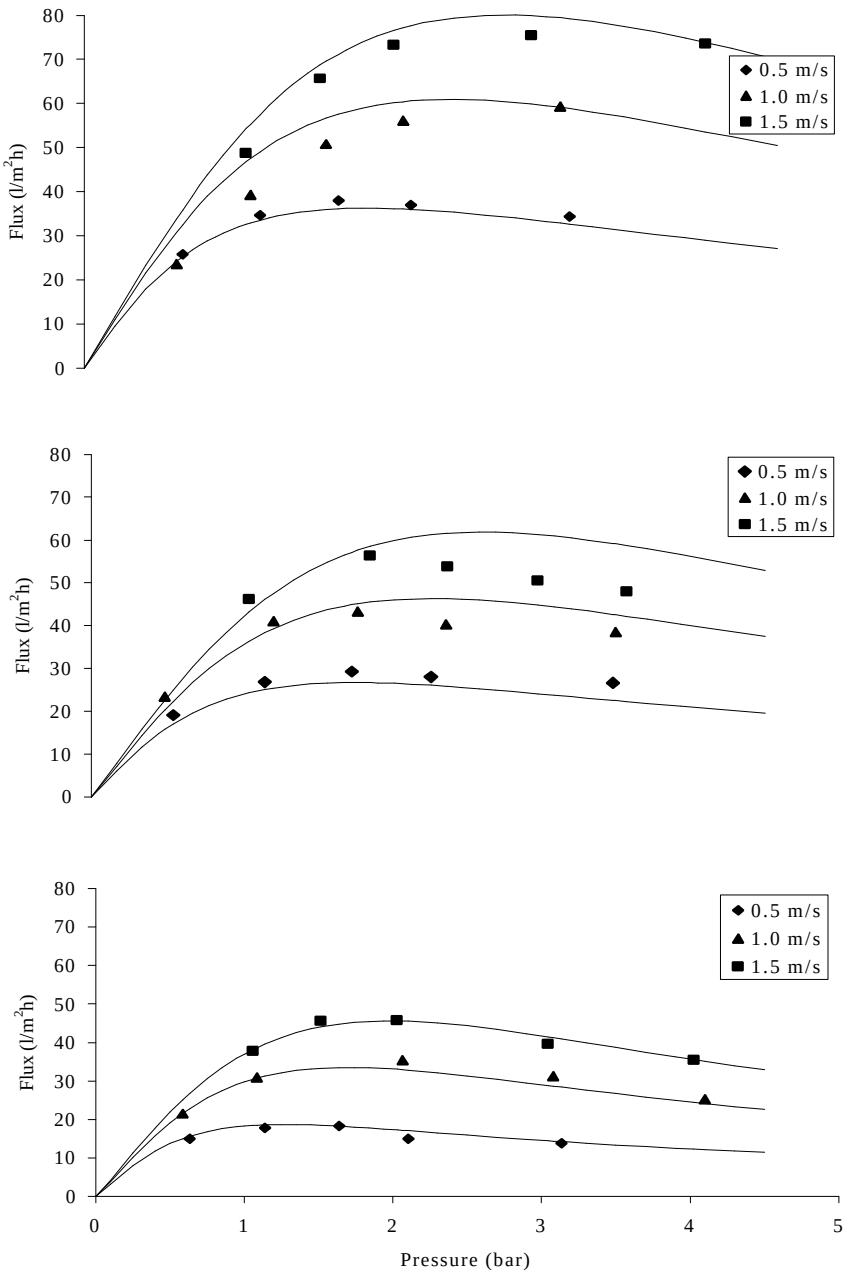

Figure 5.25. Prediction of the effect of process variables on the permeate flux from ultrafiltration of MWI (40000 g/mol) starch solution using ES625 membrane (M-V). The dots are experimental points and the solid lines are fitting of the modified resistances-in-series model (Equation 5.3) where a and b are predicted from Equation 5.4.

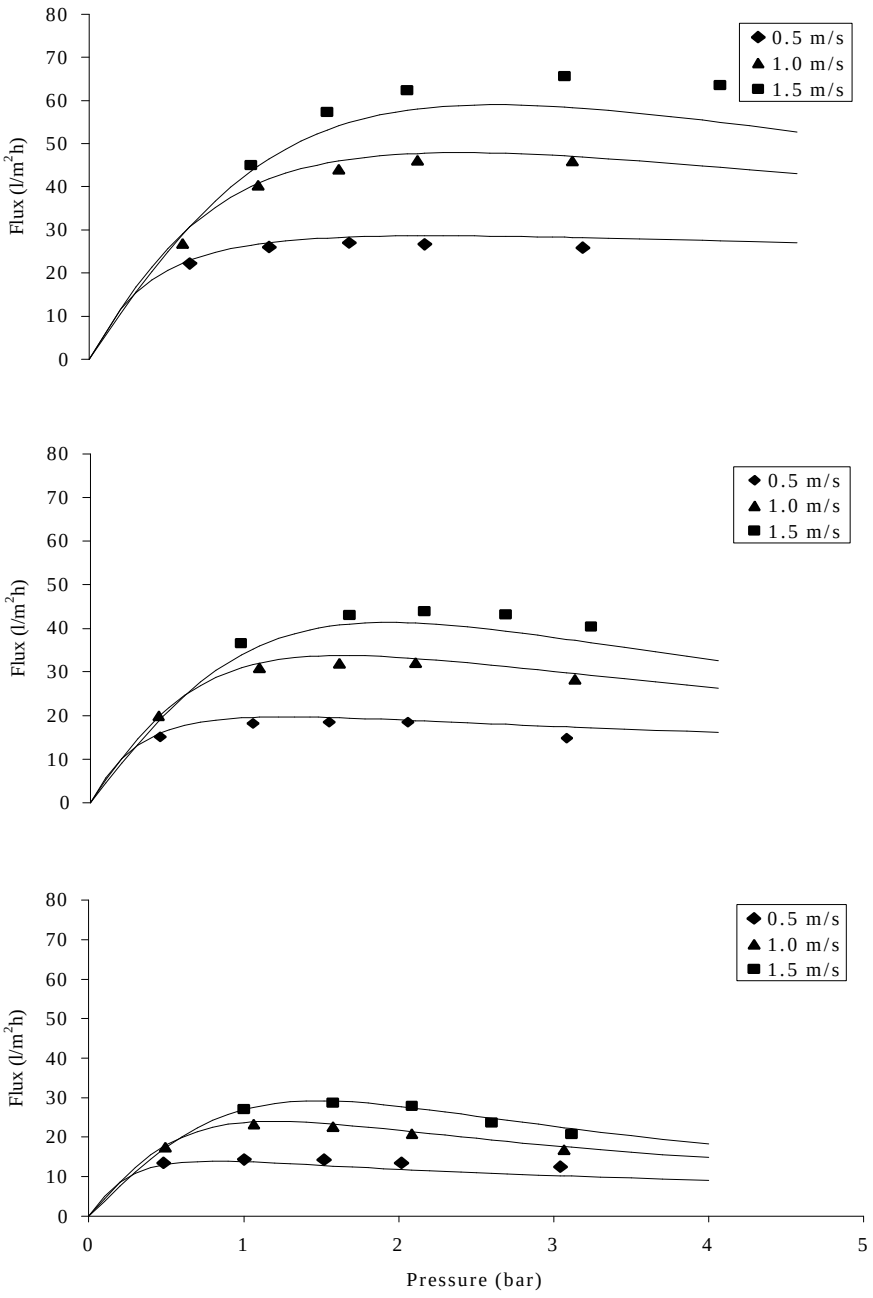

Figure 5.26. Prediction of the effect of process variables on the permeate flux from ultrafiltration of MWII (170000 g/mol) starch solution using ES625 membrane (M-V). The dots are experimental points and the solid lines are fitting of the modified resistances-in-series model (Equation 5.3) where a and b are predicted from Equation 5.4

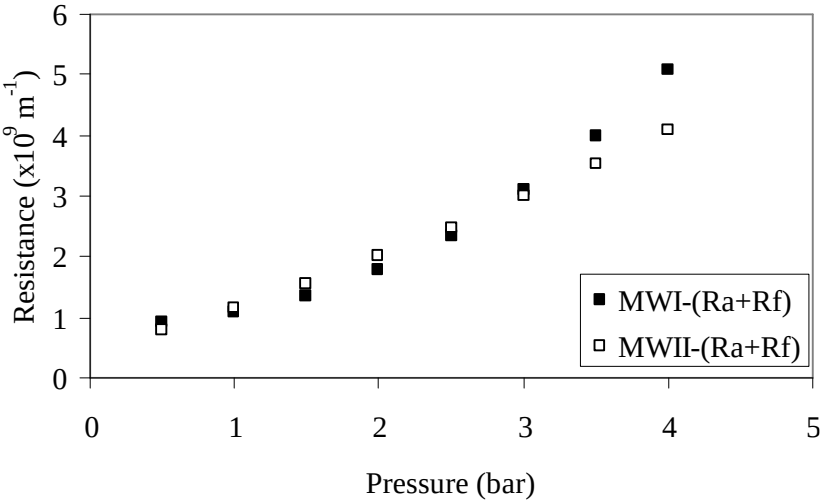

Figure 5.27. Estimation of the resistance due to an irreversible fouling resistance ($R_a + R_f$) using modified resistances-in-series (Equation 5.4) for ultrafiltration of 0.5 wt % MWI (40000 g/mol) and MWII (170000 g/mol) starch solution at CFV=1.0 m/s and pH=6.5.

5.5.3. Summarizing remarks

The permeate flux of degraded starch solution may be fitted with a resistances-in-series model. If the effect of concentration polarization is accounted for by introducing the osmotic pressure, the model becomes more physically meaningful. The model gives good permeate flux prediction and estimate of contribution of the reversible fouling and irreversible for the flux decline. If the relation between osmotic pressure and degraded starch concentration determined experimentally were available, the estimate would be better and realistic. When we want to know the contribution of each fouling mechanism, the flux loss ratio principle can be used to determine the resistances from the fluxes data obtained experimentally. But its procedure is costly; it takes much time, and it is chemical and energy intensive. Besides, since the adsorption is independent of the operating conditions, the modified resistance-in-series model may give sufficient physical information about the ultrafiltration of degraded starch solution provided the adsorptive fouling contribution at a given operating condition is determined.

The osmotic pressure accounts for flux decline due to concentration polarization. And the contribution of the fouling mechanisms at given operating conditions gives information on the fraction of the adsorptive fouling in the irreversible fouling resistance. Thus, the modified resistances-in-series model seems to be a reasonably good model in prediction of the permeate flux of ultrafiltration of partially degraded starch solutions and in the estimation of the contribution of each fouling mechanisms.

5.6. Concentrating mode operation of ultrafiltration

About 20 liters of 0.5 wt % MWI degraded starch solution was ultrafiltered by continuously withdrawing the permeate until the solution was concentrated to 3 liter (85 % of the volume was withdrawn) using 0.09 m^2 membrane area (M-IV membrane, two tubular membranes). The operating conditions were maintained at ΔP=1.6 bar, T=25^oC and pH=6.5. The ultrafiltration took 5 hours to attain the target concentrate volume. During this time, the initial 0.5 wt % starch solution was concentrated to slightly over 2.2 wt %. In the following section, we will see the flux and retention vs. time profiles, and then how the rejection vs. molecular weight profiles changed with time.

5.6.1. Flux and retention profile with time

The permeate flux, retention of the membrane and the concentration in the feed tank vs. time were measured. The results are shown in Figures 5.28, 5.29 and 5.30. As seen in Figure 5.28, during the first hour run, the flux increased and retention decreased. Beyond one hour the run, the flux was decreasing while retention was increasing steadily. This trend was exactly the same for the replicate runs we made. The explanation for the increase of the flux during the first hour run is not obvious. Commonly, the flux is expected to decrease as the concentration is increased as a result of an increase in osmotic pressure across the membrane and of the viscosity of the feed solution. For shear thinning polymers, however, there could be a range of concentration where the flux could increase with the retantate get

concentrated [Howell et al., 1996]. Starch solution is shear thinning, in particular, for native molecular size [Heitmann et al., 1997; Morawetz, 1975]. Perhaps, for degraded starch used in our study, the shear thinning effect may surpass the effect of concentration on the viscosity as the solution was concentrated from 0.5 to 0.7 wt % (for about an hour). When the solution was subjected to shearing as ultrafiltration was started, the big molecules and their entanglement could break down [Heitmann et al., 1997; Morawetz, 1975], and the molecules might be stretched [Thorsen, 2000]. That is, molecules change in the conformation and size in the solution, as the solution is flow through the module. This results in a decrease of the viscosity of a polymer solution with time. On the other hand, the smaller and the more stretched the molecules, the less resistance the molecules might encounter when they are slipped or dragged through the membrane pores. Hence, the flow resistance will decrease with time until the shearing thinning is cancelled out by the effect of an increase in concentration on the viscosity and/or the fouling resistance added to the membrane, which increases with concentration. Thus, as we observed in our result, this might result in an increase in the flux with time for some time at an early stage of ultrafiltration where the concentration change in the feed tank is not significant. The later decrease in flux was due to an increase in viscosity, osmotic pressure and depositional fouling as the concentration in the feed tank was increased.

Figures 5.28 and 5.29 show that there was a strong relationship between flux and retention. This relation is partly explained by the earlier discussion in Section 5.4. In brief, the decrease in retention as the flux increased was due to the increase in the concentration gradient across the membrane and the drag force on the molecules that forces them to slip through the pores. The increase in retention as the flux was decreasing could be attributed to the pore blockage as a result of depositional fouling. In addition, in concentrating mode ultrafiltration, the fraction of the larger molar mass components in the solution increase as the solution gets concentrated, which results in turn in an increase in retention.

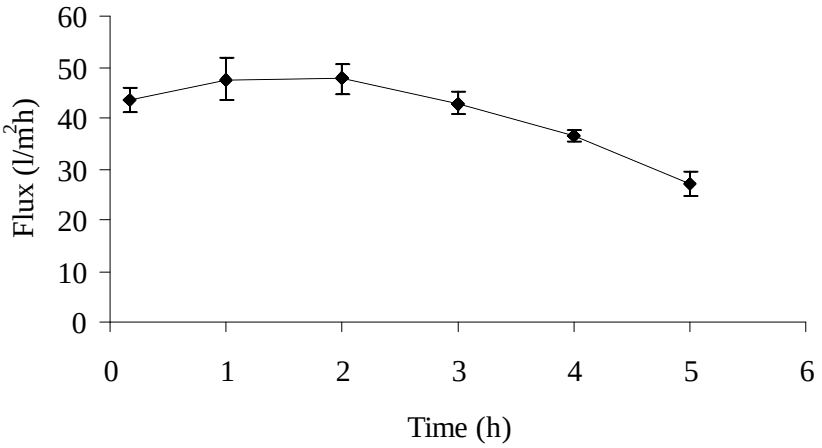

Figure 5.28. Permeate flux profile for UF of model solution MWI (40000 g/mol) operating concentrating mode atΔP=1.6 bar, T=25^{o}C and pH=6.5

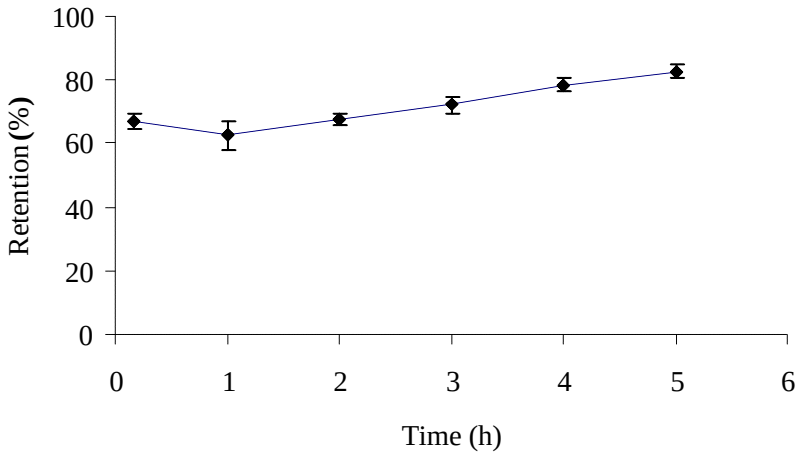

Figure 5.29. Retention profile for UF of model solution MWI (40000 g/mol) operating concentrating mode atΔP =1.6 bar, T=25^{o}C and pH=6.5

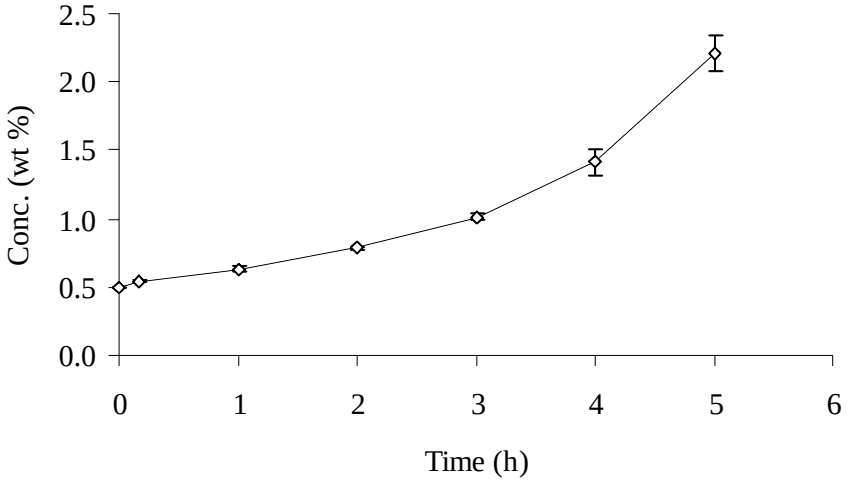

Figure 5.30. Concentration profile for UF of model solution MWI (40000 g/mol) operating concentrating mode atΔP=1.6 bar, T025^{o}C and pH=6.5

5.6.2. Rejection of macromolecules vs. run time

The HPLSEC chromatographic analysis was made for the permeate and the concentrate samples drawn after the solution was concentrated for 1 h, 3 h and 5 h runs. The molar mass distributions of the starch in the samples are plotted in Figure 5.31. The figure shows that larger molecules (more than 100,000 g/mol) were removed from the permeate. As it was concentrated, intermediate size (3000 to 30000 g/mol) molecules in the permeate were gradually depleted. This is a result of a decrease in the MWCO of the membrane because the fouling layer reduces the accessibility and the effective pore size of the pores on the membrane surface. As the concentration of larger molar mass molecules increased in the concentrate, the fraction of lower molar mass molecules in the concentrate became smaller. On the other hand, the depletion of larger molecules from the permeate makes the fraction of lower molecules to increase in the permeate with time. This in what is reflected in Figure 5.29. From molar mass distribution of the starch in the concentrate and in the permeate, the rejection vs. molar mass was also calculated and shown in Figure 5.32. This shows

that the MWCO of the membrane decreased to a lower molar mass region, as the solution was concentrated. As we said earlier, this was due to an increase in the concentration of relatively smaller molecules in the concentrate (or partial and complete depletion from the permeate) as a result of the decrease in the membrane MWCO due to fouling. The abnormal increase and fluctuation observed in the low molar mass region should be attributed to the limitation of the light scattering detector of HPSEC. The resolution of the light scattering detector that determines the molar mass is poor for molar masses smaller than 10,000 g/mol.

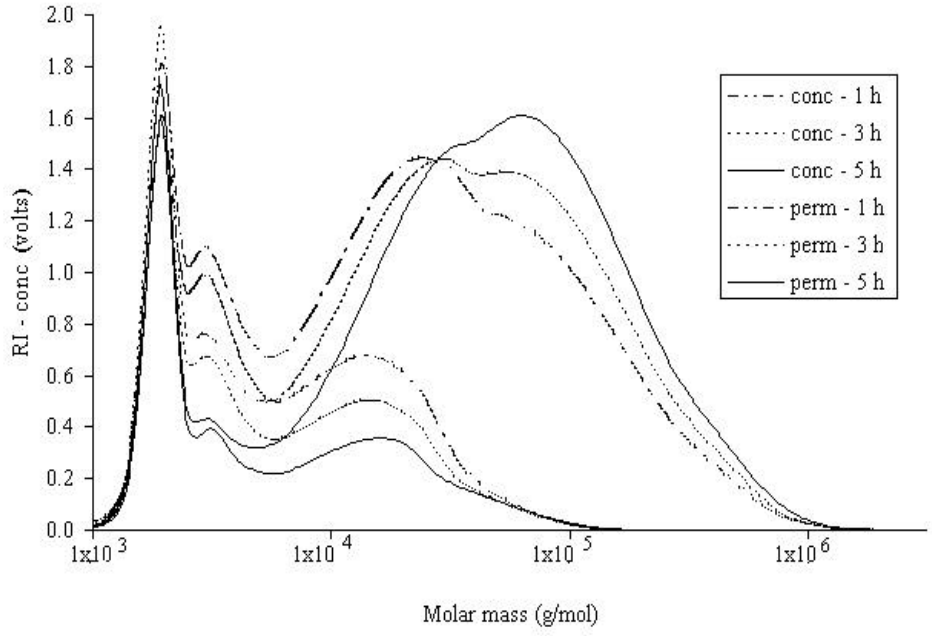

Figure 5.31. The molar mass distribution of solute in concentrates and permeates after 1 h, 3 h and 5 h UF run determined using HPSEC.

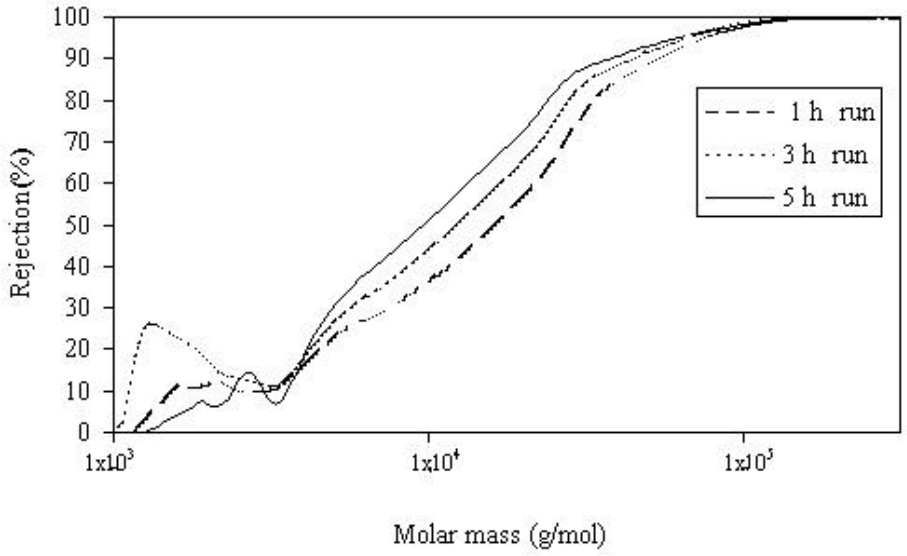

Figure 5.32. The rejection of solute as function of molar mass at 1 h, 3 h and 5 h UF concentrating mode run time determined from the data obtained using HPSEC.

5.6.3. Summarizing remarks

During the first hour of the concentrating mode run, the flux was slightly increasing. This might be attributed to shear thinning effect as result of changes in the conformation and degradation of the starch macromolecules by the shear force when solution was pumped through the system. Afterward, as expected, the permeate flux was decreasing as the solution was concentrated. The observed relation of the permeate flux and the retention was also as expected and discussed in the previous section. The retention was decreasing when the flux was increasing and vise-versa. The increase of retention as the flux was decreasing might be attributed to a decrease of the force on the solute, an increase of the size of the solute in the solution and a decrease in accessible membrane pores due to pore blocking. On the other hand, the rejection of the membrane was shifted to lower molar mass. This might be attributed to the depletion of a relatively larger molar mass starch from the permeate as the solution was concentrated as the result of an increase in retention of the membrane due to fouling.

Chapter 6

Conclusions and recommendations

6.1. Conclusions

For both types of membranes, all the three fouling mechanisms (concentration polarization, adsorption and deposition) were responsible for the flux decline in ultrafiltration of the degraded starch solution. The major contributors were, however, adsorption and deposition. Adsorption was largely responsible at low-pressure operation while the deposition effect increased with pressure and became dominant at higher pressures (near or beyond the limiting flux). Generally, the overall fouling resistance increased with the pressure, the feed concentration and the molar mass while it decreased as the cross flow velocity and the temperature was increased. The effect of the operating parameters on the contribution of the fouling mechanisms to the flux decline for the ES625 membrane is summarized as follows.

Adsorption: The contribution of adsorptive fouling increased with concentration decreased as the molar mass and the temperature was increased. The alkaline environment also caused the least adsorptive fouling.

Deposition: The contribution of depositional fouling was observed to increase with an increase in pressure (which can be expressed by a power function with power larger than 1.0), feed concentration and molar mass, and to decrease with an increase in cross flow velocity. This is in line with the cited literature.

Concentration polarization: The contribution of concentration polarization to the flux decline decreased as the molar mass and the cross flow velocity was increased (from the laminar flow regime to the turbulent flow regime), and increased as the feed concentration and the temperature were increased. In the turbulent flow regime the relation between its contribution to flux decline and transmembrane pressure was almost linear. In the laminar flow regime, however, the contribution increased for the lower range of pressure

(below the limiting flux) and decreased for the higher range of pressure (above the limiting flux) as the pressure was increased.

For MPT-U20 membrane, the trends of the contribution of depositional fouling to the flux decline and the effect of pH on the adsorption are similar to that of ES625 membranes. However, the trends of the contribution of the adsorption and the concentration polarization as the feed concentration and the molar mass were increased are somehow different. The difference seems to be a result of the difference in the morphological property of the two membranes; the ES625 membrane seems to have a smaller pore size than the MPT-U20 membrane.

Overall performance: The permeate flux in ultrafiltration of partially degraded starch solution was observed to be limited and controlled as a result of an increase in thickness and compaction of the gel/deposit layer on the membrane. The resistance added by the gel/deposit decreases as the cross flow velocity is increased and increases as the concentration and molar mass of starch in the solution are increased. The resistances-in-series model gives good fitting to the permeate flux data. However, the modified model, by introducing the osmotic pressure to account for the effect of concentration polarization, makes better estimation for the contribution of the reversible fouling and irreversible fouling to the flux declines.

In concentrating mode operation, at an early stage of filtration, the flux was slightly increasing, which might be attributed to the effect of shear thinning property of the starch solution. As the retantate gets more concentrated, however, the permeate flux decreased with an increase in concentration. The retention decreased where the flux was increasing and increased where flux was decreasing as the concentration was increased. The rejection of the membrane was shifted to lower molar mass as the concentration was increased. This is due to the depletion of the relatively largemolar mass starch from the permeate as the solution was concentrated as the result of the fouling of the membrane.

.

The flux of ultrafiltration of partially degraded starch solution by ES625 membrane tubular membrane is good enough to give equal or better performance than the existing ultrafiltration plant that has been used to recover synthetic sizing agent (PVA) from desizing wastewater. The retention is, however, very low. So two or more stages of treatment should be used to get all starch components recovered and reusable treated water.

6.2. Recommendation and future works

In this study, model degraded starch solution was used for the ultrafiltration experiments. However, the desizing wastewater from the textile industry would contain, in addition to degraded starch, textile fibers and other foreign materials. These additional particles could block the ultrafiltration module and the performance of the membrane. The flux would also be different from the model solution flux. Thus, first a prefiltration unit should be used to treat the wastewater before using ultrafiltration. Since the retention of the membranes is low; for example, ES625 membrane has retention of about 60 % for ultrafiltration of MWI (40000 g/mol) starch solution. In order to get a water that can be reused, the permeate should be treated further by using a lower MWCO membrane, maybe by a nanofiltration membrane. As the feed solution is concentrated, larger molar mass starch molecules dominate the concentrate. This increases the severity of the fouling of the membrane. In such a case, the flux can be improved buy using a membrane with a larger MWCO.

Therefore, when membrane filtration processes are used to treat wastewater containing a broad molar mass distribution, partially degraded starch, a process with two or more stages should be designed to attain the target purity of the clarified water and recover all components of starch in the wastewater. Each stage should have different MWCO; at least, one should be able to remove the smallest starch components in the permeate, and the other should take care of the large molecules, say larger than 10,000 g/mol. In order to design membrane processes that may be used to treat such wastewater, it is necessary to make further study in the following area:

1. Ultrafiltration tests for the textile wastewater from the desizing process to verify the results obtained using partially degraded starch solution and to account for the difference.
2. Ultrafiltration test using lower MWCO membranes or nanofiltration membranes on the permeate/solution containing lowermolar mass starch molecules in order to evaluate their performance: separation efficiency and flux.
3. Optimizing the number of stages to be used in treating wastewater containing partially degraded starch so that the required purity of the water and concentration level of the concentrate are attained with the least costs.
4. The performance of cleaning procedure depends on the type of cleaning agent, alkalinity, temperature and transmembrane pressure

drop. Thus, it is also important to study the effect of these parameters and their combinations on the performance of the cleaning procedure and find the optimal one.

References

Abaticchio P., A. Bottino, C. Roda, G. Capannelli, and S. Munari. Characterization of ultrafiltration polymeric membranes. Desalination. 78, 235 (1990).

Aberle T. and W. Burchard. Starches in semi-dilute aqueous solution. Starch 49 (6), 215 (1997).

Aberle Th., W. Burchard, W. Vorweg and S. Radoosta. Conformational contributions of amylose and amylopectin to the structural-properties of starches from various. Starch 46 (9), 329 (1994).

Aberle T., W. Burchard and G. Galinsky, R. Hanselmann, R. W. Klingler and E. Michel. Particularities in the structure of amylopectin, amylose and some of their derivatives in solution.Macromol. Symp. 120, 47 (1997).

Banks W. and C. T. Greenwood. Starch and its components. Edinburgh Unversity Press. Edinburgh, Great Britain. 1975.

Banks W. and C. T. Greenwood. The conformation of amylose in neutral, aqueous salt solution. Carbohydrate Res. 7, 349 (1968).

Bayazeed A. and J. Trauter. Investigation on changes in physical and technological properties of water-soluble sizing agents during ultrafiltration of process. (2) Ultrafiltration of carboxy methyl (potato) starch. Starch 43 (7), 262 (1991).

Bayazeed A. and J. Trauter. Investigation on changes in physical and technological properties of water-soluble sizing agents during ultrafiltration of process. (1) Ultrafiltration of hydroxylpropyl starch. Starch 43 (1), 18 (1991).

Belfort, G., J.M. Pimbley, A. Greiner and K.Y. Chung; Diagnosis of membrane fouling using a rotating annular filter. 1. Cell culture media. J. Membrane Sci. 77, 1 (1993).

Belfort, G., R.H. Davis, and A.L. Zydney. The behaviour of suspensions and macromolecular solutions in crossflow microfiltration. J. Membrane Sci. 96, 1 (1994).

Bhattacharjee, S., A. Sharma and P. K. Bhattacharya. Surface interactions in osmotic pressure controlled flux decline during ultrafiltration. Langmuir 10, 4710 (1994).

Biresaw, G. and C.J. Carriere. Correlation between mechanical adhesion and interfacial properties of starch/biodegradable polyester blends. J. Polymer. Sci. 39 920 (2001).

Blanchard P. H. and F. R. Katz. Starch hydrolysates: in Food-Polysaccharides and their Applications (A.M. Stephen, Ed.). Marcel Dekker, Inc. New York. 1995.

Blanshard, J. M. V. Starch granule structure and function: A physicochemical approach. In: Starch: properties and potential (T. Galliard, Ed.). John Wiley & Sons, London, 1987.

Blatt, W.F., A. Dravid, A.S. Michael, and L. Nelsen,; Solute polarization and cake formation in Membrane Ultrafiltration: Consequences, and Control Techniques; In Membrane Science and Technology (J.E. Flinn, Ed.), Plenum Press, New York, NY, 1970, pp 47-97.

Buckley, C. A., R.B. Townsend, and G.R. Groves. Treatment of desizing effluents for recovery and reuse of polymer sizes: pilot plant performance and economics, Proceeding symposium on new technologies for cotton: in Textile,Stavanger, 1982.

Burchard, W. Light scattering from reacting polmer systems associating polymers in a good solvent. Macromol. Chem., Macromol. Symp., 39, 179 (1990).

Cardew P.T. and M. S. Le. Membrane processes: A technology guide.The Royal Society of Chemistry. UK, 1998.

Chaing, B. H. and M. Cheryan. Ultrafiltration of skim milk in hollow fibers. J. Food Sci. 51, 340 (1986).

Chen, G., X. Chai, P. Yue, & Y. Mi. Treatment of textile desizing wastewater by pilot scale nanofiltration membrane separation. J. Membr. Sci. 127 (1) 93 (1997).

Cheng, T.W., H.M. Yeh, and C.T. Gau; Resistance Analysis for ultrafiltration in tubular membrane module. Sep. Sci. Techn. 32(16), 2623 (1997).

Clifton, C. N., Abidine, P. Aptel, and V. Sanchez; Growth of polarization layer in ultrafiltration with hollow-fiber membranes. J. Membr. Sci. 21, 233 (1984).

Cooper, S. G. Textile Industry, Environmental Control and Energy Conservation. Noyes Data Co. Park Ridge, New Jersey, 1978.

Cuperus, F. P. and C.A. Smolders. Characterization of UF membranes: Membrane characteristics and characterization techniques. Adv. Col. and Inter. Sci. 34, 135 (1991).

Dal-Cin, M.M., F. McLellan, C. N. Striez, C. M. Tam, T. A. Tweddle andA. Kumar. Membrane perforamnce with a pulp mill effluent:

Relative contributions of fouling mechanisms. J. Membr. Sci. 120, 273 (1996).

DeGennes, P.G. Scaling Concepts in Polymer Physics. Cornell University Press. Ithaca New York, 1979.

Dubois, M., K.A. Gilles, J.K. Hamilton, P.A. Rebers,. and F. Smith. Colorimettric for determination of sugars and related substances. Anal. Chem. 28 (3), 350 (1956).

Eaton, A. D., L. S. Clesceri and A. E. Greenberg. Standard methods for the examination of wate and wastewater. American Public Health Association. Washington, Dc., 1995

Eckner, K. F., E. A. Zottola. Partitioning of skim milk components as a function of pH acidulant, and temperature during membrane processing. J. Dairy Science 75 (8), 2092 (1992).

Elgal, G. M., Ruppenicker, G. F. and Knoepler, N. B. Sizing and desizing with degraded and ultrasonic techniques to conserve energy: in Energy conservation in textile and polymer processing. (L.V. Tyrone and J. N. Louis, Eds), American Chemical Society, Washington, 1979.

Fane, A. G. Ultrafiltration of suspension. J. Membr. Sci. 20, 249 (1984)

Fane, A. G., C. J. D. Fell, and A. G. Waters. The Relationship between Membrane Surface Pore Characteristics and Flux for Ultrafiltration Membrane. J. Membr. Sci. 9, 245 (1981)

French, D. Organization of starch granules: in Starch chemistry and Technology. (R.L. Whistler, J.N. Bemiller and E.F. Paschall, Eds) Academic Press, Orlando, San Diego, New York, London, Toronto, Motreal, Sydney, Tokyo, 1984.

Gaddis, J. L., T.C. Amond III and R.L. Thomas. Ultrafiltration of gelatinous corn starch suspensions. Sep. Sci. Techn. 34 (6&7), 1253 (1999).

Galinsky G and W. Burchrad. Starch fractions as examples for non-randomly branched macromolecules. 2. Behavior in the semi-dilute region. Macromolecules 29, 1498 (1996).

Galinsky G and W. Burchrad. Starch fractions as examples for nonrandomly branched macromolecules. 1. Dimensional properties. Macromolecules 28, 2363 (1995).

Gekas, V. and B. Hallström. Mass transfer in the membrane concentration polarization layer under turbulent cross flow I. Critical literature review and adaptation of existing sherwood correlations to membrane operations. J. Membr. Sci. 30 (2), 153 (1987).

German, M.L., A. L. Blumenfeld, Y.V. Guenin, V.P. Yuryev and V.B. Tolstoguzov. Strcurure formation in systems containing

amylose and amylopectin and their mixtures. Carbohydr. Polymers 18 (1), 27 (1992).

Geissler, E., F. Hokay, and A.-M. Hecht. Osmotic and scattering of chemically cross-linked poly (vinyl alcohol) hydrogels. Macromoleculs 24, 6006 (1991).

Gomez-Gotor, A., P. Susial, A. Guerra, and B. Ibarra. Experimental data and behavior of starch/water solutions with ultrafiltration module. Sep. Sci. Techn. 31(2), 173 (1996).

Green, G. and G. Belfort. Fouling of ultrafiltration membranes: Lateral migration and particle trajectory model. Desalination 35,129 (1980).

Grieves, R.B., D. Bhattacharyya, W. G. Schomp and J. L. Bewley. Membrane ultrafiltration of nonionic surfactant. AIChE J. 19, 766 (1973).

Guilbort, A. and C. Mercier. Fractionation and characteristics of the macromolecular components of starch: in Polysaccharides, Vol. III. (G. O. Aspinall, Ed). Academic press, Inc. Orlando, 1985.

Hanemaaijer, J. H., T. Robbertsen, D. Boomgaard, Th. Van, C. Oliema, P. Both, and D. G. Schmidt. Characterization of clean and fouled ultrafiltration membranes. Desalination 68, 93 (1988).

Heitmann, T., E. Wenzig, A. Mersmann. Characterization of three different potato starches and kinetics of their enzymatic hydrolysis by an alpha-amylase. Enz. Microb. Techn.. 20 (4), 259 (1997).

Hermans, J.J. Thermodynamics of long-chain molecules: in Colloid Science (H. R. Kruyt, Ed.). Elsevier Publishing Company, Inc., The Netherlands. 1949.

Howell, J., R. Field and D. Wu. Ultrafiltration of high-viscosity solutions: Theoretical developments and experimental findings. Chem. Eng. Sci. 51 (9), 1405 (1996).

Howell, J. A. and M. Nystrom, Fouling phenomena, in: Membranes in Bioprocessing: Theory and Applications (J. A. Howell, V. Sanchez, and R.W. Field, Eds.), Chapman and Hall, London, 1993.

Jonsson, A. S. Influence of shear rate on the flux during ultrafiltration of colloidal substances. J. Membr. Sci. 79, 93 (1993).

Jönsson, B., B. Lindman, K. Holmberg and B. Kronberg. Surfactants and Polymers in Aqueous Solutions. John Wiley & Sons, Inc. New York. 1998.

Kalichevsky, M.T. and S. G. Ring. Incompatibility of amylose and amylopectin in aqueous solution. Carbohyd. Res. 162, 323 (1987).

Kedem O. and A. Katchalsky. Thermodynamic analysis of permeability of biological membranes to non-electrolytes. Biochim. Biophys. Acta. 27, 229 (1958).

Ko, M.K. and J.J. Pellegrino. Determination of osmotic pressure and fouling resistances and their effects on the performance of ultrafiltration membranes. J. Membr. Sci. 74, 141 (1992).

Kozinski, A. A. and E. N. Lightfoot. Protein Ultrafiltration: A general example of boundary layer filtration. AIChE J. 18, 1030 (1972).

Lawton, J.W., I.L. Peoria. Surface energy of extruded and jet cooked starch. Starch 47 (2), 62 (1995).

Lee, S. H. and E. Ruckenstien. Adsorption of proteins on to polymeric surface of different hydrophilicities – A case study withbovin serum albumin. J. Collo. Inter. Sci. 125, 365 (1988).

Leung, W. and R. F. Probstein. Low polarization in laminar ultrafiltration of macromolecular solutions. Ind. Eng. Chem. Fundam. 18, 274 (1979).

Li, J-Y. and A-I. Yeh. Relationships between thermal, rheological characteristics and swelling power for various starches. J. Food Eng. 50, 141 (2001).

Ma, R. P., C. H. Gooding, and W. K. Alexander. A dynamic model forlow pressure hollow-fiber ultrafiltration. AIChE J. 31, 1728 (1985).

Manners, D. J. Recent development in our understanding of amylopectin structure. Carbohyd. Poly. 11, 87 (1989).

Marchal, L. M., J. Jonkers, K. Th. Franke, C. D. de Gooijer and J. Tramper. The effect of process conditions on the α-amylolytic hydrolysis of amylopectin potato starch: Anexperiemtal design approach. Biotechn. Bioeng. 62 (3), 348 (1999).

Marsciola, D.A., R.C. Viadero Jr. and B.E. Reed. Tubular ultrafiltration flux prediction for oil-in-water emulsions: analysis of series resistances. J. Membr. Sci. 184, 197 (2001).

Masashi Iwata, S. Koda, and H. Nomura. Theory of compression and expansion of hydrogels. J. Chem. Eng. Japan 32 (5), 684 (1999).

Miller, G. L. Use of Dinitrosalisylic acid reagent for determination of reducing sugars. Anal. Chem. 31, 426 (1959).

Mochizuki, S. and A.L. Zydney. Effect of protein adsorption on the transport characteristics of asymmetric ultrafiltration membranes. Biotechnol. Prog. 8, 553 (1992)

Morawetz, H. Macromolecules in Solution. 2nd Edition. John Wiley & Sons, Inc. New York, 1975

Mulder M. Basic Principles of Membrane Technology. Kluwer Academic Publishers. The Netherlands. 1996.

Nabetani, H., M. Nakajima, A. Watanabe, S. Nakao and S. Kimura. Effects of osmotic pressure and adsorption on ultrafiltration of ovalbumin. AIChE J. 36, 233 (1990)

Nakatsuka, S. and A.S. Michaels. Transport and separation of proteins ultrafiltration through sorptive and non-sorptive membranes. J. Membr. Sci. 69, 189 (1992).

Nguyen, Q. T. and J. Neel. Characterization of ultrafiltration membranes. Part IV: Influence of the deformation of macromolecular solutes on the transport through ultrafiltration membranes. J. Membr. Sci. 14, 111 (1983).

Ousman, M. and M. Bennasar. Determination of various hydraulic resistances during cross-flow filtration of a starch grain suspension through inorganic membranes. J. Membr. Sci. 105 (1-2), 1 (1995).

Opwis, K., D. Knittel, A. Kele, E. Schollmeyer and Krefeld. Enzymatic recycling of starch containing desizing liquor. Starch 51 (10), 348 (1999).

Parker, R. and S. G. Ring. Aspects of the physical chemistry of starch. J. Cereal Sci. 34, 1 (2001).

Persson K.M, Gekas V., G. Trägårdh. Study of membrane compaction and its influence on ultrafiltration water permeability. J. Membr. Sci. 76, 155 (1995).

Persson, K.M., G. Capannelli, A. Bottino, and G. Tragardh, Porosity and protein adsorption of four polymeric microfiltration membranes, J. Membrane Sci. 76, 61 (1993).

Pfannemüller, B. & G. Ziegast. Properties of aqueous amylose and amylose-iodine solutions. ACS Symp. Ser. 150, 528 (1981).

Pfannemüller, B., H. Mayerhöfer, R.C. Schulz. Conformation of amylose in aqueous solution: Optical rotary dispersion and circular dichroism of amylose iodine complexes and dependence on chain length of retrogradation of amylose. Biopolymers 10, 243 (1971).

Pitt, A. The nonspecific protein binding of polymeric microporous membranes, J. Parent. Sci. Techn. 41, 110 (1987)

Porter, J. J. Recovery of polyvinyl alcohol and hot water from the textile wastewater using thermally stable membranes. J. Membr. Sci. 151, 45 (1998).

Porter, M.C. Concentration polarization with membrane ultrafiltration. Ind. Eng. Chem., Prod. Res. Dev. 11, 234 (1972).

Porter, M.C. Membrane fltration: in Handbook of Separation Techniques for Chemical Engineers (P.A. Schweitzer, Ed.), McGraw-Hill, New York, NY, 1979.

Pouliot, M., Y. Pouliot, M. Britten and N. Ross. Effects of pH and ionic environment on the permeability and rejective properties of alumina microfiltration membrane for whey proteins. J. Membr. Sci. 95, 125 (1994).

Radley, J. A. Industrial Uses of Starch and Starch Derivatives. Applied Science Publishers LTD, London, 1976.

Razavi, S.K.S., J.L. Harris and F. Sherkat. Fouling and cleaning of membranes in the ultrafiltration of the aqueous extract of soy flour. J. Membr. Sci. 114 (1), 93 (1996).

Ring, S. G., l'Anson J. Kenneth and V.J. Morris. Static and dynamic light scattering studies of amylose solutions. Macromolecules 18, 182 (1985).

Ring, S.G. and M.A.Whittam. Linear dextrins-solid forms and aqueous-solution behavior. ACS Symp. Ser. 458, 273 (1991).

Roger, P., L.A. BelloPerez and P. Colonna. Contribution of amylose and amylopectin to the light scattering behaviour of starches in aqueous solution. Polymer 40 (25), 6897 (1999).

Rundle, R.E., L. Dasch, and D. French. The structure of the "B" modification of starch from film and fiber diffraction diagrams. J. Amer. Chem. Soc. 66, 130 (1944).

Sheb, J. J. S. and R. F. Probstein. On the prediction of the limiting flux in laminar ultrafiltration of macrosolutions. Ind. Eng. Chem. Fundam. 16, 459 (1977)

Snyder, E.M. Industrial microscopy of starches: in Starch, Chemistry and Technology. (R.L. Whistler, J.N. Bemiller, and E.F. Paschall, Eds.) Academic Press, Orlando, 1984.

Suki, A., A.G. Fane, and C.J.D. Fell. Flux decline in protein ultrafiltration. J. Membr. Sci. 21, 269 (1984).

Sun, S.F. Physical chemistry of macromolecules: basic principles and issues. Wiley, Inc. New York, 1994.

Swinkels, J.J.M. Sources of starch, its chemistry and physics, in: Starch Conversion Technology (G.M.A. Van Beynum and J.A. Roels, Eds.), Marcel Dekker, Inc. New York, 1985.

Tager A. Physical Chemistry of Polymers. MIR publisher. Moscow, 1972.

Tanford, C. Physical Chemistry of Macromolecules. John & Sons, Inc, New York, London, 1961.

Thorsen, T. Fundamental studies on membrane filtration of colored surface water. Ph.D. Thesis. NTNU. 2000.

Thurn, A and W. Burchard. Heterogeneity in branching of amylopectin. Carbohyd. Poly. 5, 441 (1985).

Tokita, M. and T. Tanaka. Friction coefficient of polymer networks of gels. J. Chem. Phys. 95, 4613 (1991).

Tokita, M., Friction coefficient of polymer networks of gels and solvent: in Advances in Polymer Science 110. Responsive Gels: Volume Transitions II. (K. Dusek, Ed). Springer –Verlag, Berlin, 1993.

Toyomoto, K. and Higuchi. A. Microfiltration and ultrafiltration: in Membrane Science and Technology. (Y. Osada, Y. and T. Nakagawa, Eds.). Marcel Dekker, Inc., New York, 1992.

UNEP The Textile Industry and the Environment. United Nations Publication, 1994.

Utracki, L., and R. Simha. Corresponding state relations for the viscosity of moderately concentrated polymer solutions. J. Polymer Science. Part A 1, 1089 (1963).

Van Oss, C. J., K. Arnold, R. J. Good, K. Gawrisch and S. Ohki. Interfacial tension and osmotic pressure of solutions of polar polymers.J. Macromol. Sci.-Chem., A27 (5), 563 (1990).

Van Oss, C.J. and R. J.Good. Surface tension and solubility of polymers and biopolymers: the role of polar and apolar interfacial free energies. J.Macromol. Sci.-Chem., A26 (8), 1183 (1989).

White, M. L. The permeability of an acrylamide polymer gel. J. Phys. Chem. 64, 1563 (1960).

Wijmans, J. G., S. Nakao, J. W. A. van den Beg, F. R. Toelstra and C. A. Smolders, Hydrodynamic resistance of concentration polarization boundary layers in ultrafiltration. J. Membr. Sci. 22, 117 (1985).

Wijmans, J. G., S. Nakao, and C. A. Smolders. Flux limitation in ultrafiltration: Osmotic pressure model and Gel layer Model. J. Membr. Sci. 20, 115 (1984).

Yamakawa, H. Modern Theory of Polymer Solutions. Herper & Row, New York, 1971.

Yeh, H. M. and T. W. Cheng. Resistance-in-series for membrane ultrafiltration in hollow-fibers of tube-and-shell arrangement. Sep. Sci. Techn. 28 (6), 1341 (1993).

Yeh, Ho-Ming. Modified gel-polarization model for ultrafiltration in hollow-fiber membrane modules.Sep. Sci. Techn. 31 (2), 201 (1996).

Zeman, L.J. Adsorption effects in the rejection of macromolecules by ultrafiltration membranes. J. Membr. Sci. 15, 213 (1983)

Zydney A. L. Membrane fouling: in Microfiltration and Ultrafiltration – Principles and applications. (L. J. Zeman and A. L. Zydney, Ed.). Marcle Dekker, Inc. New York. 1996.

URN:NBN:no-3327

Appendix

A. Reproducibility of degraded starch

A.1. Degraded starch preparation and evaluation of its reproducibility

In principle, the preparation of the degraded starch for this study was similar to Heitmann et al. (1997). In our case, however, we degraded native potato starch without any refinement and buffering medium. First, we evaluated the reproducibility of the degradation and the relation between the degree of degradation and the degradation time. The reproducibility was checked by determining the molar mass distribution and the concentration of the reducing end as function of degradation time using HPSEC and DNS analysis methods, respectively. Herein, we reported all the information about the material used, the procedure followed and the analysis principle of the samples and the result we obtained and their discussion. At last, the concluding remarks and the degradation times that were used in preparing the model starch solutions that were used in our study were selected.

Material

Starch: we used potato starch from Norske Potetindustrier. The starch had the following properties:

- Carbohydrate: 78-80 wt. %
- Moisture content: max. = 20 wt. %
- Protein: < 0.1 wt. %
- Fat: < 0.1 wt. %

Enzyme: α-amylase enzyme - Bactosol MTN Liquid (BIOLASE PCL 150) from SANDO. The enzyme was diluted to get 1 wt %, 0.1 wt % and 0.01 wt

% enzyme per gram of dry starch in deionized water. These concentrations were used in order to see the effect of concentration of the enzyme on the degree of degradation of the starch.

Apparatus: In order to check the reproducibility of degradation of the starch as function of time, we used a small reactor. The reactor had a diameter of 10 cm and a volume of 1 liter. In preparation of the degraded starch for our experimental work, we built a reactor with a diameter of 15 cm and a volume of about 4 liter. It was equipped with a mixer. The mixer was adjusted at about 150 rpm. The reactor was heated and cooled by a water bath and a thermostat was used to control the temperature of the water bath. A magnetic thermometer was used to measure the temperature in the reactor.

Procedure: The reactor was fixed in the water bath and the water bath was heated to about 90^{o}C and a suspension of 15 g. of starch in 750 mldeionized water was prepared and added to the reactor and the mixer was started right away. When the starch in the reactor was gelatinized and the temperature in the reactor had been at 90^{o}C for 30 min, the water bath was drained and replaced by cool tape water and the thermostat was adjusted to 40^{o}C. After 30 min, when the temperature of the water bath reached 40^{o}C, the sample of the gelatinized starch was taken and the enzymatic degradation was initiated by adding a given volume of diluted α-amylase solution (that gave 1.0, 0.1 or 0.01 % enzyme per dry starch in the gelatinized solution). In order to see the degree of degradation as a function of the degradation time, samples were collected after 5, 10, 20, 40, 60, 90 and 120 min. A sample of about 20-ml was withdrawn at each time. Enzymatic degradation was stopped by boiling the samples right away at 100^{o}C for over 5 minute in a test tube cocked by a marble ball. For the feed preparation the procedure was somewhat modified due to the larger volume of the solution, see Appendix A.2.

Analysis

Molar mass distribution: HPLSEC was used to determine the molar mass distribution of the degraded starch. The HPLSEC was performed at 40^{o}C using a Perkin Elmer (series 2000) HPLC pump with an auto sampler, operating at a flow rate of 0.5 ml/min. Injected samples contained 50-200μg of degraded starch of different degradation times. The elution was monitored by a refractive index (Shimadzu RID-10A) and a multi-angle laser light scattering detector (MALLA,Wyatt Dawn DSP,633nm) equipped with an in-line filter holder (Millipore) with a 0.2 μm PTFE filter

(Fluoropore-FG,Millipore). Data acquisition and molecular weight calculations were performed using the ASTRA software (Wyatt Technologies)

Concentration of the reducing sugar: The concentration of the reducing sugar end depends on the degree of degradation of the starch. As the degradation increases, the concentration will also increase. The sample was diluted to less than 5 mg/ml. The concentration of the reducing end was measured by using the DNS method [Miller, 1959]. The absorbance was read using a Shimadzu UV-260 (CME101-264) at 540 nm wave length and room temperature.

Result and discussion

In the degradation, three different concentrations, 0.01%, 0.1 % and 1.0 % (wt enzyme/dry wt. of starch), were used. The result of HPSEC for native starch was bad. That was because the column we used was not designed to handle such high molar mass and branched macromolecules. The column used in the equipment was best for molar mass lessthan a million g/mol and the light scattering detector was good for molar mass larger than 10,000 g/mol. For an enzyme concentration of 0.01 %, the degradation was poor. The degradation was hardly detected by the HPLSEC for degradation times less than 40 min. After 2 h, the average molar mass was still larger than 100,0000 g/mol. In addition, it seemed that the reproducibility was very poor. On the other hand, when 1.0 wt % enzyme was used, the degradation was so fast that in less than 40 min it was difficult to separate peaks of degraded starch from the peaks of the salt of the carrier medium. Thus, we only gave emphasis to the degradation of starch with 0.1 % enzyme concentration and its reproducibility. We got a clear trend of degradation with time when we degraded a 2.0 wt. % starch solution at 40^{o}C and a mixer speed of 150 rpm. For three replicates the molar mass of the starch and the corresponding concentration in solution in IR are given as a function of elution time in Figures A-1*a* to A-1*e* for 10, 20, 40, 60 and 90 min degradation. The reproducibility of degradation was somehow poor for low degradation times but it improved as the degradation time was increased. This might be due to the limitation of the apparatus, which works well for molar masses from 10,000 to 600, 000 g/mol. If we only compare the IR as the function of elution time, which was supposed to be inversely proportional to molar mass, we see better reproducibility. The reproducibility of the degradation was also checked by DNS analysis made on the samples. The average absorbance measured for the three replicates as

a function of degradation time are plotted in Figure A-2. Thus, we think that even for a lower degradation time, reproducibility was also good enough. The average molar mass of the starch in each sample was calculated and is given in Table A-1. The average molar mass calculated accounted for the mass of starch that was detected by the light scattering detector. The mass injected, the mass recovered (mass of the molar mass detected by the detector) and the mass loss (difference between injected and recovered) calculated for the sample analyzed by HPLSEC are also given in Table A-1. Except for 10-min degradation, the mass loss was increased with an increase in degradation time as a result of an increase of smaller molar mass components in the degraded starch which could not be detected by the light scattering detector. In the case of 10 min degradation, the sample should also have larger molecules that could not be measured by the column we used. This means that the actual average molar mass of the degraded sample was much smaller than what is given in Table A-1. Assuming the average molecular weight of smaller starch molecules that escaped the detector to be 3000 g/mol, we estimated the average molecular weight to be 1360000, 146000, 33000, 19000 and 13000 g/mol for 10, 20, 40, 60 and 90 min degradation time, respectively.

In addition, the samples were also tested for stability at ambient temperature for one week and for retrogradation at 3 ^{o}C for 1, 7, 14 days to see whether there is significant change in molar mass distribution due to bacterial action or removal of large molar mass molecules on settling. The stability was tested by DNS test and after 2 and 6 weeks. In both cases, the absorption measurements were the same with negligible standard deviation. The retrogradability test was conducted by running the phenol-sulfuric acid test to measure the glucose content before and after centrifuging a portion of the sample at 7000 rpm assuming the precipitate would settle at this speed. There was neither significant change in the absorption measurement nor a clear trend of variation. This shows that the retrogradation is insignificant, at least for the given conditions. There was also no detectable color change of the solution by the naked eye the first 2 days, but later the solution started to become whitish from time to time. However, on heating to 60^{o}C and mixing, it disappeared very fast for solutions kept for not more than one week. At higher concentrations things could be different. According to Elgal et al. (1979), however, the degraded starch solution can be stored for up to two weeks depending on the mode of starch degradation selected and it can be used for sizing. Longer storage of the degraded starch is not detrimental, but prior to its use it has to be mixed to uniform fluidity. This means that there will not be serious retrogradation that will change initial properties of

the degraded starch during the short storage time. In our case, however, as long as there is somewhat retrogradation, the size distribution of the starch in the solution changes which affects ultrafiltration. Therefore, it is better to use the solution experiment before it starts to retrograde or degrade further.

Concluding Remarks

A required degradation of the starch could be achieved by selecting the enzyme concentration and degradation time for a given starch concentration. Heating the degraded starch to 100^{o}C sample will kill the activity of the enzyme. In ultrafiltration studies we chose starch degraded for 40 minutes as reference starch. The other two qualities that are used in our study are chosen depending on the retention of the membrane. Since we have to use a larger reactor to prepare the model degraded starch that is used in the ultrafiltration, at a chosen degradation time we may get somewhat different reactor performance and average molecular weight of the degraded starch.

Table A-1. The mass injected, mass recovered and lost during the HPSEC analysis and the average molar mass for each sample and degradation time.

Degradation time (min)	Replicate run	Injected mass for analysis (μg)	Mass recovered (μg)	Mass lost (%)	Average molar mass (g/mol)
10.00	Run I	50.00	33.70	32.60	1644000
	Run - II	50.00	41.10	17.80	634300
	Run - III	50.00	39.60	20.80	1310000
	Average	50.00	38.10	23.73	1196100
	Run I	125.00	107.00	14.40	2848000
	Run - II	125.00	104.00	16.80	613300
	Run - III	125.00	107.00	14.40	2848000
	Average	125.00	106.00	15.20	2103100
20.00	Run I	100.00	77.80	22.20	235900
	Run - II	100.00	81.20	18.80	126300
	Run - III	100.00	78.90	21.10	166200
	Average	100.00	79.30	20.70	176133
	Run I	250.00	200.80	19.70	246900
	Run - II	250.00	205.10	17.96	128700
	Run - III	250.00	207.80	16.88	181600
	Average	250.00	204.60	18.18	185733

Table A-1. Continued…

Degradation time (min)	Replicate run	Injected mass for analysis (µg)	Mass recovered (µg)	Mass lost (%)	Average molar mass (g/mol)
40.00	Run I	300.00	205.30	31.57	48580
	Run - II	300.00	207.40	30.87	44460
	Run - III	300.00	220.20	26.60	47640
	Average	300.00	211.00	29.68	46893
	Run I	750.00	530.00	29.33	43950
	Run - II	750.00	518.80	30.83	44100
	Run - III	750.00	569.80	24.03	46590
	Average	750.00	539.50	28.06	44880
60.00	Run I	300.00	194.10	35.30	28460
	Run - II	300.00	184.00	38.67	27360
	Run - III	300.00	195.90	34.70	27920
	Average	300.00	191.30	36.22	27913
	Run I	750.00	482.60	35.65	28260
	Run - II	750.00	469.20	37.44	26690
	Run - III	750.00	487.60	34.99	27780
	average	750.00	479.80	36.03	27577
90.00	Run I	300.00	161.80	46.07	20460
	Run - II	300.00	160.90	46.37	20550
	Run - III	300.00	169.30	43.57	20650
	Average	300.00	164.00	45.33	20553
	Run I	750.00	392.30	47.69	21360
	Run - II	750.00	411.10	45.19	22410
	Run - III	750.00	402.60	46.32	21520
	average	750.00	402.00	46.40	21763

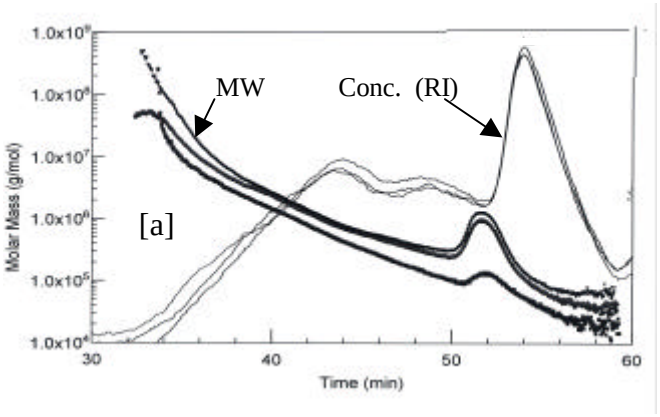

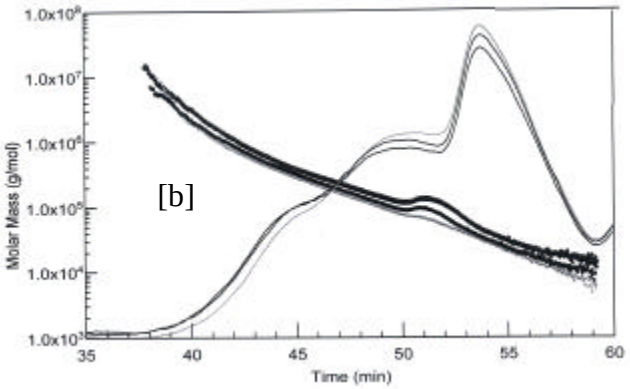

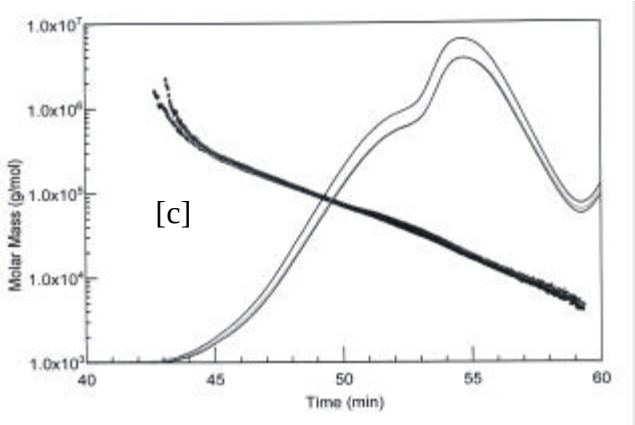

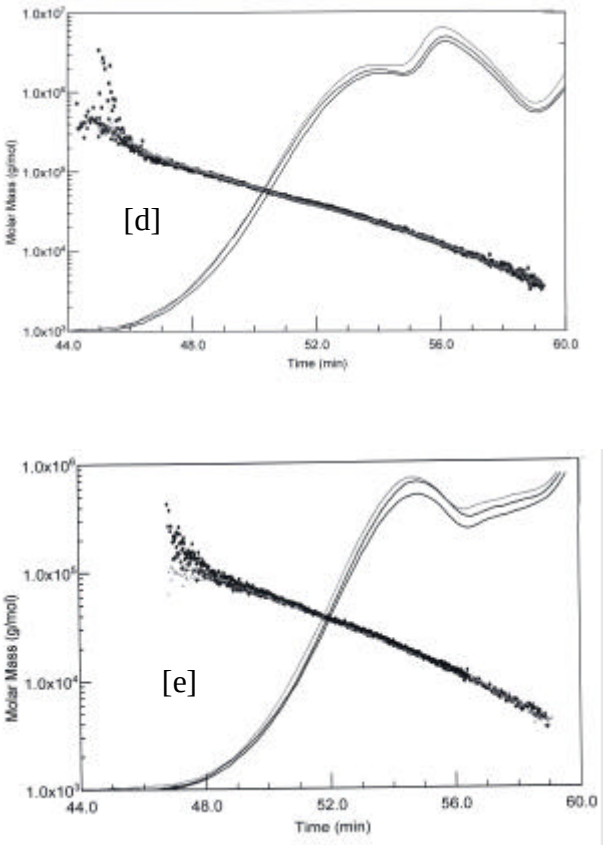

Figure A-1 Molar mass and its corresponding concentration [in RI] as a function of elution time of starch degraded for [a] 10, [b] 20, [c] 40, [d] 60 and [e] 90 min using 0.1 wt % enzyme per dry starch in gelatinized starch C=2.0 wt %, T=40 ^{o}C and mixer speed=150 rpm.

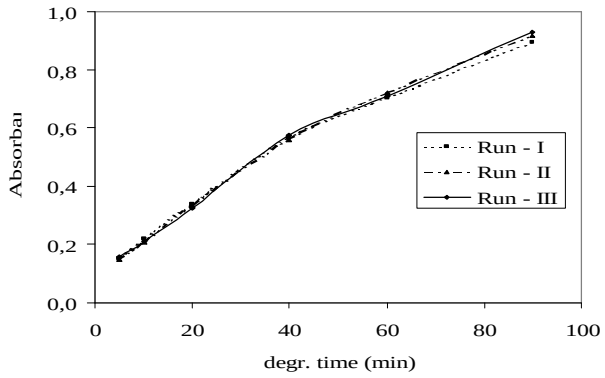

Figure A-2. The concentration of reducing end in absorbance for the degraded starch as function of degradation time (based on DNS method).

A.2 Procedure used for the preparation of feed degraded starch solution

Gelatinization of the starch

Gelatinization of 2 % (on dry basis, 75 g/3 l for 20 % water containing starch) starch

- Heat the water bath to 95 ^{o}C
- Add the suspension of 2 % starch (total 3 l) in the degradation tank
- Maintain the temperature for 45 min.
- Replace the hot water in the bath by cooled water (29 to 30^{o}C)
- Set the bath temp. controller at 40^{o}C and start the heater
- Maintain the temperature for 45 min.

Enzyme solution preparation

- Add 1g of enzyme into 100 g of distilled water, i.e. 1.0 % standard enzyme solution that was diluted further when it was applied.

Degradation of the starch to the required degree

- Measure 6 g of standard enzyme solution (gives 0.1 % enzyme/dry starch, and add to it 24 g of distilled water
- Add the enzyme prepared in the gelatinized starch, start the stirrer and the stop watch
- Run the degradation for the time that gives the required degradation
- Stop the stirrer and dismantle the degradation tank and pour into the boiling tanks
- Boil for 30 min.

A.3. Molar mass distribution of degraded starches used as a feed in the ultrafiltration experiment.

The molar mass distribution in the three model starch solutions used as a feed for ultrafiltration experiment in this study. For MWI, five different feeds, for MWII – three different feeds and for MWIII – three different feed solution samples were analyzed by HPSEC.

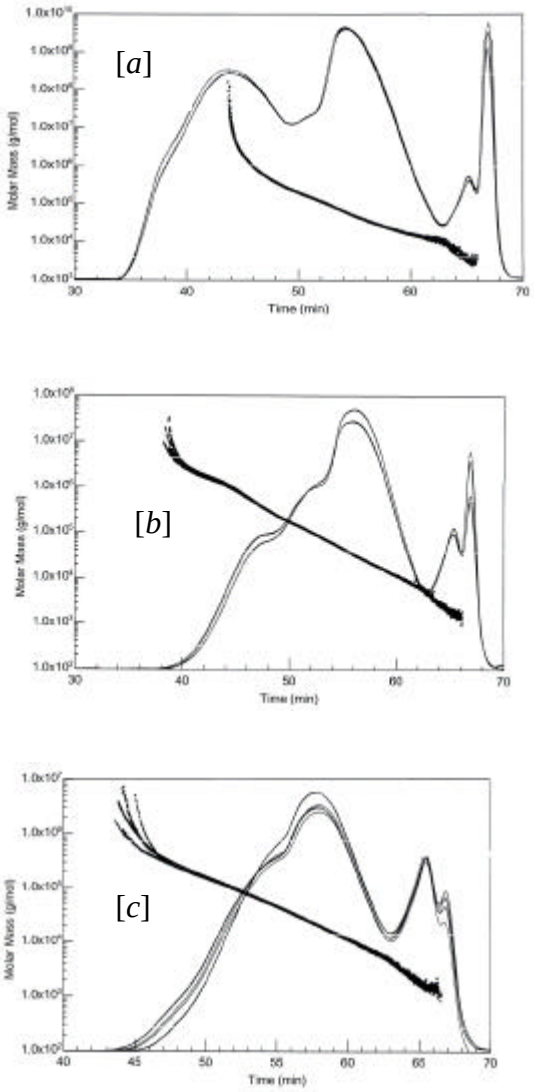

Figure A-3. The molar mass and corresponding concentration for [*a*] 10 min degradation, MWIII; [*b*] 20 min degradation, MWII; [*c*] 40 min degradation, MWI.

Table A.2. The molar mass, radius of gyration and polydispersity determined by HPSEC for some of the feed starch solutions used in the ultrafiltration experiment.

Model starch	Degradation Time (min)	Feed No.	Molar mass (g/mol)		Radius of gyration (nm)		Polydispersity (Mw/Mn)	
			Average	StDev.	Average	StDev.	Average	StDev.
MWI	40	F111	46260	0.4 %	9.6	15.0 %	5.5	3.7 %
		F112	45940	0.5 %	6.6	32.0 %	5.9	4.0 %
		F121	42460	0.4 %			5.7	5.0 %
		F122	41100	0.4 %			5.7	5.0 %
		F131	39690	0.4 %	9.8	15.0 %	5.0	3.5 %
		F132	38750	0.4 %	7.2	29.0 %	5.4	5.0 %
		Average	42367	0.4 %	8.3	22.8 %	5.5	4.4 %
MWII	20	F211	167500	0.3 %	14.2	4.0 %	12.3	5.0 %
		F212	166800	0.3 %	13.2	4.0 %	12.8	5.0 %
		F221	167700	0.2 %	12.7	5.0 %	12.6	5.0 %
		F222	167000	0.3 %	12.3	6.0 %	11.8	5.0 %
		Average	167250	0.3 %	13.1	4.8 %	12.4	5.0 %
MWIII	10	F311	1217000	4.0 %	21.3	1.5 %	33.19	18.0 %
		F312	1791000	17.0 %	21.3	1.5 %	50.95	18.0 %
		F321	1555000	13.0 %	36.2	0.5 %	29.48	13.0 %
		F322	1420000	7.0 %	14.6	1.4 %	27.36	7.0 %
		Average	1495750	10.3 %	23.4	1.2 %	35.245	14.0 %

B. Pure water flux of new ES625 and MPT-U20 membranes

Pure water flux vs. pressure for new membranes used in the ultrafiltration experiments at a temperature of 25^{o}C and a cross flow velocity of 1.0 m/s after the membranes were pretreated as prescribed in chapter 4.

1. Pure water flux of new ES625 membrane (M-I)

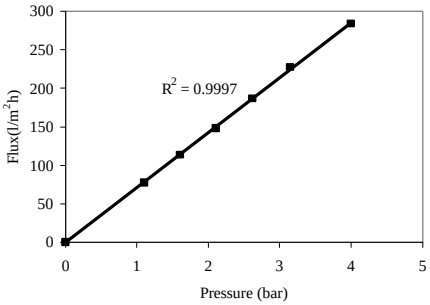

2. Pure water flux of ES625 membrane (M-II)

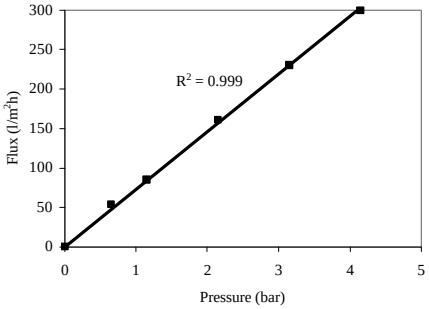

3. Pure water flux of new ES625 membrane (M-III)

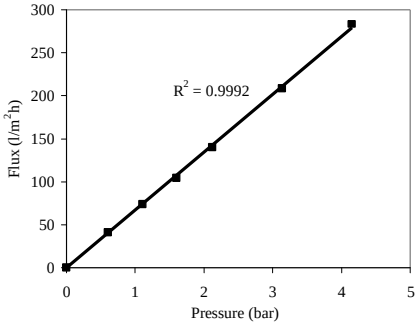

4. Pure water flux of ES625 membrane (M-IV)

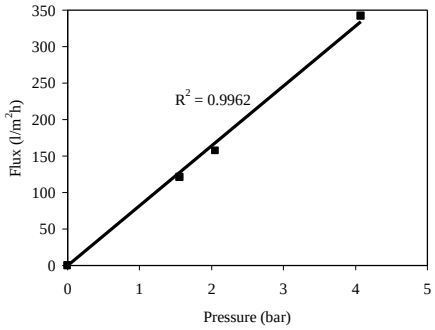

5. Pure water flux of ES625 membrane (M-V)

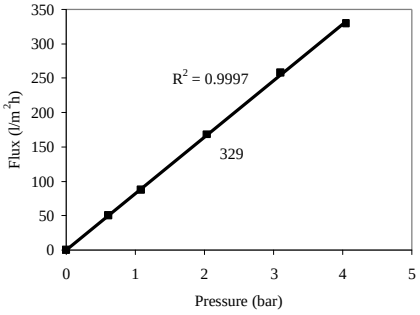

6. Pure water flux of new MPT-U20 membrane

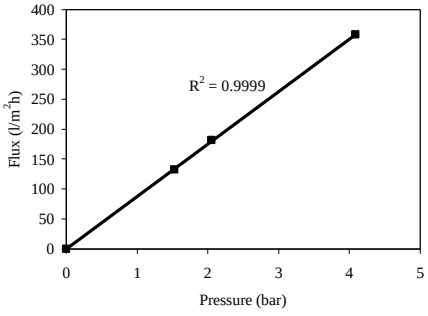

C. Significance of the pure water flux and retention variation between membranes.

The significance of the variation of the pure water flux and retention between the membranes were determined by MINTAB statistical soft.

C.1. Pure water flux of cleaned membranes

One-way ANOVA of pure water flux for ES625 membranes:M-I; M-II; M-III; M-IV; M-V

```
Analysis of Variance
Source     DF        SS        MS        F        P
Factor      4    8693.3    2173.3    44.88    0.000
Error      88    4261.7      48.4
Total      92   12955.0
                                    Individual 95% CIs For Mean
                                    Based on Pooled StDev
Level    N     Mean     StDev  -+---------+---------+---------+-----
M-I     12   143.63      9.41   (---*---)
M-II    16   172.00      9.10                                  (--*--)
M-III   20   163.52      5.89                        (---*--)
M-IV     8   159.36      9.54                  (----*----)
M-V     37   172.67      4.57                                   (--*-)
                               -+---------+---------+---------+-----
Pooled StDev = 6.96           140       150       160       170
```

One-way ANOVA of pure water flux for ES625 and MPT-U20 membranes

```
Analysis of Variance
Source     DF        SS        MS        F        P
Factor      1     29856     29856   226,48    0,000
Error     109     14369       132
Total     110     44225
                                    Individual 95% CIs For Mean
                                    Based on Pooled StDev
Level    N     Mean     StDev  --+---------+---------+---------+----
ES625   93   165,70     11,87   (*-)
MPT-U20 18   210,19      9,12                                 (--*---)
                               --+---------+---------+---------+----
Pooled StDev = 11,48            165       180       195       210
```

C.2. Retention of ES625 and MPT-U20 membranes

One-way ANOVA for the retention of ES625 membranes: M-I, M-II, M-III and M-V

```
Analysis of Variance
Source     DF        SS        MS        F        P
Factor      3    196.36     65.45    12.01    0.018
Error       4     21.80      5.45
Total       7    218.16
                                  Individual 95% of the retention
of ES625
                                  membranes For Mean Based on
Pooled StDev
Level    N     Mean     StDev  ----+---------+---------+---------+--
M-I      2   66.350     1.44              (------*-----)
M-II     2   62.850     1.28         (------*-----)
M-III    2   71.880     0.48                      (------*-----)
M-V      2   58.330     4.130   (-----*------)
                               ----+---------+---------+---------+--
Pooled StDev = 2.34             56.0      63.0      70.0      77.0
```

One-way ANOVA of the retention of ES625 and MPT-U20 membranes

```
Analysis of Variance
Source     DF        SS        MS        F        P
Factor      1     194.9     194.9     6.69    0.032
Error       8     233.2      29.2
Total       9     428.2

                                  Individual 95% of the retention of
ES625 and
                                   MPT-U20 membranes For Mean Based
on Pooled
                                  StDev
Level    N     Mean     StDev  ------+---------+---------+---------+
ES625    8   64.852     5.583                       (------*-----)
MPT-U20  2   53.815     3.882  (------------*-----------)
                               ------+---------+---------+---------+
Pooled StDev =5.399               49.0      56.0      63.0      70.0
```

D. Flux and retention data generated from each of the membranes used in the experiment

The flux data collected during the experimental ultrafiltration of degraded starch in the solution using different membranes.

D.1. ES625 membrane (M-I)

Table D-1. The flux data collected to determine the cleaning effectivity of the cleaning procedure used. J - pure water flux of a clean membrane, J_v – permeate flux, J_f – pure water flux of a fouled membrane, J_{NaOH} - pure water flux after the membrane was cleaned with caustic soda and J_{H2O2} – pure water flux after the membrane was treated by H_2O_2 solution. The experimental condition for the ultrafiltration: T=25°C, conc. = 0.5 wt %, pH=6.5, model solution – MWI, CFV=1.0 m/s.

Flux type	Run – I		Run-II	
	Pressure (bar)	Flux ($lm^{-2}h^{-1}$)	Pressure (bar)	Flux ($lm^{-2}h^{-1}$)
J	2.13	148.16	2.12	140.55
J_v	2.12	54.72	2.14	50.14
J_f	2.15	94.70	2.14	93.87
J_{NaOH}	2.12	120.48	2.13	116.28
J_{H2O2}	2.12	140.55	2.15	149.12

Table D-2. Pure water fluxes and permeate flux as function of pressure for two replicates at a temperature of 25°C and a cross flow velocity of 1 m/s.

Run - I			Run-II		
Pressure (bar)	J_i ($lm^{-2}h^{-1}$)	J_v ($lm^{-2}h^{-1}$)	Pressure (bar)	J_i ($lm^{-2}h^{-1}$)	J_v ($lm^{-2}h^{-1}$)
1.13	65.9	41.1	1.07	75.3	36.9
1.63	102.3	52.3	1.61	114.1	44.8
2.15	148.2	54.7	2.10	140.6	50.1
3.11	210.8	52.6	3.15	227.3	49.2

Table D-3. The retention of the membrane as a function of pressure at the start and end of the experiment at the operating conditions: T=25°C, conc. = 0.5 wt %, pH=6.5, model solution – MWI, CFV=1.0 m/s. The retention data were determined from the SF and COD analysis of the samples obtained from replicate II.

Pressure (bar)	Average retention (%)			
	From SF measurement		From COD measurement	
	At the start expt.	At the end expt.	At the start expt.	At the end expt.
1.07	70.7	67.2	70.4	72.1
1.61	65.4	67.3	62.6	68.1
2.10	65.1	65.8	64.3	66.7
3.15	61 .7	67.7	61.1	69.5

D.2. ES625 membrane (M-II)

Table D-3. Pure water fluxes for clean, adsorbed and fouled ES625 membrane (M-II) and permeate flux as function of pressure and cross flow velocity for two replicate runs. Operating conditions: T = 25°C, conc. = 0.5 wt %, pH=6.5, Model solution – MWI.

Cross flow (m/s)	Replicate	Pressure (bar)	J_i ($lm^{-2}h^{-1}$)	J_a ($lm^{-2}h^{-1}$)	J_f (($lm^{-2}h^{-1}$)	J_v ($lm^{-2}h^{-1}$)
0.25	Run – I	0.60	45.69	31.49	20.48	15.14
		1.09	88.32	61.28	38.74	19.60
		1.59	128.21	87.84	41.04	21.66
		21.0	181.88	113.70	42.27	21.70
	Run – II	0.44	49.46	27.57	21.10	12.54
		0.99	93.68	57.62	35.03	17.84
		1.51	142.39	91.44	48.36	20.64
		2.01	184.45	117.94	50.96	21.88
1.00	Run – I	0.60	51.77	31.91	21.80	19.85
		1.09	87.46	60.41	37.84	32.98
		1.59	132.76	91.89	59.52	47.52
		2.10	178.30	122.71	70.51	48.60
	Run – II	0.59	51.85	23.88	19.51	18.72
		1.08	90.98	47.07	36.97	30.86
		1.59	132.44	74.52	54.05	43.03
		2.09	176.62	97.43	62.41	45.34

Table D-4. The retention of ES625 membrane (M-II) as a function of pressure at the start and at the end of the experiment at the operating conditions: T=25°C, conc. = 0.5 wt %, pH=6.5, model solution – MWI, CFV=1.0 m/s. The retention data were determined from SF analysis of the samples from replicate II.

Pressure (bar)	Average retention (%)	
	At the start expt.	At the end expt.
1.07	72.08	72.26
1.61	67.60	70.98
2.10	61.84	63.86
3.15	60.64	63.70

D.3. ES625 membrane (M-III)

Table D-5. Pure water fluxes for clean, adsorbed and fouled ES625 membrane (M-II) and permeate flux as function of pressure and cross flow velocity for two replicate runs. Operating conditions: T = 25°C, conc. = 0.5 wt %, pH=6.5, Model solution – MWI.

pH	Temp (°C)	Model starch	Conc (wt %)	Flux type	Run - I		Run - II	
					Pressure (bar)	Flux ($lm^{-2}h^{-1}$)	Pressure (bar)	Flux ($lm^{-2}h^{-1}$)
6.5	25	MWI	0.1	J_i	1.61	115.77	1.59	111.90
				J_a	1.60	80.20	1.60	85.30
				J_f	1.62	52.12	1.59	58.27
				J_v	1.62	47.36	1.61	55.06
			0,5	J_i	1.60	104.26	1.61	115.38
				J_a	1.62	53.17	1.61	64.51
				J_f	1.61	41.65	1.61	51.34
				J_v	1.63	35.93	1.60	43.06
			1,0	J_i	1.60	108.82	1.63	91.34
				J_a	1.61	60.52	1.63	48.50
				J_f	1.61	42.53	1.61	37.86
				J_v	1.60	34.47	1.60	31.75
		MWII	0.5	J_i	1.61	103.43	1.61	104.59
				J_a	1.60	57.62	1.61	62.29
				J_f	1.61	40.29	1.60	38.74
				J_v	1.61	34.89	1.61	36.54
		MWIII		J_i	1.60	111.22	1.61	110.76
				J_a	1.59	83.41	1.60	75.07
				J_f	1.60	36.32	1.61	38.17
				J_v	1.60	33.94	1.60	34.93
	50	MWI		J_i	1.56	194.18	1.57	165.96
				J_a	1.57	175.86	1.55	153.76
				J_f	1.55	110.23	1.54	108.06
				J_v	1.56	90.54	1.54	89.24
3.6	25			J_f	1.55	97.86	1.56	54.81
				J_v	1.56	108.42	1.57	63.79
10				J_I	1.53	107.70	1.54	64.20
				J_a	1.57	112.23	1.55	76.02

Table D-6. The retention of ES625 membrane (M-III) at the start and at the end of the experiment at operating conditions: ΔP=1.6 bar, T=25°C, conc. = 0.5 wt %, pH=6.5, model solution – MWI, CFV=1.0 m/s. The retention data are calculated from the SF test of the feed and the permeate for replicate II.

Model starch	Pressure (bar)	Average retention (%)	
		At the start of expt.	At the end of expt.
MWI	1.63	71.21	72.55
	1.60	64.68	68.03
MWII	1.61	87.41	87.79
	1.61	82.45	84.18
MWIII	1.60	92.20	91.90
	1.60	91.50	9380

D.4. ES625 membrane (M-IV)

Table D-7. The permeate fluxes, concentration and retention of the membrane determined as function of time for two replicate concentrating model ultrafiltration runs using two ES625 membranes.

Time (hr.)	Run - I			Run - II		
	Flux ($lm^{-2}h^{-1}$)	Conc (wt.%)	Retention (%)	Flux ($lm^{-2}h^{-1}$)	Conc (wt.%)	Retention (%)
0.02	49.86	-	-	42.18	-	-
0.17	41.95	0.55	67.09	45.31	0.54	67.09
0.50	44.65	-	-	50.64	-	-
1.00	45.73	0.65	62.62	49.84	0.62	64.82
2.00	41.36	0.79	67.55	44.38	0.78	68.44
3.00	35.65	1.03	72.16	37.37	0.99	73.81
4.00	25.55	1.48	78.59	28.76	1.35	77.56
5.00	20.59	2.30	82.72	20.90	2.11	76.45

D.5. Membrane M-V

Table D-8. Permeate flux on ultrafiltration of model solution MWI and MWII for five transmembrane pressure drops, three cross flow velocities and feed concentrations for two replicate runs at T = 25°C and pH=6.5.

Model starch	Feed conc. (wt %)	Cross flow velocity (m/s)	Run - I		Run - II	
			Pressure (bar)	J_v ($lm^{-2}h^{-1}$)	Pressure (bar)	J_v ($lm^{-2}h^{-1}$)
MWI	0.50	0.50	0.66	25.67	0.62	25.81
			1.14	33.77	1.14	35.35
			1.65	37.33	1.65	38.66
			2.13	37.80	2.12	36.22
			3.14	35.32	3.17	33.26
		1.00	0.59	22.61	0.61	24.44
			1.08	38.12	1.08	40.39
			1.58	50.00	1.57	51.66
			2.07	56.16	2.07	56.12
			3.08	60.30	3.11	58.32
		1.50	1.04	47.56	1.07	49.75
			1.52	64.98	1.55	66.28
			2.01	72.90	2.01	73.58
			3.05	74.84	3.06	76.00
			4.04	73.48	4.03	73.69
	1.00	0.50	0.49	19.73	0.49	18.50
			1.04	27.94	1.03	23.69
			1.55	31.32	1.55	25.16
			2.03	29.92	2.01	24.08
			3.09	28.08	3.11	23.11
		1.00	0.42	21.74	0.46	23.76
			1.07	40.21	1.10	40.03
			1.56	42.62	1.61	41.36
			2.12	39.24	2.10	38.99
			3.09	37.44	3.14	37.19
		1.50	0.94	43.63	0.94	44.71
			1.64	55.62	1.68	57.02
			2.13	53.57	2.11	53.96
			2.67	50.08	2.64	50.98
			3.14	46.94	3.22	49.03

Table D-8. Continued…

Model starch	Feed conc. (wt %)	Cross flow velocity (m/s)	Run - I		Run - II	
			Pressure (bar)	J_v ($lm^{-2}h^{-1}$)	Pressure (bar)	J_v ($lm^{-2}h^{-1}$)
MWI	2.00	0.50	0.64	14.36	0.64	15.55
			1.15	17.10	1.14	18.65
			1.63	16.06	1.66	20.59
			2.14	13.86	2.08	16.02
			3.17	14.80	3.11	12.89
		1.00	0.58	21.28	0.60	21.89
			1.09	29.27	1.09	32.76
			2.07	33.73	2.07	37.26
			3.10	27.11	3.07	35.35
			4.11	22.10	4.10	28.58
		1.50	1.07	32.36	1.06	34.74
			1.53	36.22	1.51	41.62
			2.05	37.87	2.02	40.36
			3.08	30.92	3.02	34.67
			4.04	28.08	4.02	28.80
MWII	0.50	0.50	0.65	22.79	0.64	21.60
			1.16	26.28	1.14	25.63
			1.63	27.47	1.69	26.46
			2.15	27.07	2.13	26.21
			3.17	25.96	3.12	25.70
		1.00	0.60	26.82	0.60	26.68
			1.09	39.49	1.07	41.26
			1.59	44.24	1.60	43.70
			2.09	46.58	2.10	45.68
			3.09	45.83	3.07	46.04
		1.50	1.03	44.57	1.04	45.29
			1.52	56.63	1.52	57.74
			2.03	61.49	2.03	63.25
			3.04	63.47	3.02	67.68
			4.02	62.32	4.02	64.58

Table D-8. Continued…

Model starch	Feed conc. (wt %)	Cross flow velocity (m/s)	Run - I		Run - II	
			Pressure (bar)	J_v ($lm^{-2}h^{-1}$)	Pressure (bar)	J_v ($lm^{-2}h^{-1}$)
MII	1.00	0.50	0.46	15.08	0.44	15.19
			1.04	18.22	1.04	18.00
			1.53	18.29	1.52	18.61
			2.03	18.50	2.02	18.36
			3.06	15.05	3.02	14.58
		1.00	0.44	20.02	0.44	19.73
			1.09	30.92	1.07	30.82
			1.59	31.79	1.59	32.18
			2.08	31.54	2.07	32.62
			3.09	27.32	3.09	29.27
		1.50	0.99	37.01	0.94	36.04
			1.66	42.52	1.65	43.34
			2.14	43.34	2.13	44.28
			2.63	42.48	2.67	43.88
			3.20	40.10	3.19	40.64
	2.00	0.50	0.48	15.75	0.49	11.23
			0.98	14.47	1.03	11.23
			1.53	16.64	1.51	10.87
			2.02	16.34	2.02	9.61
			3.03	16.00	3.06	7.92
		1.00	0.57	18.25	0.43	16.67
			1.07	20.77	1.07	21.78
			1.58	20.09	1.58	21.38
			2.09	17.93	2.09	19.94
			3.07	14.08	3.07	15.62
		1.50	0.99	27.58	1.01	26.57
			1.51	29.12	1.66	28.12
			2.01	28.44	2.17	27.25
			2.54	24.73	2.67	22.72
			3.03	21.49	3.21	19.87

Table D-9. The retention of ES625 membrane (M-V) at steady state as a function of pressure, cross flow velocity for two model starch solution at T=25°C, conc. = 0.5 wt %, pH=6.5.

Model starch	Cross flow velocity (m/s)	Run - I		Run - II	
		Pressure (bar)	Retention (%)	Pressure (bar)	Retention (%)
MWI	0.50	0.66	48.48	0.62	-
		1.14	34.75	1.14	36.17
		1.65	30.50	1.65	33.42
		2.13	31.08	2.12	33.48
		3.14	36.88	3.17	37.30
	1.00	0.59	70.83	0.61	66.14
		1.08	67.23	1.08	63.82
		1.58	61.25	1.57	55.41
		2.07	54.89	2.07	49.11
		3.08	53.86	3.11	50.97
	1.50	1.04	56.00	1.07	56.01
		1.52	50.57	1.55	50.62
		2.01	43.93	2.01	45.68
		3.05	40.51	3.06	40.22
		4.04	45.94	4.03	49.25
MWII	0.50	0.65	64.75	0.64	61.90
		1.16	53.22	1.14	53.10
		1.63	51.94	1.69	52.33
		2.15	52.01	2.13	51.75
		3.17	56.02	3.12	59.86
	1.00	0.60	71.50	0.60	72.25
		1.09	63.64	1.07	65.38
		1.59	56.23	1.60	58.57
		2.09	58.91	2.10	56.45
		3.09	54.95	3.07	59.02
	1.50	1.03	70.21	1.04	70.57
		1.52	64.24	1.52	63.48
		2.03	58.14	2.03	59.18
		3.04	59.25	3.02	57.81
		4.02	69.36	4.02	67.97

D.6. MPT-U20 membrane - Only one membrane was used in the experiment

Table D-10. Pure water fluxes for clean, adsorbed and fouled MPT-U20 membrane and permeate flux for two replicate runs. Operating conditions: for three different feed concentrations, pHs and model solutions at transmembrane pressure drop≈ 1.5 bar, T ≈ 25°C and CFV ≈ 1.0 m/s.

PH	Model solution	Feed conc. (wt %)	Type of flux	Run - I		Run - II	
				Pressure (bar)	Flux ($lm^{-2}h^{-1}$)	Pressure (bar)	Flux ($lm^{-2}h^{-1}$)
3.5	MWI	0.5	J_i	1.57	160.85	1.58	162.83
			J_a	1.58	107.42	1.58	108.83
			J_f	1.58	56.05	1.58	61.27
			J_v	1.58	40.75	1.57	42.66
6.5		0.1	J_i	1.57	163.55	1.57	168.52
			J_a	1.56	110.48	1.56	120.02
			J_f	1.56	8456	1.56	88.13
			J_v	1.56	69.19	1.57	72.29
		0.5	J_i	1.56	131.77	1.56	156.89
			J_a	1.56	88.16	1.57	99.07
			J_f	1.56	60.54	1.57	68.18
			J_v	1.57	44.64	1.57	49.43
		1.0	J_i	1.56	169.26	1.57	170.03
			J_a	1.57	106.61	1.57	109.48
			J_f	1.57	60.90	1.58	61.49
			J_v	1.58	35.12	1.58	37.76
	MWII	0.5	J_i	1.58	162.79	1.58	162.14
			J_a	1.59	114.55	1.58	116.60
			J_f	1.59	79.09	1.59	80.75
			J_v	1.59	45.94	1.58	47.81
	MWIII		J_i	1.58	159.88	1.58	158.11
			J_a	1.58	110.66	1.59	106.31
			J_f	1.59	67.25	1.59	68.58
			J_v	1.58	35.39	1.58	34.85
10	MWI		J_i	1.58	163.04	1.58	153.83
			J_a	1.58	129.02	1.59	115.74
			J_f	1.57	95.87	1.57	84.82
			J_v	1.58	64.91	1.57	59.62

Table D-11. The retention of MPT-U20 membrane at the start and end of the experiment at the operating conditions: TMPD=1.5, T=25°C, conc. = 0.5 wt %, pH=6.5, model solution for three model starch solutions. The retention data was determined from SF analysis of the samples.

Model solution	Pressure (bar)	Average retention (%)	
		At the start of expt.	At the end of expt.
MWI	1.57	53.55	56.56
	1.57	48.46	51.07
MWII	1.59	55.44	54.65
	1.58	52.24	53.28
MWIII	1.58	64.14	65.58
	1.58	63.40	65.45

E. Physical constants and dimensions used

Table E.1. Physical data

Water density	997 kg/m^3 (at 25°C)
Water viscosity	0.000897 Pa.s (at 25°C)
Macromolecules hydrodynamic diameter (calculated from the radius of gyration)	
For MWI,	d = 12.038 nm
For MWII,	d = 23.966 nm
Diffusion coefficient (calculated from Equation 3- assuming idea assuming independent of conc.)	
For MWI,	D = 4.09 x 10^{-11} (m^2/s)
For MWII,	D = 2.04 x 10^{-11} (m^2/s)
Tubular membrane data	
Diameter	= 0.012 m
Length	= 1.200 m
Boltzman's constants	1.38E-23 J/K
Universal gas constant	8.3145 J/mol.K

F. Cleaning procedure and conditions

1.Caustic soda cleaning

- Concentration (in pH): 12
- Volume of water: 5 l
- Temperature: 50°C
- Flow rate: 200 l/h.
- Treatment time: 20 min.

First flushing

Flow rate:	400 l/hr
Volume:	30 l
Temperature:	16 °C

2. H_2O_2 cleaning

- Concentration (in ppm): 350 ppm
- Volume of water: 5 l
- Temperature: 50°C
- Flow rate: 200 l/h
- Treatment time: 20 min

Second flushing

Flow rate:	400 l/hr
Volume:	30 l
Temperature:	16 °C